The effects of turbulent wave-driven water motion on interactions of the
intertidal kelp *Egregia menziesii* with its herbivores

By

Nicholas Phillip Burnett

A dissertation submitted in partial satisfaction of the
requirements for the degree of
Doctor of Philosophy

in

Integrative Biology

in the

Graduate Division

of the

University of California, Berkeley

Committee:

Professor Mimi A.R. Koehl, Chair
Professor Todd Dawson
Professor Evan Variano

Summer 2017

The effects of turbulent wave-driven water motion on interactions of the
intertidal kelp *Egregia menziesii* with its herbivores

ABSTRACT

The effects of turbulent wave-driven water motion on interactions of the
intertidal kelp *Egregia menziesii* with its herbivores

by

Nicholas Phillip Burnett

Doctor of Philosophy in Integrative Biology

University of California, Berkeley

Professor Mimi A.R. Koehl, Chair

Kelp are ecologically important organisms because they provide food and habitat to many other
creatures. On wave-swept rocky shores, kelp must withstand the force of moving water from
waves and currents, while also growing to large sizes to outcompete neighboring macroalgae for
light and space. If the forces from moving water (e.g. drag) exceed the strength of the kelp, the
kelp can be damaged or dislodged from the shoreline, effectively removing the kelp from the
ecosystem. Here, I use the intertidal kelp *Egregia menziesii*, one of the largest kelp found in the
rocky intertidal zone along the west coast of North America, to investigate how the kelp's
growth and structure are affected by, and alter its interaction with, moving water in waves, as
well as the animals that use the kelp for food and habitat.

In Chapter One, I examine how the gas-filled bladders (pneumatocysts) of kelp help keep the
fronds of *E. menziesii* afloat in wave-driven flow. Field surveys revealed that this species shows
great variation in pneumatocyst size, number, and location on fronds. In laboratory towing-tank
studies, I found that drag on pneumatocysts was reduced when they were bent over by flowing
water. The drag due to pneumatocysts was small compared to the drag on a whole frond. At
flow speeds up to 0.58 m s^{-1}, the buoyant force exerted by a pneumatocyst was greater than the
drag it experienced. In wave-tank experiments using models of fronds with pneumatocysts at
different positions, the pneumatocysts were most effective at lifting fronds high in the water
column when they were located at the distal tips of the fronds, both in small and large waves.
However, if fronds had pneumatocysts that were not at the tip, an increase in the peak velocities
of waves led to an increase in the heights of the fronds in the water column. In the field,
pneumatocysts did not affect the back-and-forth horizontal motion of *E. menziesii* exposed to
waves, but fronds with pneumatocysts were higher in the water column than fronds with no
pneumatocysts, even when the number of pneumatocysts on a frond was low. My results
indicate that pneumatocysts can exhibit great variability in size, number, and location with only a
small effect on hydrodynamic forces on a kelp, that pneumatocysts at frond tips are most
effective at holding kelp high in the water column, but that only a few pneumatocysts at any
location along a frond can enhance the frond's height in waves.

In Chapter Two, I examine the consequences of long, flexible kelp fronds being knotted (a single frond tied around itself) and tangled (multiple fronds intertwined) as they move back and forth with ocean waves. I found that knots increased the drag forces on fronds while also making those fronds break under small forces than unknotted fronds. Tangled fronds of *E. menziesii* provided spatially complex habitats that hosted more and larger herbivores than did untangled fronds, and that herbivore damage, coupled with the higher hydrodynamic forces and mechanical stresses experienced by knotted fronds, made them more vulnerable to being broken by waves. Breakage of knotted fronds can enhance the survival of kelp by pruning individuals to smaller size, thereby reducing their risk of being dislodged by large waves during winter storms. Although earlier studies have documented that the physical environment can affect ecological processes, I found that this is a 'two-way street' where ecological interactions in turn can alter how organisms perform in the physical environment. By analyzing the organismal-level, biomechanical mechanisms underlying the ecological interactions between kelp, herbivores, and the physical environment as all three changed with the seasons, I found that reconfiguration and damage caused by both physical and biological processes affect both kelp survivorship and community structure.

In Chapter Three, I examine how the morphology of *E. menziesii*, and the types of epifauna on the kelp, change over seasons at sites exposed to heavy wave action ("exposed") or to moderate wave action ("moderate") in northern California. Sessile suspension-feeding animals (mussels, barnacles) were more prevalent on kelp at exposed sites, whereas motile herbivorous epifauna (amphipods, limpets, isopods, crabs) were found on more of the kelp at moderate sites. Kelp at both wave exposures showed similar seasonal patterns of morphological change, growing longer fronds from spring through autumn and decreasing in size during winter while maintaining the same number of fronds. The variation in frond lengths on a kelp decreased in summer when the proportion of intact fronds was high, but increased as more fronds broke during autumn and winter. Although patterns of change were similar, some aspects of kelp morphology differed between exposed and moderate sites. During spring, kelp at exposed sites had fewer fronds than those moderate sites. During spring through autumn, the kelp at exposed sites had longer fronds, a greater proportion of intact fronds, and less variation in frond length than those at moderate sites. Frond breakage at wounds inflicted by herbivores, which infest a greater proportion of the kelp at moderate sites than at exposed sites, may be responsible for these morphological differences. In winter, large waves prune kelp to similar morphologies at exposed and moderate sites.

This work is dedicated to the memory of my sister,

Veronica Gray Burnett

Contents

ACKNOWLEDGEMENTS

All of this work is the product of countless meetings and consultations with my adviser, Prof. Mimi A.R. Koehl. I thank her for the multi-faceted mentorship that she has provided me over these five years.

I owe a tremendous amount of thanks to the people who provided assistance in the field. The numerous early mornings and long, cold hours that we spent together in the intertidal zone were the only way that I could build the dataset that has been the foundation of my dissertation. The time volunteered by my field assistance is particularly apparent in Chapter 3 of this work. These people are: Eric Armstrong, Anna Belk, Hannah Bourne, Tessa Burnett, Reina Carissa, Doris Chan, Sofia Chang, Blair Conklin, Katie Horton, Justin Jorge, Jenna Judge, Emily King, Adit Kothari, William Kumler, Dana Lin, Leeann Louis, Jesyka Melendez, Rosemary Romero, Charlotte Runzel, Erik Sathe, Dwight Springthorpe, Richelle Tanner, and Doriane Weiler. Institutional support was provided by Tom Libby (UC Berkeley's Center for Interdisciplinary Bio-inspiration in Education and Research), and Jackie Sones and Kitty Brown (UC Davis' Bodega Marine Laboratory).

Lastly, I would like to acknowledge my family. My parents, Louis and Karen Burnett, have enthusiastically supported me at every stage of my life and education. I cannot thank them enough for all the opportunities, and all the love, they have given me. My wife, Tessa, also deserves special recognition. She has provided me with unconditional support, love, and patience throughout my time at Berkeley. My field work often occurred at inopportune times, but she was always happy to accommodate my schedule, most significantly in the case of our wedding and various holiday trips. I am grateful for her unwavering support of my research.

Chapter 1: Pneumatocysts provide buoyancy with minimal effect on drag for kelp in wave-driven flow

1.1 INTRODUCTION

The intertidal zones of many temperate rocky shores are populated by large seaweeds whose abundance is highly correlated with increased biodiversity because they serve as a food source and habitat for many other organisms (e.g. Abbott and Hollenberg, 1976; Graham, 2004; Christie *et al.*, 2009). Moving water from ocean currents and waves impose hydrodynamic forces on the seaweeds (e.g. Koehl, 1984; Denny, 1988; Gaylord, 1999). On the west coast of North America, waves generally have periods between 8 and 20 seconds (NOAA Buoy Center, www.ndbc.noaa.gov), resulting in thousands of waves each day that move onto the shore and exert forces on the seaweeds. If the magnitudes of the forces exceed the seaweed strength, the seaweeds can be dislodged from the substratum or suffer a partial breakage of the thallus (Koehl and Wainwright, 1977; Carrington, 1990; Demes *et al.*, 2013), resulting in the removal of the seaweed and its epibiota from the ecosystem (Krumhansl and Scheibling, 2012).

The morphological and mechanical traits of a seaweed can alter the hydrodynamic forces it experiences. A seaweed with a flexible thallus can be reconfigured by moving water into a small, streamlined shape that reduces hydrodynamic forces on the seaweed (Koehl, 1984; Carrington, 1990; Martone *et al.*, 2012). In back-and-forth wave-driven flow, flexible seaweeds move with the water in the direction of flow, thus the water velocity relative to the seaweed is reduced and hydrodynamic forces on the seaweed are lower than they would be if the seaweed were rigid (Koehl, 1984). However, moving with the ambient water motion may not always minimize forces on the seaweed: when the seaweed becomes fully extended it can experience inertial loading (i.e. "jerk" *sensu* Denny *et al.*, 1998) due to the sudden thallus deceleration, in addition to the hydrodynamic forces from water that continues moving past the seaweed (Koehl, 1984).

Many flexible seaweeds rely on buoyancy to remain upright in the water column and to access light for photosynthesis (e.g. Stewart *et al.*, 2007). When hydrodynamic forces become sufficiently large, a buoyant seaweed can be pushed closer to the substratum, but return to its upright position once the water motion slows (Stewart, 2004). However, buoyancy has also been shown to interfere with the passive reconfiguration of a seaweed into a compact, streamlined shape when in flowing water, and thus buoyancy counteracts this mechanism of hydrodynamic force reduction (Stewart, 2006a).

The buoyancy of many species of seaweeds is provided by gas-filled bladders (pneumatocysts), which have a variety of forms across seaweed taxa (Abbott and Hollenberg, 1976). For example, *Nereocystis luetkeana* has a single, large pneumatocyst at the end of its stipe, whereas *Macrocystis pyrifera* has numerous small pneumatocysts at regular intervals along the thallus, with pneumatocysts near the holdfast being larger than more distal pneumatocysts. Most studies on the biomechanics and hydrodynamics of seaweed buoyancy have focused on small species (thallus less than 0.5 m in length; pneumatocysts smaller than 2 cm in diameter) to investigate the trade-off between the flexibility of the whole thallus and pneumatocyst buoyancy (e.g. Stewart, 2004, 2006a,b, 2007). However, little is known about the influence of pneumatocysts on the forces on and movement of large seaweeds (thallus longer than 1 m) in ambient flow. Furthermore, the consequences to drag of the size and deformability of a

pneumatocyst have not been explored, and the effects of the positions of pneumatocysts along fronds on the behavior of seaweeds in flowing water are not understood.

I used the feather boa kelp, *Egregia menziesii*, to study the hydrodynamic consequences of having pneumatocysts of different sizes, numbers, and locations along the thallus of a long seaweed. *E. menziesii*, which is one of the largest species of kelp abundant in the rocky intertidal zone along the west coast of North America, has numerous strap-like fronds that grow to lengths of 3 m or more from a perennial holdfast (Abbott and Hollenberg, 1976) (Fig. 1.1A). The rachis of each frond (about 1 to 2 cm wide) bears ellipsoidal pneumatocysts (up to 2 cm long) and narrow lateral blades (up to 5 cm in length) along both edges (Henkel and Murray, 2007) (Fig. 1.1B).

The objective of the present study was to determine how the number, size, flexibility, and location of pneumatocysts on long kelp fronds affect the motion of and hydrodynamic forces on the fronds in wave-driven water flow. The specific questions investigated were: (1) Where do pneumatocysts occur on the fronds of *Egregia menziesii*, and how abundant and large are those pneumatocysts? (2) What is the magnitude of the hydrodynamic force on a single pneumatocyst, and how do the size and the reconfiguration of a pneumatocyst in moving water affect the force on the pneumatocyst? (3) How much do pneumatocysts increase the drag on a frond? (4) How does the location of pneumatocysts on a frond affect the depth of the frond in the water column under different wave conditions? (5) How do pneumatocysts in natural arrangements on kelp in the field affect the horizontal movement and depth of fronds in ambient waves?

1.2 METHODS

1.2.1. Pneumatocyst surveys

1.2.1.1 Field sites

Pneumatocysts on *Egregia menziesii* were surveyed at four rocky intertidal sites in northern California (Fig. S1.1). Two moderately wave-exposed sites were located near Bodega, CA, USA: Horseshoe Cove (HC) (38°18'59" N, 123°4'12" W) and Miwok Beach (MW) (38°21'25" N, 123°4'2" W). Two wave-exposed sites were located in the Point Reyes National Seashore, CA, USA: Kehoe Beach (KB) (38° 9'56.08" N, 122° 57'6.04" W) and McClures Beach (MC) (38°11'2.70" N, 122°58'2.33" W).

1.2.1.2. Abundance of pneumatocysts

The abundance of pneumatocysts on the fronds of intertidal *E. menziesii* were surveyed at HC, KB, and MB in February and June, 2016. At each site, kelp were surveyed along a horizontal transect through the *E. menziesii* zone (low intertidal), selecting every third individual that was encountered. The lengths of all the fronds on the selected kelp were measured to the nearest 1 cm, and the number of pneumatocysts on each frond was recorded.

1.2.1.3. Location of pneumatocysts

The locations of pneumatocysts on the fronds of *E. menziesii* were measured at HC and MW in October and November, 2013. At each site, kelp were surveyed as described above. One frond from each kelp was haphazardly selected, and locations of all pneumatocysts longer than 0.5 cm on the frond, as well as the total length of the frond, were measured to the nearest 1 cm.

For each frond, the locations of the proximal-most and distal-most pneumatocysts were calculated from the survey data.

1.2.1.4. Size of pneumatocysts

The sizes of pneumatocysts on the fronds of intertidal *E. menziesii* were surveyed at MW and MC in September 2016. At each site, 10 kelp were selected as described above. All the pneumatocysts on each kelp were removed, bagged according to the individual kelp, and then photographed. The projected planform area (hereafter planform area) of each pneumatocyst was measured to the nearest 0.01 cm^2 using ImageJ software (ImageJ, v.1.47, National Institutes of Health, USA).

1.2.2. Reconfiguration and drag on pneumatocysts

The reconfiguration of and drag on individual pneumatocysts were measured before and after the pneumatocyst's buoyancy or the stiffness of the pneumatocyst's petiole was changed. Individual fronds with pneumatocysts were collected from MW and MC in January and February, 2016. Fronds were cut into sections (length = 10 cm) with a single pneumatocyst in the middle of each section, and all lateral blades (Fig. 1.1A) were trimmed away (Fig. 1.2). The pneumatocysts were grouped into one of two treatments, and all pneumatocysts within each group originated from separate kelp. In one group, each pneumatocyst's petiole was stiffened by reinforcing the petiole with a short length of aluminum foil. In the second group, the pneumatocyst was punctured and filled with water, rendering it neutrally buoyant (Stewart, 2004). The fronds and their pneumatocysts were towed through a tank of water (working section with a cross-section = 30 x 30 cm, length = 100 cm) at a constant velocity (mean = 0.58 m s^{-1}, see *1.3 Results*), and a spring scale was used to measure drag on the fronds and pneumatocysts (Ohaus Model 8261-M, Pine Brook, NJ, USA). While the fronds were towed through the water, the fronds and pneumatocysts were videotaped at 50 frames per second (Fastec Imaging, San Diego, CA, USA). The deflection angle of the pneumatocysts in each frame of the videos was measured to the nearest 0.01° using ImageJ and calculated by

$$Deflection\ (°) =\ cos^{-1}\left(\frac{l_a^2+l_b^2-l_c^2}{2l_al_b}\right) - 90°$$

(eqn. 1.1)

where l_a is the distance from the leading edge of the frond to the base of the pneumatocyst, l_b is the distance from the base of the pneumatocyst to the top of pneumatocyst, and l_c is the distance from the leading edge of the frond to the top of the pneumatocyst (Fig. 1.2).

The reconfiguration of and drag on each frond and pneumatocyst were measured during three tows in their unmanipulated state (i.e. not stiffened or punctured) and during three tows after manipulation. After the control and treatment measurements were made, the pneumatocyst was removed from the frond to measure drag on the frond by itself (3 times for each frond). The drag coefficient C_D of the pneumatocysts was calculated by:

$$C_D = \frac{2F_p}{\rho Au^2}$$

(eqn. 1.2)

where F_p is the drag on the pneumatocyst by itself (i.e. drag on pneumatocyst and frond minus the drag on frond), ρ is the density of the water in the tow tank (998 kg m^{-3} at 20 $^{\circ}$C, Vogel, 1994), A is the projected planform area of the pneumatocyst, and u is the tow velocity. Projected planform area was measured to the nearest 0.01 cm^2 using ImageJ.

The buoyancy forces of intact pneumatocysts were measured by removing them from the frond and using a spring scale to measure the force required to submerge each pneumatocyst in water. The planform areas of the pneumatocysts were measured to the nearest 0.01 cm^2 using ImageJ.

1.2.3. Force to pull a pneumatocyst off a frond

The force required to detach a pneumatocyst from the rachis was measured with an Instron materials-testing machine (Model 5544, Norwood, MA, USA). The Instron machine pulled a nylon cord that was loosely tied around the pneumatocyst's petiole (strain rate = 20 mm min^{-1}). The rachis was held in place with a clamp and the force required to separate the pneumatocyst from it was recorded the nearest 0.01 N (Fig. 1.3). Sections of fronds bearing pneumatocysts were kept moist in air between 4 and 10 °C until they were tested in air at 20 °C; tests only lasted 2 minutes, so specimens remained cool. Planform areas of pneumatocysts were measured to the nearest 0.01 cm^2 using ImageJ.

1.2.4. Physical models to test the effect of pneumatocyst location on frond height

Physical models of flexible fronds were videotaped in a wave tank to test the effect of pneumatocyst location along a frond on the height of the frond in the water. Models of fronds were constructed of flagging tape (Presco, Sherman, TX, USA) with pneumatocysts that were air-filled silicon spheres, approximately 1 cm in diameter (H&P Sales, Vista, CA, USA). The flagging tape was negatively buoyant in fresh water; its mass density was 1455 kg m^{-3} and its flexural stiffness was 3.27x10^{-9} N m^2. Mass density of the flagging tape was calculated by weighing a section of flagging tape on a digital balance to the nearest 0.0001 g and measuring the section volume with digital calipers to the nearest 0.01 mm.

Flexural stiffness of the flagging tape was determined by hanging a point mass from the end of a section of tape, positioned as a horizontal cantilever beam, and measuring the deflection of the free end of the tape cantilever from the horizontal axis. By approximating the tape as a rectangular beam, linear beam theory was used to calculate the flexural stiffness, EI:

$$EI = \frac{1}{3}\frac{F_B l_B^3}{d}$$

(eqn. 1.3)

where F_B is the applied force to the beam, l_B is the length of the beam, and d is the deflection of the beam from the horizontal axis (e.g. Wainwright et $al.$, 1976). For equation (1.3) to hold, the deflection of the beam had was less than 10% of the beam length.

Model fronds were 30.0 cm long and 2.5 cm wide, and a pair of model pneumatocysts was attached by thread at 10, 20, or 30 cm from the frond base. The locations of pneumatocysts on the models represented real fronds with pneumatocysts at the tip, middle, or bottom of the frond. Models with no pneumatocysts were also made. Five replicate models of each configuration were constructed.

Models were scaled to be dynamically-similar to fronds of $E.$ $menziesii$ in waves in the field. Models were attached to the bottom of a paddle-driven wave tank (working section with a

cross-section 30 x 30 cm and a length parallel to the flow of 100 cm; Hunter, 1988). At rest, the water in the wave tank was 20 cm deep. The ratio of model length to water depth (3:2) was similar to that of *E. menziesii* fronds in shallow surge channels. The wave tank paddle was driven at 0.24 and 0.07 Hz, producing waves with maximum horizontal water velocities of 0.296 m s^{-1} and 0.078 m s^{-1}, respectively. The ratio of the model length to the distance that the water traveled before reversing for both tank settings was approximately 1:1, which mimicked that of the real fronds in the field (see *1.2.5 Movement of* E. menziesii *fronds in wave-driven flow in the field* below).

Each model was videotaped using a Fastec video camera at 20 fps at each wave frequency. In each frame of the video of a full wave cycle, the height of the distal end of each model above the substratum was measured to the nearest 1 mm with ImageJ. The time-averaged height of each model was determined, and the mean of those heights for the five replicate models of each configuration was calculated.

1.2.5. Movement of E. menziesii *fronds in wave-driven flow in the field*

The effects of pneumatocysts on horizontal frond movement were tested by measuring the water velocity relative to *E. menziesii* fronds in a surge channel at HC in October, 2013. Seven *E. menziesii* fronds were haphazardly collected from separate holdfasts near the surge channel and the proximal ends were cut off so that each frond tested was 1.5 m in length. The pneumatocysts found on each frond were located within the distal-most half of the frond. The diameters of the pneumatocysts were measured with calipers to the nearest 0.1 mm. The proximal end of each frond was anchored to the bottom of a surge channel using a brick, and the distal end of the frond was marked with surveyor's tape (3M, Saint Paul, MN, USA). The surge channel was approximately 1 m wide, 5 m long, and 1 m deep.

The water flow in the surge channel was measured while the motions of each kelp frond were videotaped. An acoustic Doppler velocimeter (ADV; SonTek 16-MHz MicroADV, San Diego, CA, USA) was placed at the mouth of the surge channel to measure water velocity to the nearest 0.01 cm s^{-1} as a function of time (sampling rate of 25 Hz) at a height of 20 cm above the substratum. A digital camera (Casio Exilim EX-F1, Dover, NJ, USA) was positioned above the channel with the horizontal component of its field of view parallel to the long axis of the surge channel so that the full range of frond motion was visible to the camera.

The movement of each frond in the surge channel was videotaped for 2 minutes (frame rate of 30 fps) while simultaneous ADV measurements of the ambient water velocities in the surge channel were measured. Water velocities and frond movements were recorded for each frond with its naturally-occurring pneumatocysts, and then recorded again after all pneumatocysts were removed. In each video, the horizontal position of the frond's distal end was tracked to the nearest 0.1 cm using ImageJ and the velocities of the frond were calculated from the position data. Time series of the frond and water velocities were paired by averaging data into 0.2 s bins. Water velocities relative to the frond were calculated by subtracting the frond velocity from the water velocity in each bin, and then those data were sorted by the instantaneous ambient water speed in intervals of 1 cm s^{-1}. Next, the relative water velocities that each frond experienced, with and without its pneumatocysts, were compared among all the fronds at each instantaneous ambient water velocity.

1.2.6. Frond height in the water column in waves in the field

The effect of pneumatocysts and ambient water velocity on the vertical position of fronds in the water column was tested using the same water velocity data and videotapes described in the previous section (1.*2.5. Movement of* E. menziesii *fronds in wave-driven flow in the field*). Each frame of the videos was scored for whether or not any part of a frond floated at the water's surface (1 = frond floating at the water surface, 0 = frond submerged below the water surface). Time series of the floating scores and ambient water speeds were paired by averaging data into 0.2 s bins and then sorted by the instantaneous ambient water speed in intervals of 1 cm s^{-1}. Within each binned ambient water speed, the proportion of time that each frond spent floating at the water's surface was determined for fronds both with and without their pneumatocysts.

The density of frond tissue was measured at a consistent location on fronds, 45 cm from the terminal lamina (Fig. 1.1A), collected from HC following the field experiment. A circular piece of rachis 5.50 mm in diameter was cut from each frond using a hole punch. The thickness of the cut section was measured to the nearest 0.01 mm using digital calipers, and then the mass of the section was weighed to the nearest 0.001 g (wet weight after being patted dry with a paper towel) using a digital balance (AG245, Mettler Toledo, Columbus, OH, USA). These data were used to calculate the mass per volume of rachis tissue.

1.3 RESULTS

1.3.1. Field surveys of pneumatocysts

Fronds with pneumatocysts were more common and occurred in larger numbers in summer than in winter. At all three sites (HC, MC, KB) in February, 10.5 to 11.3% of fronds longer than 10 cm had pneumatocysts, whereas in June, 10.6 to 49.1% of such fronds had pneumatocysts. On fronds bearing pneumatocysts in February, the mean number of pneumatocysts per length of frond ranged from 2.5 to 2.9 pneumatocysts m^{-1}, while in June there were 3.5 to 6.4 pneumatocysts m^{-1} (Fig. 1.4A, Table 1.1).

Pneumatocysts occurred over a wide range of locations on the fronds. Surveys of the locations of pneumatocysts on fronds at HC and MW in October and November 2013 showed that the most proximal pneumatocysts on each frond (i.e. closest to the holdfast) were at positions that ranged from 10 to 67% of the frond length from the base of the frond (i.e. the point where the frond branches from an older frond or from the holdfast). The most distal pneumatocysts were located at positions 10% to 96% of the frond length from the base. The median location of pneumatocysts, pooled across all surveyed fronds at MW, was close to frond midpoint (44% of the frond length from the base) (Fig. 1.4B).

Pneumatocysts were larger at the wave-exposed site, MC, than at the moderately wave-exposed site, MW (Mann-Whitney *U* test, *P* < 0.0005, n = 839 pneumatocysts from MC, 409 from MW) (Fig. 1.4C).

1.3.2. Orientation of and drag on pneumatocysts

Buoyancy of the pneumatocyst and the stiffness of the petiole both affected the reorientation of pneumatocysts in flowing water and the drag on them. Pneumatocysts that were made neutrally buoyant leaned over more in flow and experienced lower drag than they did when they were positively buoyant (paired *t*-tests, *P* < 0.005, df = 14) (Fig. 1.5). In contrast, pneumatocysts with stiffened petioles were reoriented less by flow and experienced higher drag than they did without stiffened petioles (paired *t*-tests, *P* < 0.005, df = 16). The drag on a pneumatocyst was negatively correlated to the deflection of the pneumatocyst in flow (Fig. 1.5).

Unmanipulated pneumatocysts had a mean drag coefficient of 0.013 (SD = 0.007, n = 32) and a mean deflection angle (Fig. 1.2B) of 54.65° from vertical (SD = 9.44, n = 33) (Fig. 1.5). Buoyancy was positively correlated to the planform area of pneumatocysts. Buoyant forces ranged between 0.40 and 1.74 mN for pneumatocysts between 0.70 and 6.60 cm^2 in planform area (Fig. 1.6A). Drag was smaller than buoyancy for the majority of the unmanipulated pneumatocysts (Fig. 1.6B).

1.3.3. Force to remove pneumatocysts from the frond

The force to remove a pneumatocyst from a frond was positively correlated to the planform area of the pneumatocyst (Fig. 1.7). Detachment forces ranged from 3.91 to 35.63 N for pneumatocysts between 0.77 to 8.64 cm^2 in planform area.

1.3.4. Physical models to test the effect of pneumatocyst location on frond height

The heights of model fronds above the substratum of a laboratory wave tank were affected by the positions of pneumatocysts and by the wave action. For both wave regimes tested, fronds exposed to the oscillatory flow of waves remained, on average, higher in the water column when the pneumatocysts were located at the distal tip of a frond than when they were at more proximal positions (Fig. 1.8). Fronds with pneumatocysts located at their midpoint or proximal end were higher in the water column when exposed to the high velocity, high frequency waves than when exposed to the slower low frequency waves (Mann-Whitney U tests, $P < 0.05$, n = 5 replicates of each float position in each wave condition). In contrast, the height of fronds with pneumatocysts at the distal tip, and for fronds without pneumatocysts, did not differ between the two wave conditions that were tested (Mann-Whitney U tests, $P > 0.05$, n = 5 replicates of in each wave condition).

1.3.5. Frond movement in wave-driven flow in the field

Fronds collected for the field experiments had between 3 and 21 pneumatocysts, and all pneumatocysts were between 7.5 and 20.0 mm in diameter. Fronds of *E. menziesii* moved back-and-forth with each wave (Fig. 1.9A), such that the water velocity relative to the frond surface was slower than the ambient water velocity (Fig. 1.9B). The presence of pneumatocysts only affected the relative water velocity past the distal ends of the fronds at three instantaneous ambient water velocities of -32, -30, and -1 cm s^{-1} (paired t-tests, $P < 0.05$, df > 3), which, all being negative velocities, indicate water movement in the seaward direction. All fronds, regardless of pneumatocysts, experienced approximately 82 to 83% of the instantaneous ambient water velocities -36 to 50 cm s^{-1} (Fig. 1.9B,C).

1.3.6. Frond height in water column in the field

In ambient water speeds from 0 to 40 cm s^{-1}, fronds with pneumatocysts spent more time floating at the air-water interface than did fronds without pneumatocysts (paired t-tests, $P < 0.05$, df > 4; Fig. 1.10). Even with pneumatocysts, the probability of a frond floating at the water surface decreased with increasing ambient water speed, whereas fronds without pneumatocysts were only observed floating at the water surface in very slow ambient water speeds of 2 and 4 cm s^{-1} (Fig. 1.10). The mass density of frond rachis tissue in the middle of the frond (45 cm from the intercalary meristem) was 1092 kg m^{-3} (SD = 74, n = 5), which is greater than that of sea water (1024 kg m^{-3} at 20 °C; Vogel 1994), so fronds without pneumatocysts sink in still water.

1.4 DISCUSSION

1.4.1. Reorientation of individual pneumatocysts in flow reduces drag

Reconfiguration of seaweeds in moving water has mostly been studied on the scale of the entire organism, whereas the focus of the present study was on the reconfiguration of pneumatocysts relative to the fronds of *Egregia menziesii* when in flow. Pneumatocysts floats are rigid, but the petioles can bend easily, so reconfiguration of the structure was limited to bending at the petiole such that the float leaned over closer to the rachis to a mean deflection (Fig. 1.2B) of 54.65° in a current of 05 m s^{-1} (Fig. 1.5). This deflection is in contrast to the reconfiguration of flexible leaves on terrestrial plants, which fold into cones and bend at the petiole (Vogel, 1989), or to the flexible thalli of seaweeds, the blades of which can be folded into streamlined shapes (Carrington,1990; Martone *et al.*, 2012) or pushed together into streamlined bundles (Koehl and Alberte, 1988). However, deflection by bending at the petiole was sufficient to reduce drag on the pneumatocysts, and consequently the pneumatocysts produced more buoyancy than they did drag (Fig. 1.6B). The buoyancy of the pneumatocyst is antagonistic to the flexibility of the petiole, and actually inhibits reconfiguration of the pneumatocyst to some degree (Fig. 1.5). This trade-off between flexibility and buoyancy has been shown for the entire thallus of the seaweed *Turbinaria ornata* (Stewart, 2006a), but not for individual structures on a seaweed.

The drag at field-relevant velocities of 0.5 m s^{-1} and the buoyant forces on the pneumatocysts were each less than 2 mN (Fig. 1.6), yet the force to break a pneumatocyst from the frond ranged from 3 to 36 N (Fig. 1.7). These measurements indicate that intact pneumatocysts can resist drag and buoyant forces at least 1,000 times greater than those they are likely to experience in the field, whereas the frond itself is approximately 12 times stronger than the forces it is expected to encounter from hydrodynamic forces in nature (Friedland and Denny, 1995). Other factors can cause pneumatocysts to be weakened and break from the frond, such as herbivory or abrasion against rocks (Black, 1976; Lowell *et al.*, 1991). Such pneumatocyst loss is probably a factor in producing the wide range of pneumatocyst numbers and locations on fronds measured in the field (Fig. 1.4A,B).

1.4.2. Effects of pneumatocysts on drag and photosynthesis

The magnitude of the drag on a pneumatocyst measured in this study is approximately three to four orders of magnitude lower than the total drag on an entire *E. menziesii* (e.g. Gaylord *et al.*, 2008). Therefore, it is likely that fronds of *E. menziesii* can have a wide variety of pneumatocyst sizes and numbers without paying a price in increased hydrodynamic drag. In fact, kelp at the wave-exposed site had larger and more numerous pneumatocysts than kelp at the moderately wave-exposed site (Fig. 1.4C), suggesting that the benefit of buoyancy from pneumatocysts is more important than the problem of increased drag due to pneumatocysts.

Pneumatocysts may indirectly affect the growth of the kelp. Even though pneumatocysts have lower photosynthetic rates than do the vegetative lateral blades on *E. menziesii* fronds (Henkel and Murray, 2007), they probably enhance the overall photosynthetic rate of a frond by holding it high in the water column (Fig. 1.8) where photon flux density is greater than at depth (e.g. Rohde *et al.*, 2008; Colvard *et al.*, 2014). Furthermore, buoyant seaweeds in dense aggregations encounter more light than do non-buoyant individuals (Stewart *et al.*, 2007). The flexibility of fronds that allows them to be moved around relative to each other by turbulent

waves, coupled with the buoyancy of fronds with pneumatocysts, permits *E. menziesii* to have numerous fronds and to grow in dense aggregations near other individuals without their fronds being continuously shaded by neighboring fronds. Koehl and Alberte (1988) found that motions of ruffled blades of the kelp *Nereocystis luekeana* in flowing water reduced self-shading, thereby enhancing photosynthetic rate. Growing in dense aggregations also reduces the hydrodynamic forces that the individual kelp or fronds experience in waves or currents (Holbrook *et al.*, 1991; Johnson, 2001; Stewart *et al.*, 2007), suggesting that any increase in drag from pneumatocysts on an individual frond may be counteracted by the fronds growing in dense aggregations.

1.4.3. Interaction of flexibility and buoyancy

Flexibility reduces hydrodynamic forces on seaweeds by allowing them to "go with the flow" in waves and to be bent over parallel to ambient water flow and reconfigured into streamlined shapes, whereas buoyancy enables them to hold photosynthesizing tissues high in the water column. The reduction in drag that flexibility provides and the effect that buoyancy has on drag depend on the flow regime and the size of the seaweed. In wave-driven flow, a flexible seaweed that is buoyant is able to reconfigure with the oncoming wave and then rebound to an upright posture when the flow slows. If a seaweed is short relative to the distance that the water travels in each wave before it reverses direction, then the seaweed fully reconfigures in the flow and is exposed to a period of unidirectional flow relative to its surfaces, similar to seaweeds that are exposed to unidirectional currents. In unidirectional flow, the buoyancy of a flexible body attached to a surface resists the body's ability to be bent over by the current, which can lead to higher drag than if it were not buoyant (as was measured for individual pneumatocysts, Fig. 1.5). Buoyant seaweeds that are short (length << distance of water travel in a wave) and that live in habitats exposed to waves, such as *T. ornata*, can experience a similar buoyancy-induced increase in drag compared with non-buoyant seaweeds (Stewart 2006a). In contrast, for long seaweeds such as *E. menziesii* that can move with the flow for most or all of a wave cycle, the penalty of increased hydrodynamic force due to buoyancy is very small. Waves must move water greater distances (i.e. must have longer periods and higher peak velocities) to expose long seaweeds to the drag penalty of buoyancy than to subject short seaweeds to that penalty. For example, in the present study *E. menziesii* moved at 17% of the ambient water velocity, such that the waves would have to move water more than 8 m for a 1.5 m frond to be fully reconfigured in the flow (Fig. 1.9A). Thus, long buoyant kelp can avoid a buoyancy-induced drag penalty in habitats exposed to larger waves than can short seaweeds.

The variation in pneumatocyst size, number, and location on the fronds of *E. menziesii*, as well as the variation that occurs across other seaweed taxa, show that there are many ways in which flexibility and buoyancy interact to enable seaweeds to grow to large sizes. *E. menziesii* is one of the longest and largest kelp growing in the wave-swept rocky intertidal zone, and its thallus, including the pneumatocysts, must tolerate a wide range of abiotic and biotic stressors that can negatively affect the kelp. The prominence of *E. menziesii* in this habitat suggests that the structure of the kelp, from the size of its flexible fronds to the buoyancy of its pneumatocysts and stiffness of their petioles, is a highly effective strategy for surviving turbulent hydrodynamic conditions of waves while also being large enough to outcompete other seaweeds for light and space.
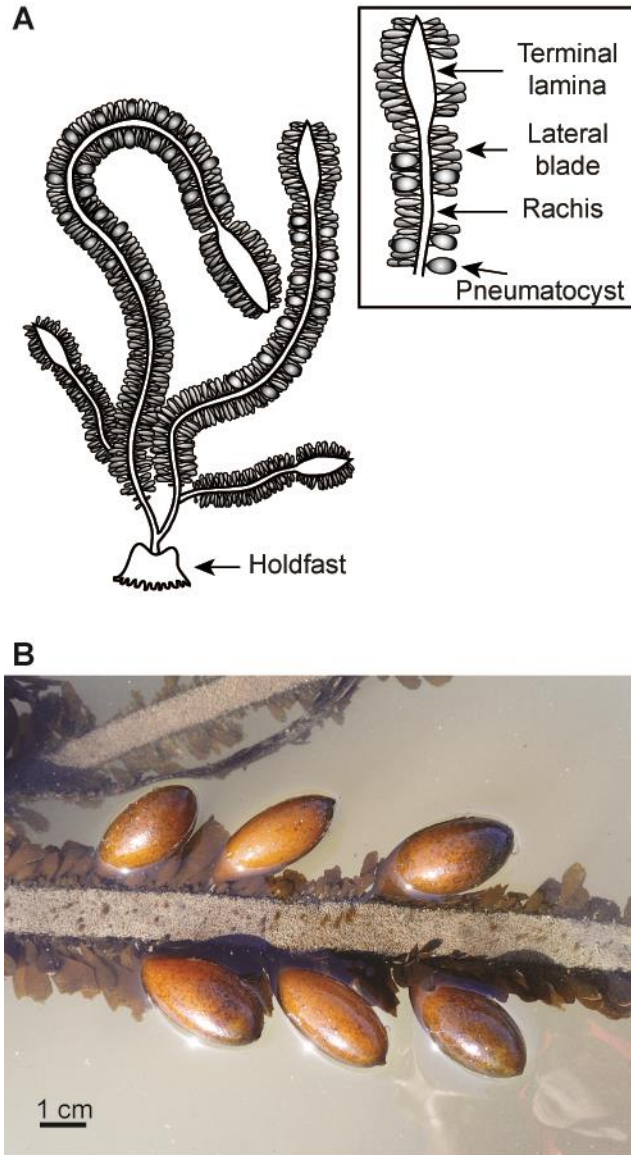
Figure 1.1: (a) Anatomy of an *Egregia menziesii* sporophyte. Individual fronds on the kelp are strap-like and can grow to more than 3 m in length. (b) Each frond's rachis bears lateral blades and ellipsoidal pneumatocysts along both edges.
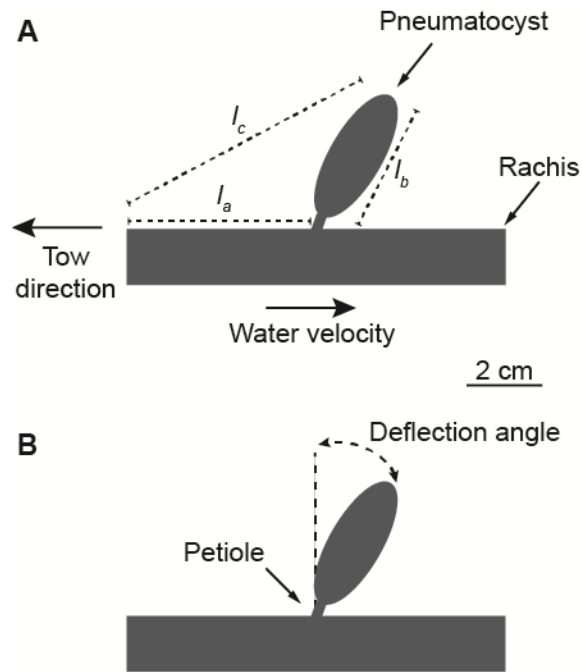
Figure 1.2: Diagram of a pneumatocyst attached to a rachis from which the lateral blades have been removed. The frond is towed from right to left, so the water flow relative to the frond is from left to right. (A) Distances (l_a, l_b, l_c) between three points on the frond and pneumatocyst. (B) Deflection angle of the pneumatocyst, calculated using equation (1.1), measures how far the pneumatocyst re-oriented in flowing water from an orientation perpendicular to the edge of the rachis.
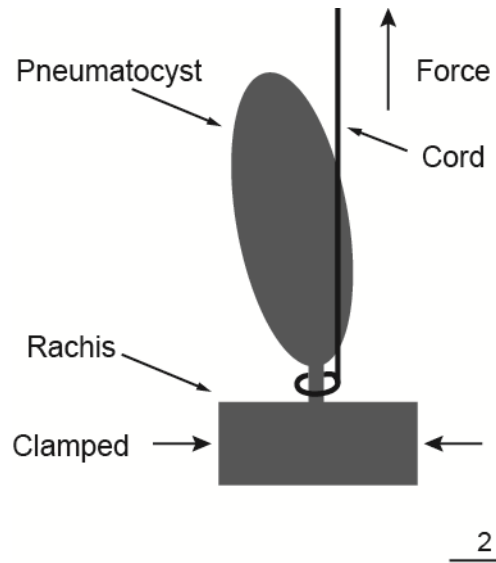
Figure 1.3: The force to break a pneumatocyst from the frond was measured by tying a nylon cord around the pneumatocyst's petiole and clamping the frond in the Instron materials-testing machine. The cord was then pulled vertically, while measuring the force on the pneumatocyst, until the pneumatocyst broke from the frond.

Figure 1.4: (A) Pneumatocyst density (number of pneumatocysts per length of frond) of the float-bearing fronds on *E. menziesii* at three sites, sampled in winter (white bars) and the

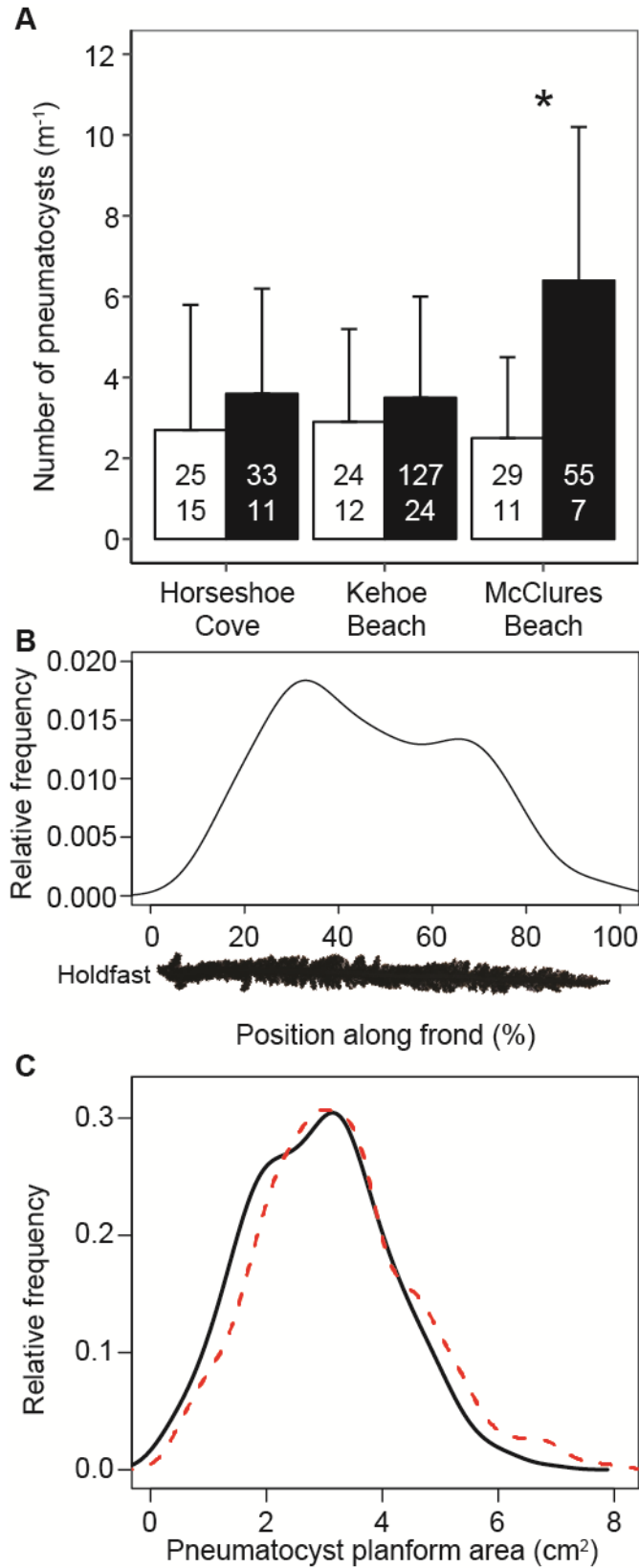following summer (black bars). Error bars indicate 1 SD. There was a significant difference (indicated by an asterisk) between seasons for the MC site (Mann-Whitney U test, $P < 0.05$), but not for the other sites. The top value in each bar indicates the number of fronds measured, and the bottom value indicates the number of individual kelp whose fronds were measured. (B) Relative frequency of the locations of pneumatocysts along the length of fronds at Miwok Beach, where 0% indicates the proximal part of the frond nearest the holdfast, and 100% indicates the tip of the frond (n = 155 pneumatocysts from 34 individuals). Pneumatocyst location is reported as a percent to standardize among fronds of different lengths. In the separate survey at Horseshoe Cove and Miwok Beach, the median distance from the base of the most proximal pneumatocysts on fronds was 32% of the frond length, and the median distance of the most distal pneumatocysts was 65% of the frond length (n = 52). (C) Relative frequency of pneumatocyst size (planform area) at Miwok Beach (black, solid line) and McClures Beach (red, dashed line). At McClures Beach, the median pneumatocyst size was 3.11 cm^2 (range = 0.39 to 8.02, n = 839), and at Miwok Beach, the median pneumatocyst size was 2.93 cm^2 (range = 0.15 to 6.89, n = 409).
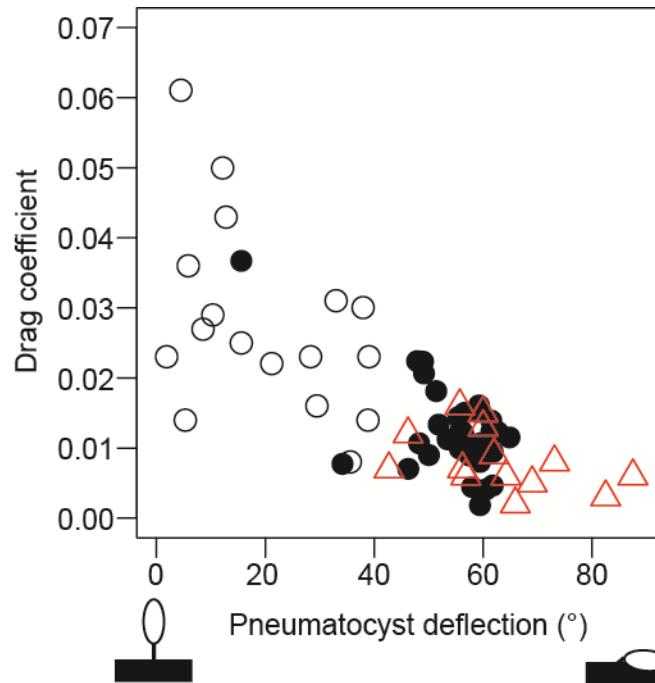
Figure 1.5: Drag coefficients (eqn. 1.2) of pneumatocysts were negatively correlated with pneumatocyst deflection (eqn. 1.1, Fig. 1.2B) in moving water (linear regression, $y = -0.0004x + 0.0360$, $P < 0.005$, $r^2 = 0.56$). Open circles indicate pneumatocysts that were positively buoyant with stiffened petioles, closed circles indicate pneumatocysts that were positively buoyant with flexible petioles (i.e. unmanipulated), and red open triangles indicate pneumatocysts that were neutrally buoyant with flexible petioles.
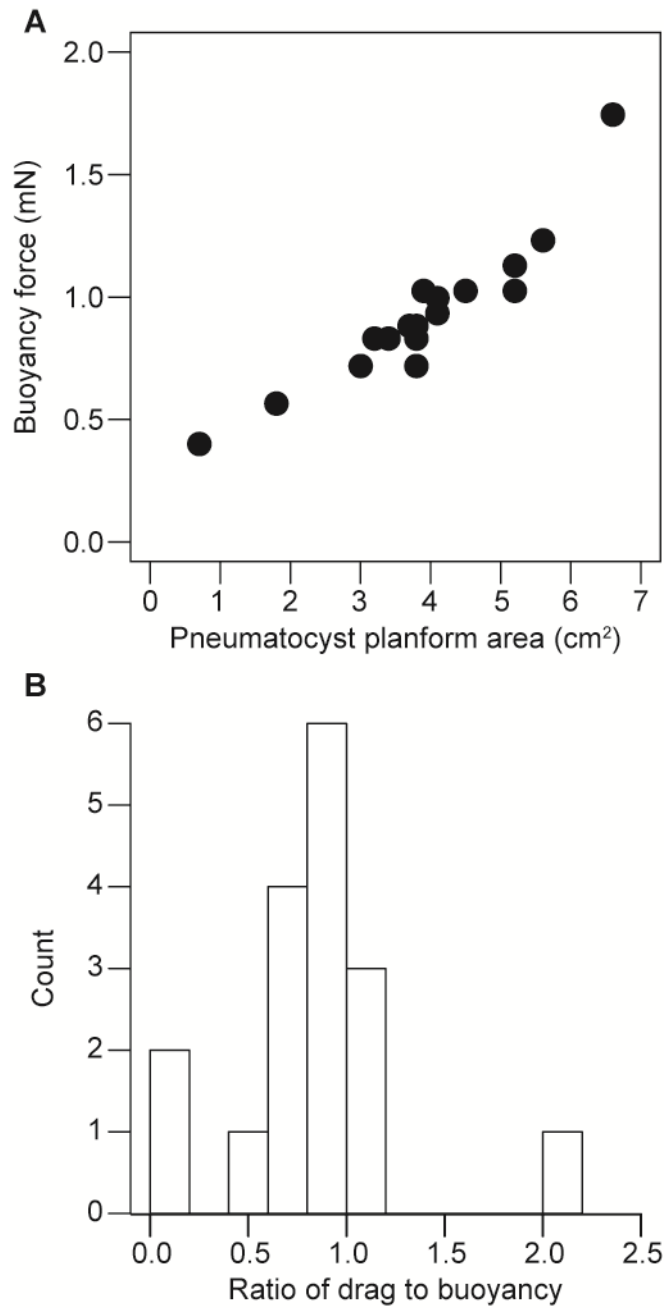
Figure 1.6: (A) Buoyancy of pneumatocysts was positively correlated to the planform area of the pneumatocysts (linear regression, $y = 0.198x + 0.156$, $P < 0.005$, $r^2 = 0.86$). (B) The number of pneumatocysts towed at a mean velocity of 0.58 m s^{-1} (SD = 0.03, n = 17) that had different ratios of drag to buoyancy (median = 0.91, minimum = 0.13, maximum = 2.03).
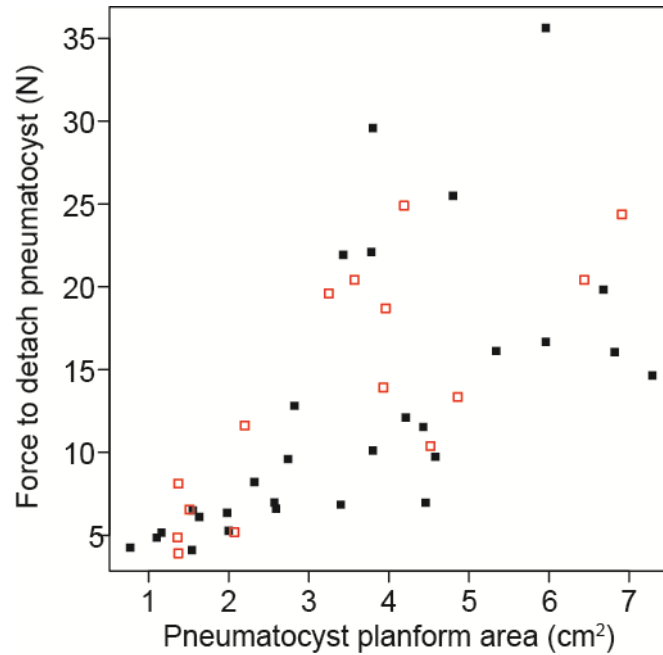
Figure 1.7: The force to remove a pneumatocyst from a frond was positively correlated to the size of the pneumatocyst (linear regression, $y = 2.88x + 2.75$, $P < 0.005$, $r^2 = 0.48$). Filled black squares are pneumatocysts from the moderately wave-exposed site, Miwok Beach, and open red squares are pneumatocysts from the wave-exposed site, McClures Beach.
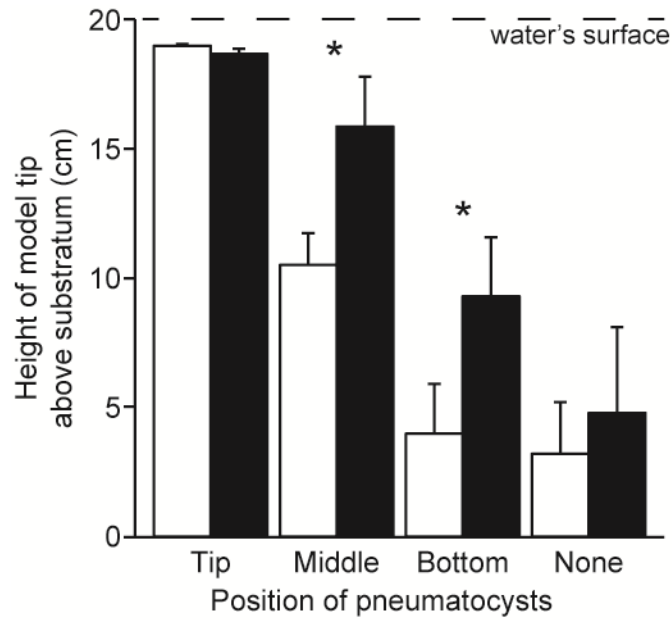
Figure 1.8: Mean height of the tip above the substratum of physical models of fronds with pneumatocysts located at the tip, middle, or base of the frond, or with no pneumatocysts. White bars are for models in the slow, low-frequency waves, and black bars are for models in the fast, high-frequency waves (error bars show 1 SD, n = 5 frond models). Asterisks indicate models whose mean heights were significantly affected by the wave setting (Mann-Whitney *U* tests, *P* < 0.05).
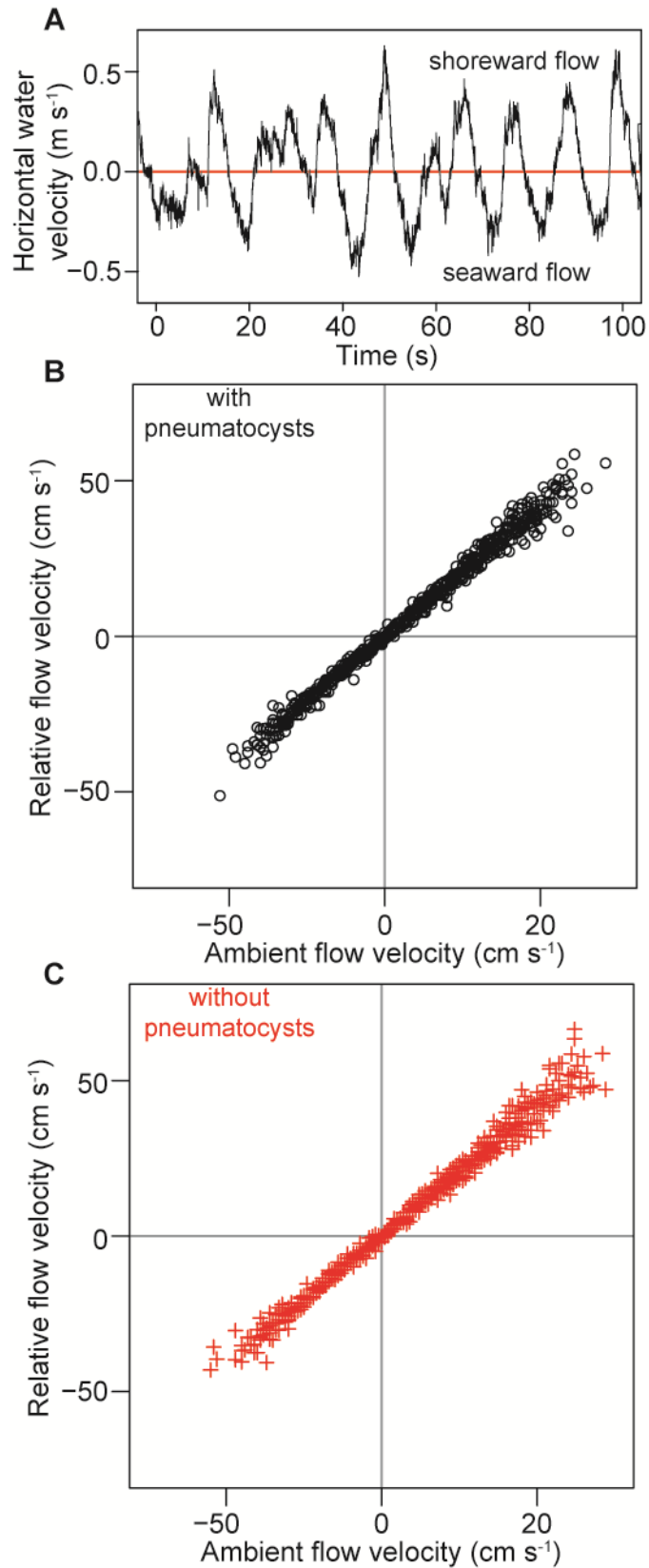
Figure 1.9: (A) Horizontal velocity plotted as a function of time for the back-and-forth flow of waves in a surge channel. Velocities above the red line indicate shoreward flow and velocities

below the red line indicate seaward flow. (B) Instantaneous water flow velocities relative to the tips of fronds with pneumatocysts (data for 7 fronds pooled) plotted at a function of instantaneous ambient flow velocity (rounded to the nearest 1 cm s^{-1}). (C) Instantaneous flow velocities relative to fronds without pneumatocysts (data for 7 fronds pooled) plotted at a function of instantaneous ambient flow velocity. There were no differences in the relative flow velocities for fronds with and without pneumatocysts across the range of ambient flow velocities measured (analysis of covariance, $P > 0.05$, covariate = ambient flow velocity, factor = presence of pneumatocysts). All frond tips experienced instantaneous water velocities relative to their surfaces that were 82 to 83% of the instantaneous ambient flow velocity (linear regression for fronds with pneumatocysts, $y = 0.83x - 0.01$, $P < 0.005$, $r^2 = 0.99$; linear regression for fronds without pneumatocysts, $y = 0.82x + 0.25$, $P < 0.005$, $r^2 = 0.99$).
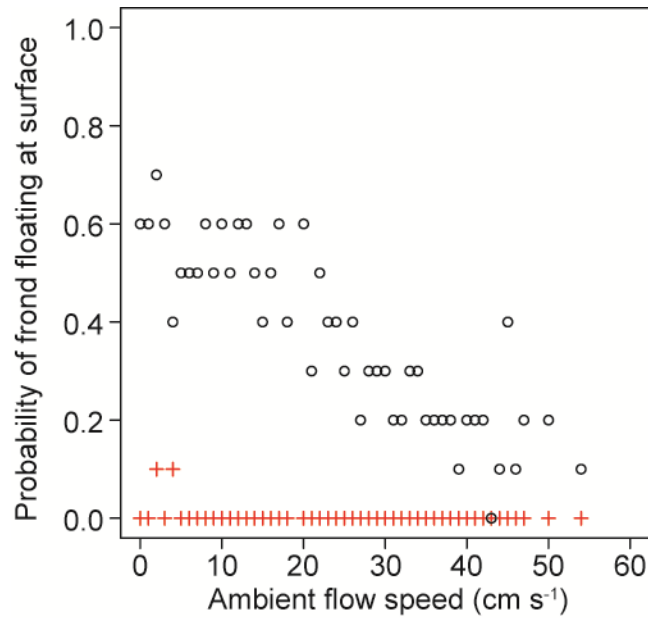
Figure 1.10: Probability of fronds floating at the water's surface (i.e. air-water interface) at instantaneous ambient flow speeds from 0 to 54 cm s^{-1}. Open circles are fronds with pneumatocysts and red crosses are fronds without pneumatocysts. The probability of floating for fronds with pneumatocysts was negatively correlated to ambient flow speed (linear regression, $y = -0.01x + 0.62$, $P < 0.005$, $r^2 = 0.76$).

Site	Season	Kelp sampled	Length of fronds with pneumatocysts (cm) (mean ± SD; fronds sampled)	Length of fronds without pneumatocysts (cm) (mean ± SD; fronds sampled)	Pneumatocyst abundance (m^{-1}) (mean ± SD)
Horseshoe Cove	Winter	26	89 ± 37; 25	42 ± 31; 214	2.7 ± 3.1
	Summary	22	91 ± 43; 33	41 ± 35; 279	3.6 ± 2.6
Miwok Beach	Winter	19	96 ± 41; 26	42 ± 36; 163	2.4 ± 1.5
Kehoe Beach	Winter	21	94 ± 33; 24	45 ± 39; 213	2.9 ± 2.3
	Summer	24	142 ± 66; 127	57 ± 64; 205	3.5 ± 2.5
McClures Beach	Winter	24	105 ± 45; 29	42 ± 29; 277	2.5 ± 2.0
	Summer	8	119 ± 82; 55	53 ± 53; 57	6.4 ± 3.8

Table 1.1: Lengths of fronds with and without pneumatocysts, and abundance of pneumatocysts on fronds (calculated only for fronds with pneumatocysts) over two seasons at four sites: Horseshoe Cove and Miwok Beach (moderately wave-exposed); Kehoe Beach and McClures Beach (wave-exposed).

Chapter 2: Knots and tangles weaken kelp fronds while increasing drag forces and herbivore loads on the kelp

2.1 INTRODUCTION

Ocean waves in shallow coastal areas impose hydrodynamic forces on the bottom-dwelling organisms in those habitats. Many attached organisms have morphologies that reduce hydrodynamic forces or have life cycles that enable them to live in habitats exposed to seasonal periods of rapid water motion (Koehl, 1999; Wolcott, 2007; Martone *et al.*, 2012; de Bettignies *et al.*, 2013). Kelp, which are among the largest sessile organisms occurring on wave-swept shores (Abbott and Hollenberg, 1976), provide habitat and food to a diversity of other organisms in these ecosystems (Graham, 2004; Norderhaug *et al.*, 2007; Christie et al., 2009). Large kelp often have flexible stipes or fronds that allow the kelp to move passively with the water flowing back and forth during each wave (Abbott and Hollenberg, 1976). By "going with the flow," long flexible kelp experience little water motion *relative* to their surfaces, and thus experience low hydrodynamic forces (Koehl, 1984, 1999). However, the back-and-forth water motion of waves can cause flexible kelp to become tangled or knotted (Meluzzi *et al.*, 2010) (Fig. 2.1). Although tangled kelp that live only one season were more likely to be broken and washed ashore than untangled kelp (Koehl and Wainwright, 1977), the effects of knots and tangles on the biomechanical performance of species of kelp that live more than one year have not been explored, nor have the effects of tangles on the assemblages of animals living on kelp.

Here, I investigate these issues using the feather boa kelp, *Egregia menziesii* (Fig. 2.1), which are abundant on wave-swept rocky shores of the west coast of North America (Abbott and Hollenberg, 1976). An individual *E. menziesii* bears many long fronds (Fig. 2.2). I studied how knots and tangles affected hydrodynamic forces on fronds, strength of fronds, assemblages of animals living on kelp, and herbivore-inflicted damage to fronds and their consequent weakening and healing. I related these biomechanical consequences of knots and tangles to temporal patterns of kelp size, knotting, and breakage measured in the field.

2.2 METHODS

2.2.1 Field sites

Collection for experiments and surveys of *Egregia menziesii* were made at sites along a 26-km range of northern California coastline between May 2015 and August 2016 (Fig. S1.1). Two wave-exposed sites were located in the Point Reyes National Seashore (CA, USA): Kehoe Beach (KB; 38°9'56.08" N, 122°57'6.04" W) and McClures Beach (MC; 38°11'2.70" N, 122°58'2.33" W). Two moderately wave-exposed sites were located near Bodega (CA, USA): Horseshoe Cove (HC; 38°18'47.55" N, 123°4'13.78" W) in the Bodega Head Marine Reserve (Bodega, California, USA), and Miwok Beach (MW; 38°21'53.10" N, 123°4'15.90" W) in the Sonoma Coast State Beach (Bodega, California, USA).

2.2.2 Hydrodynamic forces on knotted fronds

I tested whether overhand knots increased the drag on fronds in moving water. Drag is the hydrodynamic force acting parallel to the direction of water movement relative to a body (Vogel, 1994). Drag measurements were made by towing intact fronds (frond length range = 0.5 to 1.2 m) with a stepping motor at a constant velocity through still water in a tank (2.5 x 0.2 x 0.2

m). Each frond was towed at only one velocity (0.3, 0.4, 0.5, 0.6 or 1.0 m s⁻1), which was in the range of ambient water velocities experienced by the kelp (Friedland and Denny, 1995; Gaylord *et al.*, 2008). These towing velocities corresponded to Reynolds numbers ranging from 3.5 x 10^3 to 9.5 x 10^3, where the Reynolds number is the ratio of inertial forces to viscous forces, given by the formula:

$$Re = \frac{u\,l}{v}$$

(eqn. 2.1)

where u is the water velocity relative to the frond, l is a characteristic length scale, and v is the kinematic viscosity of the water (Vogel, 1994). Here, I used the rachis width as the characteristic length scale. A spring scale (Ohaus Models 8001-MN, 8261-M, 8263-M, Ohaus, Pine Brook, NJ) recorded the maximum force with which the frond resisted the movement through the water (Bell and Denny, 1994). Three replicate measurements of drag forces were made at the tow velocity for each unknotted frond. Then each frond was tied into an overhand knot and three replicate measurements of drag were made at the same velocity. The overhand knot was always positioned in the middle of each frond. Each frond was photographed prior to testing, and projected planform area was calculated using ImageJ software (National Institutes of Health, version 1.49b).

　　　The drag force on an object is determined, in part, by the object's shape, as indicated by the drag coefficient, C_D (Vogel, 1994). I calculated C_D for fronds in their knotted and unknotted configurations:

$$C_D = \frac{2F}{u^2 \rho A}$$

(eqn. 2.2)

where F was the measured drag force, u was the tow velocity, ρ was the density of the freshwater in the tow tank at 20 °C (1000 kg m⁻³, Vogel, 1994), and A was the projected planform area of the frond in its unknotted configuration.

2.2.3 Breakage of knotted fronds

　　　I tested whether knots reduced the force required to break a frond in tension. I compared the force required to break knotted sections of frond with the force required to break adjacent unknotted sections of the same frond. In December 2015, unwounded fronds that were at least 1 m in length were haphazardly collected from kelp at MC and MW, and transported to the University of California, Berkeley for testing. A model 5844 Instron (Norwood, MA, USA) materials-testing machine was used to measure the maximum tensile force required to break sections of the fronds 25 cm in length that were unknotted or tied into overhand knots (Fig. 2.1A). Overhand knots were chosen because they are the simplest knot to tie[4] and were the most common knot formed by single *E. menziesii* fronds in the field. Immediately after collection, fronds were placed in a covered container with their residual sea water. Fronds were kept in air, inside the covered container, between 4 and 10°C until testing and were measured within 12 hours of collection. For each frond, no more than 15 minutes elapsed between being removed from storage and being measured. Preliminary experiments showed no difference in breaking

force between kelp that were measured after 12 hours at 4°C and separate kelp that were measured immediately after collection (Mann-Whitney U test, $P > 0.05$, n = 5 for each time period). The fronds of *E. menziesii* have an intercalary meristem (Fig. 2.2C), such that frond tissue distal to the holdfast is younger and weaker than frond tissue proximal to the holdfast (Abbott and Hollenberg, 1976; Demes *et al.*, 2013; Krumhansl *et al.*, 2015). To control for the effects of aging on the strength of the unknotted frond tissue, the unknotted breaking force of each frond was calculated as the mean of the breaking forces for unknotted tissues immediately distal and proximal to the frond tissue used for the knotted measurement (Fig. 2.2C). Samples were blotted dry with a paper towel and secured in the materials-testing machine by gluing paper towels to the ends of the fronds with cyanoacrylate glue and placing the paper towel-covered ends into specimen grips of the Instron.

Frond specimens were stretched at a strain rate of 0.2 min^{-1} (strain rate = change in length of specimen per unit time, divided by the initial length of the specimen between the grips of the Instron). Previous *in situ* measurements of hydrodynamic forces on *E. menziesii* (Gaylord *et al.*, 2008) showed that forces on the kelp can increase at an instantaneous rate of more than 10 N s^{-1} when a wave breaks on the kelp (i.e. wave impingement) and approximately 1 N s^{-1} after the wave breaks (i.e. wave surge). Wave impingement occurs only during a brief time point in each wave cycle, whereas wave surge occurs during the remainder of the wave cycle (Gaylord, 1999). Preliminary measurements of the forces in fronds when pulled at a range of strain rates allowed me to determine a range of strain rates (between 0.20 min^{-1} and 0.89 min^{-1}) that spanned those experienced by *E. menziesii* in the field.   I found that the breaking force of *E. menziesii* fronds was independent of strain rate between 0.20 min^{-1} and 0.89 min^{-1} (linear regression analysis, $P > 0.05$). Therefore, I used a strain rate of 0.2 min^{-1} to measure breaking forces of knotted versus unknotted fronds under the conditions of wave surge. The strain rates of knotted samples were based on the total length (included the length of frond that was tied into a knot) of the specimen between the grips of the Instron.

2.2.4 Frond configuration and epifaunal communities

I investigated whether tangled and untangled fronds of *E. menziesii* had different structural characteristics (i.e. wounds, lateral blades, Fig. 2.3C,D) and epifaunal loads. From September to December 2015, I collected tangled fronds from MC and MW. I also haphazardly collected untangled fronds that were adjacent to the collected tangled fronds. Comparing the tangled fronds with adjacent fronds that were untangled allowed me to control for local environmental factors beyond frond configuration that could have influenced a frond's structure and epifauna (e.g. temperature, light, water motion, rock topography). Fronds and their epibiota were collected and immediately bagged and preserved with 45% isopropyl alcohol. Fronds were brought to the laboratory where they were untangled and all macrofauna were removed.

I measured morphological features and quantified epifauna on the collected fronds. The lengths of the fronds from each collection were measured to the nearest 1 cm. Small lateral blades generally border the edges of *E. menziesii* fronds (Fig. 2.2C), but can be removed by processes such as abrasion and herbivory. I rated the abundance of lateral blades on each frond (0 = none, 1 = lateral blades on less than half the length of the frond, or 2 = lateral blades on at least half the length of the frond; Fig. 2.3C). The total "bushiness" of each group of tangled or untangled fronds was calculated as the sum of these lateral blade scores, divided by the total length of the fronds in that group. I also counted the number of discrete wounds on each frond. Many of the wounds were obviously caused by herbivory, while the cause of damage for other

wounds was difficult to distinguish (e.g. herbivory vs. abrasion on rocks). Epifauna in each collection were separated into taxonomic groups (gammarid amphipods, isopods *Idotea* spp., kelp crab *Pugettia producta*, barnacles, mussels *Mytilus* spp., limpets *Lottia* spp., and littorinid snails), photographed, and counted. The total dry weight of each epifaunal group on each set of fronds was determined to the nearest 0.0001 g (Mettler Toledo AG245, Mettler Toledo, Columbus, OH) after drying them to a constant weight in a drying oven at 60°C.

2.2.5 Weakening of fronds by herbivore damage

Many of the epifauna found on fronds, either tangled or untangled, were herbivores that wounded the frond tissue. I measured the breaking forces of fronds that had herbivore damage using the materials-testing machine described above. Undamaged fronds were collected from MC and MW from October to December 2015. I inflicted a wound that was similar in size and shape to the wounds on the fronds that were caused by amphipods (Fig. 2.3D). I measured the force required to break a section of a frond with mimicked damage and the force to break unwounded sections of the same frond (the average breaking force of unwounded tissue distal and proximal to the wounded section of the frond, Fig. 2.2C). Sample preparation and measurement protocols were the same as described for breakage of knotted fronds.

2.2.6 Prevalence of knots and tangles

The sites were visited approximately once per month when the tidal heights were between -0.4 and 0.1 m relative to MLLW. At each site, kelp were surveyed along a horizontal transect that spanned the full range of microhabitats (e.g. surge channel, rocky bench, boulder), selecting every third kelp that was encountered. Kelp were selected if they were mature sporophytes (i.e. Type IV sporophytes *sensu* Henkel and Murray, 2007) and had stipes that were distinguishable from those of other individuals. The lengths of all fronds on the selected kelp were measured to the nearest 1 cm, and the presence of any knotted or tangled fronds was noted. When a knotted frond was encountered, I measured the length of the frond as the distance between the distal and proximal ends of the frond in its knotted configuration. I also measured the distance of the knot from the proximal end of the frond to the nearest 1 cm. Kelp with tangled fronds were untangled to measure frond lengths to the nearest 1 cm. A subset of the surveyed kelp were also marked with nylon paracord and a 2.5 x 2.5 cm acrylic identification tag. Tagged kelp were surveyed again on subsequent months and the total frond lengths were compared with those of tagged untangled kelp over the same time period and at the same sites.

I define each season as three whole months, i.e. spring = March-May; summer = June-September; autumn = August-November; winter = December-February.

2.3 RESULTS

2.3.1 Hydrodynamic forces on knotted fronds

Overhand knots increase the drag coefficient of kelp fronds by 56% (paired *t*-test, $P < 0.0005$, df = 19, Fig. 2.2A). This effect was more pronounced for short fronds than for long fronds (Fig. 2.2B, Table 2.1). Drag coefficient did not vary with Reynolds number for either knotted or unknotted fronds (linear regressions, $P > 0.05$).

2.3.2 Breakage of knotted fronds

Sections of fronds tied into an overhand knot always broke at the entrance to the knot (arrow, Fig. 2.1A), and broke at forces that were on average 18% lower than those required to break an adjacent unknotted section from the same frond (Fig. 2.2C,D,E; Table 2.2).

2.3.3 Frond configuration and epifaunal communities

The most common animals found on the fronds were amphipods, kelp crabs, isopods, littorinid snails, and limpets, all of which eat kelp tissue. Suspension-feeding mussels and barnacles were also common. Tangled fronds had more amphipods (Fig. 2.3A), mussels, and kelp crabs than did untangled fronds, whereas untangled fronds had more littorinid snails than did tangled fronds (paired t-tests, $P < 0.05$, df = 15, Table 2.3). In contrast, there was no difference between tangled and untangled fronds in the abundances of the other types of animals tallied (paired t-tests, $P > 0.05$, df = 15). On both tangled and untangled fronds, amphipods that can burrow and consume tissue from inside the fronds (Sotka, 2007) occurred in greater numbers (paired t-test, $P < 0.05$, df = 31) and higher biomass than littorinid snails (paired t-test, $P < 0.05$, df = 31), which only browse the surfaces of the fronds. Not only did tangled fronds bear more herbivores than did untangled fronds, but those grazers were bigger: amphipods (paired t-test, $P < 0.05$, df = 14, Fig. 2.3B) and isopods (paired t-test, $P < 0.05$, df = 6) each had a greater average body mass on tangled fronds than on untangled fronds.

2.3.4 Weakening of fronds by herbivore damage

Grazers can damage fronds by removing the lateral blades (Fig. 2.3C) and by making wounds in the supportive rachis (Fig. 2.3D). Tangled fronds had fewer lateral blades (Fig. 2.3C) (paired t-test, $P < 0.05$, df = 10) and more wounds (Fig. 2.3D) per rachis length than did adjacent untangled fronds (Fig. 2.3E).

To test whether the rachis wounds I found on tangled fronds made the fronds weaker, I compared the strength of fronds with wounds like those made by amphipods (Fig. 2.3E) to that of unwounded fronds. Wounded sections of frond rachises broke at forces that were on average 31% lower than the forces required to break adjacent unwounded sections of rachis from the same fronds (Fig. 2.3F, Table 2.4).

2.3.5 Prevalence of knots and tangles

Surveys of *E. menziesii* in four intertidal habitats along the northern California coast revealed that knots and tangles were most abundant in the autumn (Fig. 2.4A), and that they formed on kelp whose mean frond lengths were at least 49 cm (n = 43). Knots frequently formed on the longest frond of a kelp (68.4% of knots, total n = 13 knotted longest fronds), and those fronds ranged in length from 1.24 to 3.59 m. However, the maximum frond length of a kelp was not a good predictor of whether or not the kelp had knotted fronds (logistic regression, $P = 0.081$, $X^2 = 3.042$, df = 1; Peng *et al.*, 2002). Tangles formed on kelp whose maximum frond lengths ranged from 1.17 to 5.50 m, but maximum frond length was not a good predictor of whether kelp had tangled fronds (logistic regression, $P = 0.21$, $X^2 = 1.576$, df = 1).

Kelp whose fronds were knotted or tangled experienced more frond breakage per time than did neighboring kelp without knots or tangles (Fig. 2.4B,C). Over a period of one month, beginning when knots were first observed, kelp with knotted fronds lost 21% of their size (median, range = 72% decrease to 51% increase), while, over the same time interval, kelp without knotted fronds increased their size by 3% (median; range = 58% decrease to 140% increase in size) (paired t-test, $P < 0.05$, df = 9). Similarly, kelp with tangled fronds lost more

frond tissue than kelp without tangled fronds over one month beginning when tangles were first observed (paired *t*-test, $P < 0.05$, df = 12). Kelp with tangled fronds lost 11% of their size (median, range = 92% decrease to 64% increase in size) while kelp without tangled fronds maintained their size during the same time interval (median = 0%, range = 71% decrease to 105% increase).

2.4 DISCUSSION

2.4.1 Hydrodynamic forces on and breakage of knotted fronds

Knotted fronds of *Egregia menziesii* experienced more hydrodynamic drag (Fig. 2.2A) and were weaker than unknotted fronds (Fig. 2.2C,D), suggesting that the water motion of ocean waves can make knotted kelp fronds break more easily than unknotted fronds. However, the cross-sectional shape of *E. menziesii* fronds (Fig. 2.2E) may have limited the weakening caused by knots. The weakening of knotted structures is thought to result from the curvature of the material within the knot and the mechanical stress (force per cross-sectional area of material) that the curvature puts on the material. When a structure is bent, the material on the inside of the curve experiences compression and the material on the outside of the curve experiences tension. If the tensile stress placed on the material on the outside edge of the curve exceeds the strength of the material, then the structure can break. The maximum stress (σ, the force per area) on a material that is bending under an applied force can be quantified by

$$\sigma = \frac{E\, y_{max}}{R}$$

(eqn. 2.3)

where E is the Young's modulus (stiffness) of the material, y_{max} is the maximum distance within the material's cross-section from the neutral axis, and R is the structure's radius of curvature (Wainwright *et al.*, 1976).

Structures with circular cross-sections can be weakened by up to 50% when tied into a knot (Pieranski *et al.*, 2001; Meluzzi *et al.*, 2010), whereas *E. menziesii*, with its ellipsoidal cross-sectional (Fig. 2.2E) was only weakened by 18% (median) up to a maximum of 28% (Fig. 2.2C,D). An ellipsoidal cross-section has a smaller y_{max} than does a circular cross-section of the same total area, and because y_{max} is proportional to the maximum stress, the ellipsoidal cross-section experiences smaller stresses than the circular cross-section for any given R (Gere and Timoshenko, 1997). Therefore, when bent inside a knot, the maximum stress in the frond is much less than if the frond had a circular cross-section. Considering both the increased hydrodynamic drag and weakening caused by knots, knotted fronds are expected to break more easily than unknotted fronds when exposed to moving water, but the initial large strength of *E. menziesii* fronds (Friedland and Denny, 1995) suggests that even knotted fronds should be able to withstand much of the water flow that the kelp regularly experiences in its habitat.

2.4.2 Frond configuration, epifaunal communities, and herbivory

Tangling was associated with an increase in the numbers and body sizes of herbivores living on the kelp. The herbivores, through feeding, caused structural damage to the fronds, most notably by decreasing the number of lateral blades (Table 2.3) and by directly wounding the frond's rachis (Fig. 2.3E). Losing lateral blades, which are responsible for much of the kelp's photosynthesis (Henkel and Murray, 2007), can impact the physiology of the kelp,

whereas the wounds to the rachis can cause the whole frond to break (Fig. 2.3F), also resulting in a loss of photosynthetic tissue. Thus, while the back-and-forth motion of waves can passively tie kelp fronds into knots and tangles that enhance the kelp's role as a source of habitat and food, it can ultimately lead to the breakage of kelp fronds and loss of that valuable kelp habitat from the intertidal ecosystem (e.g. Black, 1976).

2.4.3 Prevalence of knots and tangles

Through field surveys, I observed that knots and tangles formed on kelp with long fronds, and that they were more likely to occur in the autumn. The individual mechanisms of increased drag and reduced strength through knotting, and reduced strength through herbivore damage on tangled fronds, suggest that knotted and tangled fronds are likely to break from the force of waves before unknotted and untangled fronds. The change in thallus size of individual kelp, with and without knotted and tangled fronds, followed the predictions based on the biomechanical consequences of knotting and tangling described in this study: kelp whose fronds were tangled or knotted decreased in size while untangled, unknotted kelp did not (Fig. 2.4B,C).

The timing of knotted and tangled fronds on *E. menziesii* further suggests that these complex frond configurations are important in the perennial life cycle of the kelp. Though knotted and tangled fronds were observed in every season of the year, they were most common in the autumn, which is also when the kelp will have the longest fronds and largest total size (Black, 1974). By becoming knotted and tangled in the autumn, the kelp can decrease in size just before the arrival of the large ocean waves that are typical of winter storms. A decrease in the total number and length of fronds will decrease the magnitude of hydrodynamic drag that an individual kelp's holdfast experiences, and therefore reduces the risk that the entire kelp will be dislodged from the substratum (Wolcott, 2007). Surviving the large waves of winter is an important process for perennial seaweeds, especially those that grow to large sizes.   Large reductions in size for kelp, especially *E. menziesii*, are not problematic because their fast growth rates allow them to quickly reach large sizes in the spring and summer (Black, 1974), providing habitat and food to much of the surrounding biological community (Hughes, 2010). Previous studies have described the various ways in which large seaweeds undergo decreases in body size before winter, such as herbivory-induced breakage (Black 1976; de Bettignies *et al.*, 2012), inherently weak fronds (Demes *et al.*, 2013), and the timing of reproductive tissue formation (Wolcott, 2007).

Here I show how frond breakage and a decrease in kelp size are caused by turbulent water motion that ties the kelp fronds into knots and tangles. I described the specific biomechanical and ecological mechanisms by which breakage of knotted, tangled fronds occurs, and I monitored *E. menziesii* in the field to test whether the mechanisms identified in the laboratory studies agree with what happens to real kelp.
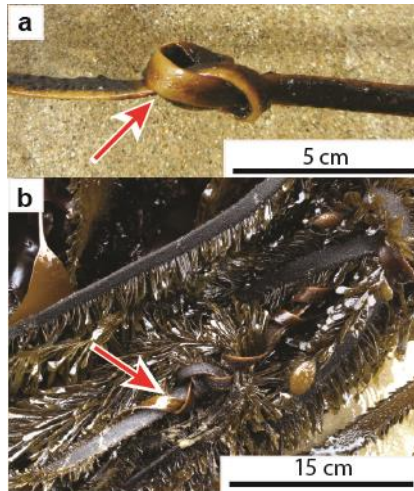
Figure 2.1: Fronds of the kelp *Egregia menziesii* tied into complex configurations. (A) Knots are formed in a single frond, whereas (B) tangles are formed by multiple fronds. The knot and tangle are indicated by the arrow in the respective photographs.
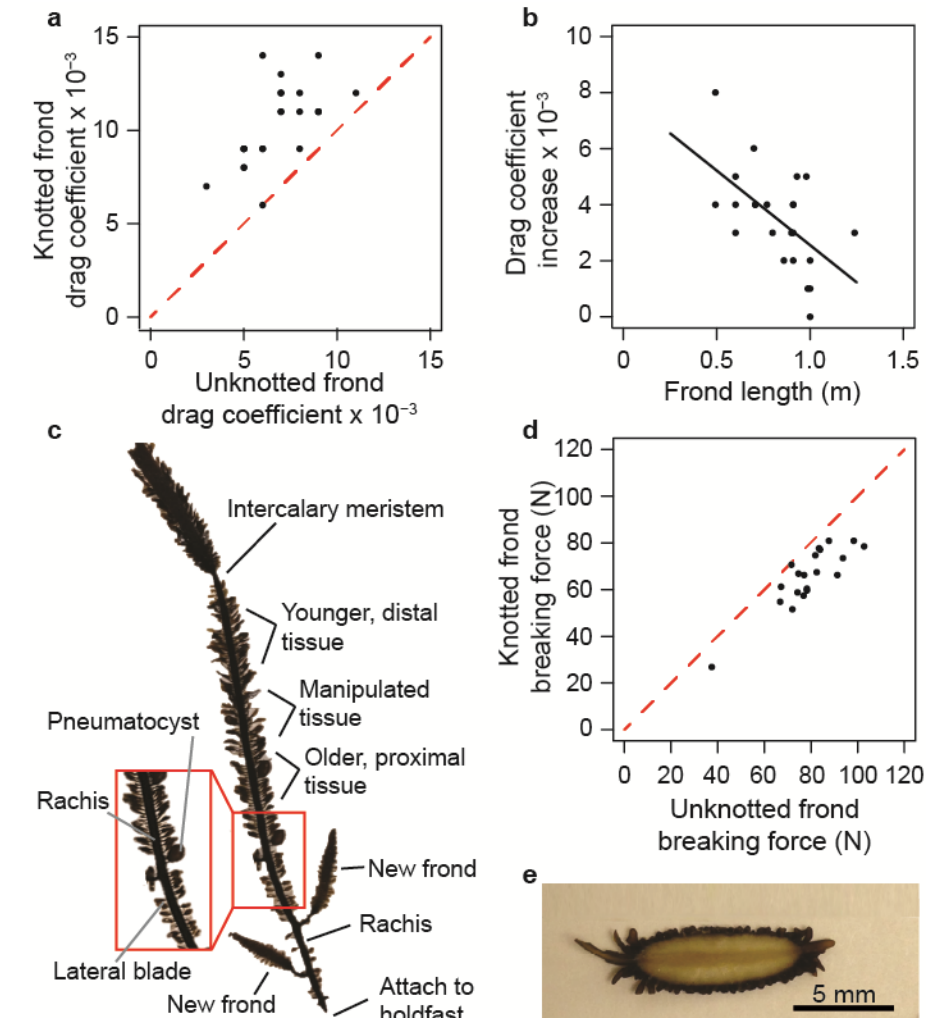
Figure 2.2: Effects of being tied into a knot for kelp fronds. (A) Drag coefficients of fronds were greater when fronds were tied into a knot than when the same fronds were unknotted (paired *t*-test, $P < 0.0005$, df = 19). Slope of dashed line = 1, thus all points above the line indicate an increased drag coefficient for knotted fronds, whereas points below the line show a decrease. (B) Knots had a larger effect on the drag of short fronds than of long fronds (linear regression: $y = -5.2x + 8.0$, $P < 0.005$, $r^2 = 0.34$). (C) The anatomy and relative age of regions of a frond of *E. menziesii*. Measurements of the breaking force can be affected by the tissue age, thus I compared the breaking force of one section of frond (knotted) to that of the breaking force of both younger and older sections. (D) Knotted sections of frond broke with 18.1% lower forces than unknotted sections of the same frond (paired *t*-test, $P < 0.0005$, df = 19). (E) Ellipsoidal cross-section of rachis.
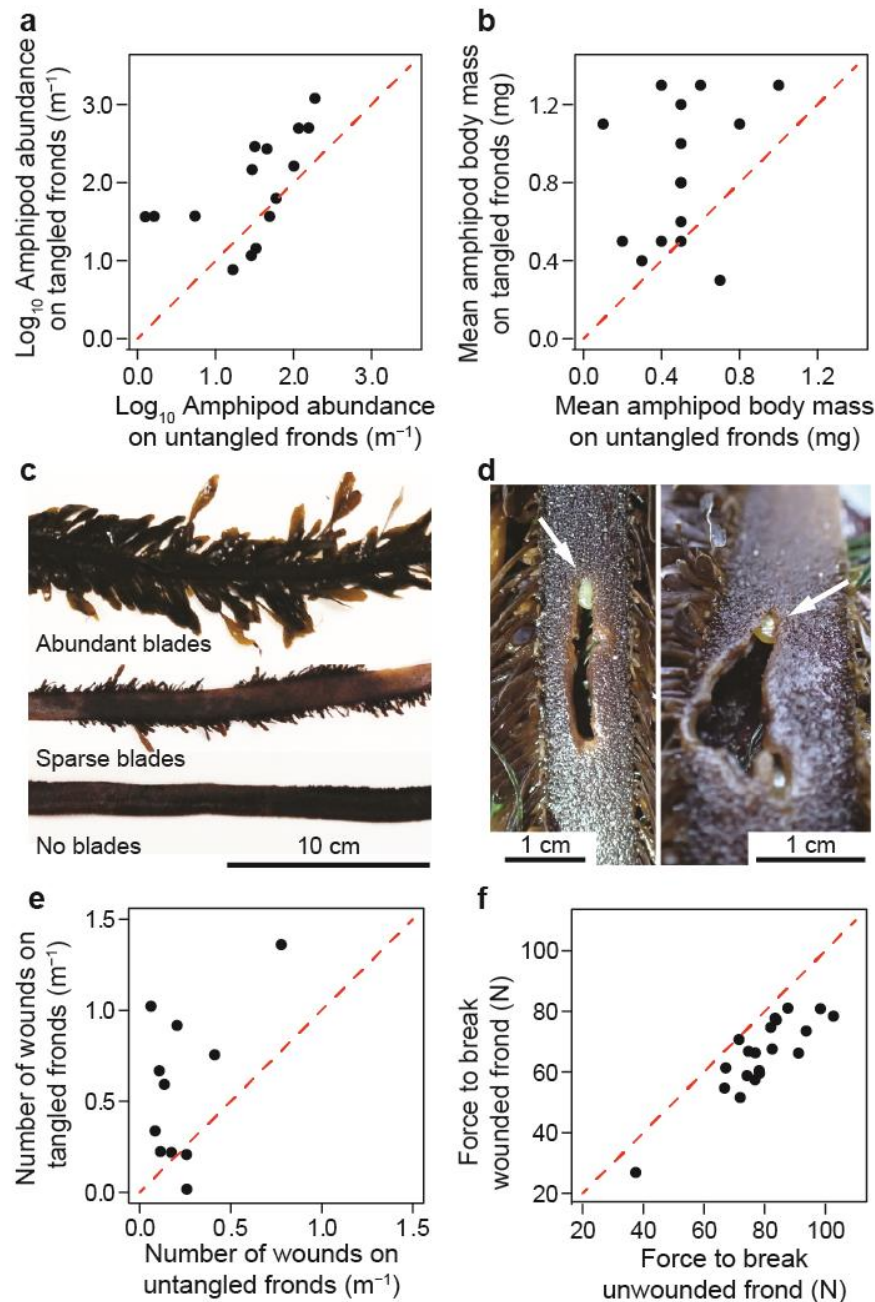
Figure 2.3: Effects of being tangled for kelp fronds. (A) Tangled fronds had more amphipods per frond length (individuals m^{-1}) than did neighboring, untangled fronds (paired t-test, $P < 0.05$, df = 15). Maximum abundance of amphipods on tangled fronds was 1,207 inidividuals m^{-1}, and 188 individuals m^{-1} on untangled fronds. Dashed lines show a slope = 1, similar to Fig. 2.2A,D. (B) Tangled fronds had bigger amphipods (mean dried weight per amphipod) than did untangled fronds (paired t-test, $P < 0.05$, df = 14). (C) Example of different abundances of lateral blades on frond. (D) Example of wounds caused by amphipods (white arrows) burrowing into and feeding on fronds. (E) Tangled fronds had more wounds than did untangled fronds (paired t-test, $P < 0.05$, df = 10). (F) Wounds mimicking damage from amphipods made fronds break at a 31.4% lower force than unwounded frond tissue from the same frond (paired t-test, $P < 0.05$, df = 15). I controlled for the tissue age as described in Fig. 2.2C.
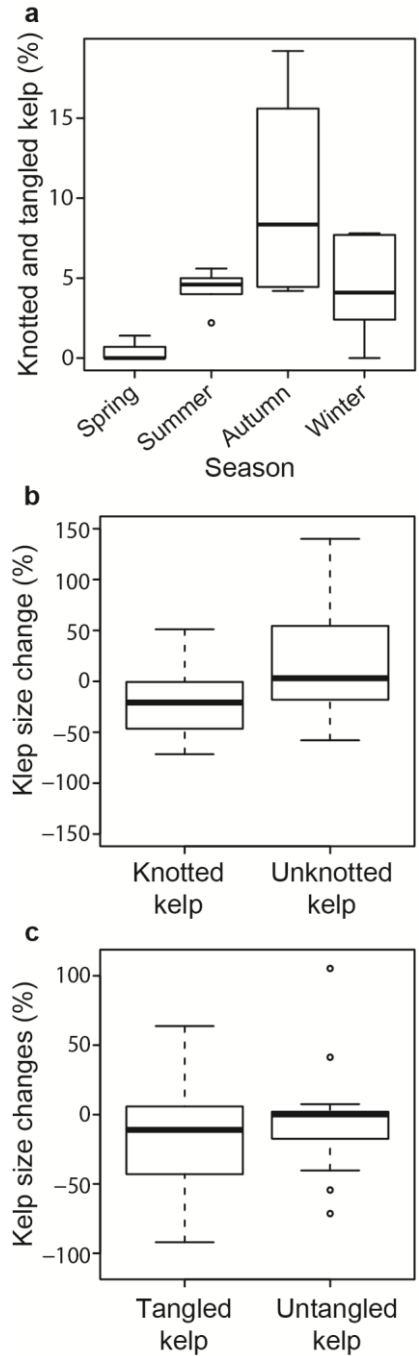
Figure 2.4: Seasonality of knotting and tangling, and the consequences for kelp. (A) Kelp with knotted or tangled fronds were most common in autumn (median = 8.4%, n = 4) and least common in spring (median = 0.0%, n = 4). Each sample is the mean of two sites per month. Change in kelp size over one month for kelp with knotted fronds versus kelp without knotted fronds (B) and kelp with tangled fronds versus kelp without tangled fronds (C).

Frond	Projected planform area (m²)	Length (m)	Mean unknotted drag coefficient	Mean knotted drag coefficient
1	0.061	1.24	0.005	0.008
2	0.025	0.93	0.009	0.014
3	0.022	0.98	0.007	0.012
4	0.011	0.60	0.008	0.012
5	0.004	0.49	0.006	0.014
6	0.006	0.71	0.005	0.009
7	0.023	0.99	0.011	0.012
8	0.013	1.00	0.006	0.006
9	0.031	0.91	0.006	0.009
10	0.032	0.91	0.007	0.011
11	0.028	0.91	0.007	0.011
12	0.019	0.60	0.007	0.012
13	0.014	0.70	0.007	0.013
14	0.017	0.86	0.009	0.011
15	0.028	0.91	0.009	0.011
16	0.019	0.80	0.008	0.011
17	0.014	0.77	0.005	0.009
18	0.024	1.00	0.009	0.011
19	0.024	0.90	0.005	0.008
20	0.038	1.00	0.008	0.009

Table 2.1: Drag coefficients of unknotted and knotted fronds. Drag coefficients were measured for fronds when they were unknotted, and again when those same fronds were tied into an overhand knot.

Frond	Knotted frond max force (N)	Unknotted frond max force; older tissue (N)	Unknotted frond max force; younger tissue (N)	Mean unknotted frond max force (N)
1	59.35	69.09	39.79	54.44
2	54.72	62.65	70.82	66.74
3	26.87	45.28	29.78	37.53
4	77.76	79.19	87.76	83.47
5	77.10	79.01	88.68	83.84
6	81.00	87.46	87.86	87.66
7	66.26	89.74	92.65	91.20
8	80.90	110.37	86.31	98.34
9	70.73	80.86	62.27	71.57
10	74.73	91.95	71.90	81.93
11	61.30	78.08	56.11	67.10
12	78.42	108.06	97.23	102.65
13	58.82	83.71	64.58	74.15
14	51.58	74.32	69.54	71.93
15	66.33	91.85	62.01	76.93
16	57.44	94.85	58.73	76.79
17	60.49	90.21	66.12	78.17
18	67.53	100.24	64.70	82.47
19	59.61	96.30	60.14	78.22
20	73.51	117.61	69.76	93.69
21	66.76	86.99	62.32	74.65

Table 2.2: Breaking force of unknotted and knotted frond tissue. The breaking force of a knotted section of frond was compared to the breaking force of unknotted tissue from the same frond. To control for the effects of tissue on the breaking force, the breaking force of unknotted tissue was calculated as the mean of the breaking force of frond tissue that was older than the knotted tissue and the breaking force of frond tissue that was younger than the knotted tissue (Fig. 2.2C).

Table 2.3 – Page 1. Lengths, abundances of lateral blades, wounds, abundances of amphipods, dried weights of amphipods.

Frond pair	Date (MM/DD/YY)	Site	Untangled frond length (m)	Tangled frond length (m)	Untangled fronds, lateral blades	Tangled frond, lateral blades	Untangled fronds, wounds (n m^{-1})	Tangled fronds, wounds (n m^{-1})	Untangled fronds, amphipods (n)	Tangled fronds, amphipods (n)	Untangled fronds, amphipods dry wt (g)	Tangled fronds, amphipods dry wt (g)
1	09/28/15	MW	2.53	16.90	-	-	-	-	254	2,745	0.2531	3.4785
2	09/29/15	MC	1.81	5.77		-	-	-	60	83	0.0243	0.1058
3	09/29/15	MC	2.01	2.89	-	-	-	-	313	1,453	0.0683	0.6826
4	09/28/15	MW	4.24	11.97	-	-	-	-	492	5,956	0.2836	7.7857
5	10/26/15	MW	3.20	10.06	-	-	-	-	191	633	0.0914	0.7454
6	10/26/15	MW	6.24	11.63	1.33	1.35	1.60	2.41	285	3,157	0.1559	2.4008
7	10/28/15	MC	6.22	13.32	1.29	0	1.61	0.23	34	497	0.0171	0.3864
8	10/28/15	MC	4.95	1.81	2	2	1.01	1.66	931	2,186	0.4022	1.1055
9	11/09/15	MW	3.93	4.85	1.03	0.94	3.05	6.60	125	1,415	0.0880	0.3958
10	11/09/15	MW	3.82	5.75	1.80	0.09	1.57	4.35	64	44	0.0306	0.0199
11	11/11/15	MC	4.80	5.66	1.40	0	0.83	1.24	6	207	0.0004	0.2180
12	11/11/15	MC	7.73	8.94	1.81	0.24	0.65	3.02	228	1,315	0.1200	1.2813
13	11/11/15	MC	7.21	6.23	1.22	0	0.97	3.69	207	73	0.0540	0.0292
14	11/11/15	MC	8.65	4.74	1.77	0.45	0.92	3.16	428	175	0.2278	0.1047
15	12/10/15	MC	8.00	3.83	1.24	0.19	0.5	3.92	13	142	0.0108	0.1492
16	12/10/15	MC	7.28	7.63	0.92	1.49	0.82	1.70	0	83	0.0000	0.0836

Table 2.3 – Page 2. Abundances and dried weights of isopods, kelp crabs, and barnacles.

Frond pair	Untangled fronds, isopods (n)	Tangled fronds, isopods (n)	Untangled fronds, isopods dry wt (g)	Tangled fronds, isopods dry wt (g)	Untangled fronds, kelp crabs (n)	Tangled fronds, kelp crabs (n)	Untangled fronds, kelp crabs dry wt (g)	Tangled fronds, kelp crabs dry wt (g)	Untangled fronds, barnacles (n)	Tangled fronds, barnacles (n)	Untangled fronds, barnacles dry wt (g)	Tangled fronds, barnacles dry wt (g)
1	2	1	0.0131	0.0995	0	1	0.0000	0.4540	0	0	0.0000	0.0000
2	0	0	0.0000	0.0000	0	0	0.0000	0.0000	0	0	0.0000	0.0000
3	1	1	0.0009	0.0560	0	1	0.0000	0.1526	0	0	0.0000	0.0000
4	6	9	0.0273	1.0540	0	10	0.0000	1.3088	0	2	0.0000	0.0089
5	1	2	0.0022	0.1794	0	2	0.0000	2.1280	0	0	0.0000	0.0000
6	9	15	1.3518	1.9197	0	1	0.0000	0.1021	0	0	0.0000	0.0000
7	1	0	0.0035	0.0000	0	2	0.0000	0.3439	0	0	0.0000	0.0000
8	7	9	0.1393	3.2190	0	0	0.0000	0.0000	0	0	0.0000	0.0000
9	0	0	0.0000	0.0000	0	2	0.0000	1.5988	1	0	0.0004	0.0000
10	0	0	0.0000	0.0000	0	0	0.0000	0.0000	0	0	0.0000	0.0000
11	0	0	0.0000	0.0000	0	1	0.0000	0.1223	0	0	0.0000	0.0000
12	0	0	0.0000	0.0000	1	0	0.0000	0.0000	0	0	0.0000	0.0000
13	0	0	0.0000	0.0000	0	0	0.3466	0.0000	0	4	0.0000	0.0010
14	2	1	0.2205	0.3661	0	0	0.0000	0.0000	0	7	0.0000	0.0085
15	0	0	0.0000	0.0000	0	0	0.0000	0.0000	0	0	0.0000	0.0000
16	0	0	0.0000	0.0000	0	0	0.0000	0.0000	0	0	0.0000	0.0000

Table 2.3 – Page 3. Abundances and dried weights of mussels, limpets, and Littorinid snails

Frond pair	Tangled fronds, Littorinid snails dry wt (g)	Untangled fronds, Littorinid snails dry wt (g)	Tangled fronds, Littorinid snails (n)	Untangled fronds, Littorinid snails (n)	Tangled fronds, limpets dry wt (g)	Untangled fronds, limpets dry wt (g)	Tangled frond, limpets (n)	Untangled fronds, limpets (n)	Tangled fronds, mussels dry wt (g)	Untangled fronds, mussels dry wt (g)	Tangled fronds, mussels (n)	Untangled fronds, mussels (n)
1	0.0516	0.0043	8	4	0.0000	0.0000	0	0	0.0066	0.0000	13	0
2	0.0214	0.0156	9	8	0.0000	0.0000	0	0	0.0000	0.0000	0	0
3	0.0015	0.0576	2	28	0.0000	0.0112	0	1	0.0001	0.0000	1	0
4	0.1935	0.1439	38	29	0.0229	0.0000	1	0	0.0181	0.0000	4	0
5	0.0158	0.0271	4	4	0.0000	0.0000	0	0	0.0006	0.0000	2	0
6	0.0066	0.0397	4	5	0.0181	0.0544	1	1	0.0000	0.0010	9	1
7	0.0165	0.0071	9	3	0.0000	0.0000	0	0	0.0000	0.0000	0	0
8	0.0198	0.1410	5	34	0.0000	0.1052	0	1	0.0000	0.0024	0	1
9	0.0083	0.0308	1	3	0.0085	0.0000	1	0	0.2229	0.0004	1	1
10	0.0096	0.3029	2	32	0.0000	0.0000	0	0	0.0000	0.0000	0	0
11	0.0000	0.0000	0	0	0.0000	0.0000	0	0	0.0000	0.0000	0	0
12	0.0224	0.1007	6	26	0.0000	0.0000	0	0	0.0000	0.0000	0	0
13	0.0165	0.0763	5	17	0.0000	0.0000	0	0	0.0003	0.0000	1	0
14	0.1854	0.5328	50	102	0.0000	0.0040	0	1	0.0075	0.0000	3	0
15	0.0349	0.0182	6	3	0.0000	0.0000	0	0	0.0000	0.0000	0	0
16	0.0372	0.0000	7	0	0.0000	0.0000	0	0	0.0000	0.0000	0	0

Table 2.3: Comparisons of lateral blades, wounds, and epifaunal abundances and biomasses on the tangled and untangled fronds.

Frond	Wounded frond max force (N)	Unwounded frond max force; older tissue (N)	Unwounded frond max force; younger tissue (N)	Mean unwounded frond max force (N)
1	16.44	27.27	33.04	30.16
2	24.64	35.81	41.04	38.42
3	15.41	19.91	32.86	26.39
4	31.52	34.96	48.86	41.91
5	27.93	31.36	48.00	39.68
6	17.98	26.72	31.17	28.94
7	43.39	44.52	60.01	52.26
8	46.15	60.82	66.02	63.42
9	31.49	38.49	51.55	45.02
10	44.60	51.27	62.22	56.75
11	23.44	24.32	45.30	34.81
12	18.44	25.19	34.75	29.97
13	18.92	23.20	34.05	28.62
14	31.69	42.30	56.51	49.41
15	29.74	33.10	51.05	42.08
16	40.47	61.43	25.73	43.58

Table 2.4: Breaking force of wounded and unwounded frond tissue. The breaking force of a wounded section of frond was compared to the breaking force of unwounded tissue from the same frond. To control for the effects of tissue on the breaking force, the breaking force of unwounded tissue was calculated as the mean of the breaking force of frond tissue that was older than the wounded tissue and the breaking force of frond tissue that was younger than the wounded tissue (Fig. 2.2C).

Chapter 3: Seasonal changes in morphology and epifauna on the kelp *Egregia menziesii* in habitats with different wave exposure

3.1 INTRODUCTION

On many rocky coastlines around the world, kelp provide habitat and food for many organisms (Bustamante *et al*., 1995; Graham *et al*., 2007). In subtidal zones, kelp forests are vital habitat for a variety of vertebrates and invertebrates (Graham, 2004, Morton and Anderson, 2013). In intertidal zones, macroalgae provide refuges that are buffered from the harsh abiotic stresses associated with aerial exposure at low tide, such as desiccation and thermal extremes (Burnaford, 2004; Beermann *et al*., 2013). Because of their important roles in marine ecosystems, the ways in which kelp respond to fluctuations in environmental conditions, such as water temperature, water chemistry, and water motion, have been studied (reviewed by Harley *et al*., 2012). At the same time, it is also important to understand how the epifauna using kelp as habitat and food affect and are affected by the responses of the kelp to the environment (Norderhaug *et al*., 2012; Poore *et al*., 2014; Simonson *et al*., 2015; see Chapter 2).

Kelp morphology can affect the roles that the kelp play in the surrounding biological community. For example, macroalgae with large, complex thallus or holdfast morphologies can provide more habitat for epibionts than do seaweeds with small, simple morphologies (Hauser *et al*., 2006; Norderhaug *et al*., 2007; Christie *et al*., 2009; Teagle *et al*., 2017). Kelp morphology also affects the temporal patterns of kelp survival in a community because it influences whether the kelp can withstand unfavorable environmental conditions. For example, the morphology of a seaweed affects it resistance to desiccation and over-heating during low tides (e.g. Bell, 1995; Bertness *et al*., 1999). Furthermore, the hydrodynamic forces on kelp can break them or wash them away when they are exposed to rapid water flow (e.g. in large waves during storms) (e.g. Black, 1976; Friedland and Denny, 1995; Wolcott, 2007; Demes *et al*., 2013). Macroalgae that are small have streamlined morphologies, or can reconfigure into streamlined shapes in flowing water, experience lower hydrodynamic forces than do seaweeds with large, bulky morphologies (e.g. Koehl, 1984; Koehl and Alberte, 1988; Carrington, 1990; Martone *et al*., 2012; de Bettignies *et al*., 2013).

In spite of the importance of the morphology of macroalgae to their ecological roles and performance, seasonal changes in their morphology are difficult to monitor. Some measurements of morphology require removal of seaweeds from the shore (e.g. biomass, blade area) (e.g. Johnson and Koehl, 1994; de Bettignies *et al*., 2013), so individuals cannot be followed with time. Studies of kelp morphological plasticity in which tagged individuals were followed with time in the field have generally only lasted weeks (e.g. Koehl and Alberte, 1988) or months (e.g. Lowell *et al*., 1991; Pfister, 1991) rather than years. As a result, our knowledge about seasonal changes in macrophyte morphology *in situ* in habitats characterized by different wave exposures is limited.

3.1.1 Egregia menziesii

In this study, I monitored the seasonal morphological changes of the kelp *Egregia menziesii* at sites exposed to different levels of wave exposure. *E. menziesii* is one of the largest and most abundant kelp in the rocky intertidal zone along the west coast of North America (Black, 1974; Abbott and Hollenberg, 1976; Hughes, 2010). The thallus of *E. menziesii* is comprised of a perennial holdfast bearing numerous strap-like fronds (Fig. 3.1), each of which

can grow to several meters in length (Abbott and Hollenberg, 1976). The size and abundance of *E. menziesii* make it important for structuring the biological community in rocky intertidal habitats (Kennelly, 1989; Sotka, 2007; Hughes, 2010), yet its size and highly-branched structure make measurements of its morphology cumbersome to do in the field. Previous descriptions of *E. menziesii* thalli in the field have been limited to easily-measured morphological characters such as the length of the kelp's longest frond or the number of fronds on the kelp (Black, 1974; Blanchette *et al.*, 2002; Hughes, 2010), although fine-scale morphological surveys have been made of the small lateral blades that line the edges of the fronds (Henkel and Murray, 2007). Nonetheless, little is known about how the morphology of this ecologically-important kelp varies over seasons and years, or how such variation is affected by the wave exposure of the sites at which the kelp are living.

     E. menziesii affects the intertidal community by scouring organisms off the rocks as its fronds sweep across the substratum, and also by providing habitat for epibionts and food for herbivores (Kennelly, 2002; Hughes, 2010). In feeding experiments, *E. menziesii* was commonly chosen by a wide range of invertebrate herbivores as a preferred food source over other kelp and seaweed species (Leighton, 1971; Sotka, 2007). *E. menziesii* is the sole host to the limpet *Lottia insessa*, which uses the kelp for both food and habitat (Black, 1976; Kuo and Sanford, 2013). While large *E. menziesii* can host more limpets than can small ones, grazing by the limpets can reduce kelp size because fronds are broken off by waves at weak points caused by limpet grazing damage (Black, 1976; de Bettignies *et al.*, 2012). Thus, while large complex morphologies may allow kelp to provide habitat and food to more animals, herbivorous epifauna can in turn alter the morphology of the kelp. *E. menziesii* is host to numerous other organisms, including amphipods (Sotka, 2007), but little is known about how the prevalence and composition of the epifauna on *E. menziesii* varies with season.

3.1.2 Objectives

     The goal of this study was to quantify how the morphology and epifauna of an ecologically-important kelp, *E. menziesii*, changes with time at sites exposed to different levels of wave action. Kelp morphology depends on growth and damage, both of which can vary with season, so I made monthly measurements over several years. Rather than simply focusing on size, I measured a variety of different morphological features. My specific objectives were:
1) to measure monthly and inter-annual variation in the morphology of *E. menziesii*,
2) to quantify during different seasons the morphological differences between the kelp at sites exposed to heavy versus to moderate wave action,
3) to measure the seasonal rates of change of a variety of morphological features and to determine how those rates depended on kelp size and on the magnitude of that feature before the change occurred, and
4) to monitor the temporal patterns in the proportion of *E. menziesii* hosting a variety of different types of herbivores and other epibionts.

3.2 METHODS

3.2.1 Field surveys

     Intertidal individuals of *Egregia menziesii* were surveyed at four sites in northern California between August 2014 and February 2017 (Fig. S1.1). Sites were visited approximately once per month when the height of low tide was less than 0.3 m above MLLW.

Two moderately wave-exposed sites were located near Bodega, CA, USA: Horseshoe Cove (HC) (38°18'59" N, 123°4'12" W) and Miwok Beach (MW) (38°21'25" N, 123°4'2" W). Two wave-exposed sites were located in the Point Reyes National Seashore, CA, USA: Kehoe Beach (KB) (38° 9'56" N, 122° 57'6" W) and McClures Beach (MC) (38°11'3" N, 122°58'2" W).

At each site, adult kelp (i.e. stage IV sporophytes, *sensu* Henkel and Murray, 2007) were surveyed along a horizontal transect that ran parallel to the shoreline, selecting approximately every third individual that was encountered. A separate transect was used during each survey. The lengths of all the fronds on the selected kelp were measured to the nearest 1 cm, and whether or not each frond had its intercalary meristem and terminal lamina (Fig. 3.2) was recorded. Broken fronds missing their intercalary meristem and terminal lamina do not grow as quickly as intact fronds (Black, 1974).   In addition, each surveyed kelp was examined for evidence of epifauna living on the kelp's fronds. For herbivores, kelp wounds characteristic of a particular type of herbivore or the presence of those animals counted as evidence (Fig. 3.3A-D), whereas for non-herbivorous epifauna, evidence was limited to the presence of the animals (Fig. 3.3E-G).

Over the course of the study period, a subset of kelp (98 kelp at moderate sites, 85 kelp at exposed sites) at each site were tagged and were followed with time. The individuals to be tagged were selected by initially distributing between 5 and 10 tags over the transect area, such that no tagged kelp were within one meter of each other and that tagged kelp covered the range of microhabitats available along the transect line. On subsequent visits to the site, newly tagged kelp were established in an area of the shore if old tagged kelp had been washed away (or the tags lost) such that there were always at least 10 tagged kelp at each site during each month of the study period. Tags were 2.5 cm x 2.5 cm acrylic plates, each with a unique identification number. The tags were tied with nylon cord around the kelp's stipe, as close to the holdfast as possible. During subsequent months, the presence of terminal laminae and meristems on the fronds of tagged kelp fronds was recorded, and the lengths of fronds were measured. Many tags were eventually lost or the whole kelp washed away, so tagged kelp were followed for as long as the tags could be found (median = 177 days, range = 26 to 677 days).

3.2.2 Kelp morphology

Data from field surveys (i.e. frond lengths, presence/absence of terminal laminae and meristems) were used to calculate seven morphological features. All fronds longer than 10 cm on a kelp were included for the calculations.
1. Kelp size (S) was the total length of all the fronds on an individual kelp.
2. Number of fronds (N_f) was the number of fronds on an individual kelp.
3. Mean frond length (L_{mean}) was the kelp size divided by number of fronds (S/N_f).
4. Maximum frond length (L_{max}) was the length of longest frond on an individual kelp.
5. Frond density (D) was the length of fronds per space through which the fronds could move, calculated assuming the kelp is attached to a flat substratum and that the fronds occupy a hemispherical space whose radius is equal to the mean frond length (Fig. 3.4):

$$D = \frac{S}{\frac{2}{3}\pi L_{mean}{}^3}$$

(eqn. 3.1)

6. Percent of fronds that were intact (I) was the percent of fronds on a kelp that had a terminal lamina and meristem (Fig. 3.2).

7. Branching exponent (B), similar to the fractal dimension described by Seuront (2010), is a measure of how uniform the lengths of the fronds on an individual kelp are. A high branching exponent indicates that there is little variety in frond lengths on a kelp, whereas a low branching exponent indicates high variation in the lengths of fronds on an individual. For each kelp, I sorted the fronds on each kelp by their length and assigned a number, i, corresponding to their rank (i.e. $i = 1$ for the shortest frond and $i = N_f$ for the longest frond). Next, I calculated F_i, the total length of fronds whose ranks were less than or equal to i, for each possible value of i. The branching exponent, B, for a kelp was the slope of the regression of a log-log plot of each value of i and the corresponding value of F_i (Fig. 5).

The rate of change of each morphological feature on a kelp was calculated by:

$$Rate\ of\ change = \frac{F_{end} - F_{start}}{Weeks}$$

(eqn. 3.2)

where F_{end} is the magnitude of the feature at the end of a sampling period, F_{start} is the magnitude of the feature on the first day of the period, and *weeks* is the number of weeks between the two measurements (days between measurements divided by 7).

3.2.3 Statistical analyses

All analyses were run in R Statistical Software (v 3.3.2, R Development Core Team 2016). Kelp morphology data were rarely normally distributed and had variable sample sizes. Therefore, I used non-parametric statistical tests to compare morphologies of kelp at sites with different wave exposures, and of kelp at each site at different seasons. Mann-Whitney U tests were used for two-sample comparisons, and Kruskal-Wallis tests with a post hoc Dunn test ('FSA' package in R; Ogle, 2017) were used for comparing more than two samples.   For seasonal comparisons, I considered spring to be March through May, summer to be June through August, autumn to be September through November, and winter to be December through February.

3.3 RESULTS

3.3.1 Monthly variation in kelp morphology at a single site

The morphology of *Egregia menziesii* changed over time at each site. I present the results here for a single moderately wave-exposed site, HC, where I had the most thorough temporal coverage, and data for the other sites are presented in the Appendix (Figs. S3.1-S3.4). Measurements at HC were made during each month for two years, and data for both years were pooled for each month to calculate monthly medians and conduct statistical analyses. During summer and autumn months, the kelp were larger (S, Fig. 3.6A) and had more fronds (N_f), higher mean (L_{mean}) and maximum (L_{max}, Fig. 3.6B) frond lengths, a greater proportion of intact fronds with terminal laminae and meristems (I), and a higher branching exponents (B, a measure of how uniform the fronds were in length) than did kelp in late winter and in spring, but had a lower frond density (D, the length of fronds per space through which the fronds could move) (Figs. S3.5A-E) (Kruskal-Wallis tests with post hoc Dunn tests, $P < 0.05$).

3.3.2 Inter-annual variation in kelp morphology at a single site

During winter and spring, the morphology of *E. menziesii* was different in 2016 than it was during 2015 and 2017 (Table 3.1) (Mann-Whitney *U* tests and Kruskal-Wallis tests with post hoc Dunn test, $P < 0.05$). For example, from February through May, the mean frond lengths of kelp were significantly higher in 2016 than in either 2015 or 2017 (Fig. 3.7). Similarly, kelp in spring 2016 had larger sizes (*S*), more fronds (N_f), longer fronds (L_{mean} and L_{max}), lower frond densities (*D*), relatively more intact fronds (*I*), and higher branching exponents (*B*) than did kelp in spring 2015 (Table 3.1).

3.3.3 Kelp morphology at sites with different wave exposure

I tested whether the morphology of *E. menziesii* differed between sites with heavy versus moderate wave exposure. Since wave size varies with season (e.g. Denny, 1988), I compared sites during each season separately. Because of their close proximity and similar wave-exposure level, data from HC and MW were pooled to represent moderately wave-exposed sites (which I call "moderate"), and data from KB and MC were pooled to represent wave-exposed sites (which I call "exposed"). Kelp size (*S*) was not different between the exposed and moderate sites in all seasons (Mann-Whitney *U* tests, $P > 0.05$) (Table 3.2) (Fig. S3.6A). However, in the summer and autumn, kelp at the exposed sites had greater mean frond lengths (L_{mean}) than did kelp at moderate sites (Fig. 3.8A). In the spring, kelp at exposed sites had fewer fronds per kelp (N_f) than at moderate sites (Mann-Whitney *U* test, $P < 0.05$), but there were no differences in N_f between sites with different wave exposures during the other seasons (Fig. S3.6B). Furthermore, during spring, summer, and autumn, kelp at the exposed sites had relatively more intact fronds (*I*, Fig. 3.8B) and lower frond densities (*D*, Fig. 3.8C) than did those at moderate sites (Table 3.2). Although various morphological features differed between kelp from the exposed and moderate sites during spring, summer, and autumn (Figs. S3.3A-E), there were no significant morphological differences between the kelp from different sites during the winter (Table 3.2).

3.3.4 Rates of morphological change of kelp at sites with different wave exposure

The morphology of a kelp can change with time due to growth and to damage (e.g. by herbivores and hydrodynamic forces), all of which can vary between sites and seasons. I examined the direction and rates of change of a variety of morphological features of *E. menziesii* at exposed and moderate sites during spring, summer, autumn, and winter (Table 3.3).

The rate of change in the size (*S,* the total length of all the fronds on a kelp) of individual *E. menziesii* depended on season, wave exposure (Table 3.3), and on the size of the kelp at the beginning of the month over which growth rate was measured (Table 3.4) (Fig. 3.9). At both the exposed and the moderate sites, all the kelp grew in the summer (i.e. the growth rates for the measured kelp were all positive), whereas during the other seasons, some kelp increased in size while others got smaller (i.e. the range of growth rates spanned positive and negative values). However, at the exposed sites there was a net increase in kelp size during all seasons (i.e. the median value for growth rate was positive, Table 3.3), whereas at the moderate sites there was a net increase in size in spring, summer, and autumn, but a net decrease in size (i.e. the median value for growth rate was negative, Table 3.3) in winter. Thus, during the winter there was a significantly higher growth rate for kelp at exposed sites than at moderate sites (Table 3.3). At the exposed sites, large kelp increased in size at significantly greater rates than did smaller kelp during the summer, but size had no effect on growth rates during the other seasons. (Table 3.4). In contrast, at the moderate sites large kelp grew more rapidly in both spring and summer, but got smaller at greater rates during autumn and winter (Table 3.4) (Fig. 3.9).

There were only a few cases, all at the moderate sites, in which the rate of change of other morphological features depended on total kelp size (S): the rate of decrease was greater for large kelp than for small ones in maximum frond length in autumn, in percent of intact fronds in summer, and in the number of fronds on a kelp in autumn, whereas the rate of increase in frond number during spring was positively correlated with S during spring (Table S3.1). The observation that total size did not usually affect rates of change of other morphological parameters is not surprising because kelp with very different morphologies can have the same size (e.g. kelp with a few long fronds or many short fronds can be the same total size). Therefore, I explored how morphological features other than total size depended on their magnitude at the start of the period over which changes in that feature were measured.

The rate of change of the number of fronds on a kelp (N_f) sometimes correlated with the number of fronds on that kelp at the beginning of the period over which the change in N_f was measured (Table 4), and was also affected by season and wave exposure (Table 3.3) (Fig. S3.7A). At both exposed and moderate sites, some kelp gained and some lost fronds during all seasons, but there was a net increase in frond number during summer and winter at the exposed sites, and a net increase during spring and summer at the moderate sites, while there was no net change during other seasons. The rate of increase in frond number was significantly greater at the exposed sites than at the moderate sites only during the winter (Table 3.3). Exposed-site kelp with many fronds lost fronds during spring at a greater rate than did kelp with few fronds, but added fronds at a greater rate during summer (Table 3.4). In contrast, at moderate sites, kelp with many fronds lost fronds at a greater rate than did kelp with few fronds during autumn and winter.

The rate at which mean frond length (L_{mean}) increased showed a net rise during all seasons at the exposed sites, whereas at the moderate sites L_{mean} increased only during spring and summer, but decreased during autumn and winter (Table 3.3) (Fig. 3.10B). The rate of increase in L_{mean} was significantly higher at the exposed sites than at the moderate sites during both winter and spring (Table 3.3). At exposed sites, kelp that had a high mean frond length became shorter at a greater rate than did those with a low mean frond length during the spring, whereas at the moderate sites this occurred during spring, autumn, and winter.

The maximum frond length (L_{max}) of kelp at both the exposed and moderate sites increased during spring, summer and autumn, but decreased during winter (Table 3.3) (Fig. S3.7B). There were no significant differences in the rates of change of L_{max} between exposed and moderate sites (Table 3.3). The longest fronds on kelp with high maximum frond lengths grew more slowly than did the longest fronds on kelp with lower maximum frond lengths during autumn at the exposed sites, and during both autumn and winter at the moderate sites (Table 3.4).

Frond density (D, the length of fronds per space in the water through which the fronds can move) is a measure of how closely-spaced the fronds are to each other. Frond density decreased (i.e. fronds became sparser) during summer at both exposed and moderate sites (Table 3.3) (Fig. 3.10C). However, opposite trends in frond density were seen at different wave exposures during other seasons. During spring and autumn D decreased at the exposed sites while it increased at the moderate sites, and during winter D increased at the exposed sites but decreased at moderate sites. Frond density decreased at significantly greater rate at the exposed sites than at the moderate sites during spring, but decreased at greater rates at the moderate sites during summer (Table 3.3). Kelp with high frond densities changed D at lower rates than did those with lower frond densities at both wave exposures (Table 3.4). Kelp with high D lost frond

density at a greater rate during the spring at the exposed sites and during the spring, summer, and winter at the moderate sites.

The rate of change of the percent of fronds on a kelp that were intact (*I*) was also affected by season, site, and number of intact fronds on a kelp at the start of the measurement period. At the exposed sites, the percent of intact fronds decreased during summer and autumn, whereas at the moderate sites *I* increased during the spring (Table 3.3) (Fig. S3.7C). The rate at which kelp lost intact fronds was significantly greater at the exposed sites than at the moderate sites only during the summer (Table 3.3). Kelp with a high percentage of intact fronds lost intact fronds at a lower rate than did kelp with fewer intact fronds during spring, autumn, and winter at the exposed sites and during spring, summer, and winter at the moderate sites (Table 3.4).

Branching exponent (*B*) is a measure of how uniform the frond lengths are for an individual kelp. At the exposed sites, the branching exponent increased during spring and decreased during winter, whereas at the moderate sites *B* increased in summer and autumn, and decreased in winter (Table 3.3) (Fig. S3.7D). Kelp with high *B* increased their *B* at slower rates than those with lower *B* during all seasons at the exposed sites, and during spring at the moderate sites Table 3.4).

In conclusion, for all the morphological features of *E. menziesii* that I monitored in the field, the direction and rate at which they changed depended on season, wave exposure, and the magnitude of the feature at the start of the period over which change was measured. Furthermore, kelp size alone was not a good predictor of rates of change in morphological features other than size.

3.3.5 Epifauna

The most abundant epifauna on *E. menziesii* were herbivorous and suspension-feeding invertebrates. Among the herbivores, amphipods were found on the greatest percentage of the kelp (Fig. 3.3A), followed in order of prevalence by limpets, *Lottia insessa* (Fig. 3.3B), isopods, *Idotea* spp. (Fig. 3.3C), and kelp crabs, *Pugettia producta* (Fig. 3.3D) (ranking based on the median of the median values for each type of herbivore for each month). Amphipods were found on many more kelp than were limpets at both exposed and moderate sites (paired *t*-tests by month for each wave exposure, $P < 0.05$, n =15 months for exposed sites, and n = 20 months for moderate sites). Among the suspension-feeding epifauna on *E. menziesii*, mussels, *Mytilus* spp. (Fig. 3.3E) were found on a greater percentage of the kelp than were gooseneck barnacles, *Pollicipes polymerus* (Fig. 3.3F), and acorn barnacles (order Sessilia) (Fig. 3.3G) (ranking based on the median of the median values for each type of suspension feeder for each month).

The animals living on *E. menziesii* had different seasonal patterns of prevalence. Among the herbivores at both moderate and exposed sites, amphipods were found on the greatest percentage of kelp in the autumn (Fig. 3.11A), limpets were on the most kelp during the summer (Fig. 3.11B), and isopods and kelp crabs showed no seasonal pattern (Fig. 3.11C,D). At both exposed and moderate sites, the suspension-feeding gooseneck barnacles were found on the greatest percentage of kelp during winter and spring (Fig. 3.11F), while the acorn barnacles were most prevalent in autumn (Fig. 3.11G). In contrast, the seasonality of the suspension-feeding mussels depended on wave exposure: at exposed sites, mussels were found on more of the kelp during spring, but at moderate sites they were most prevalent in the summer (Fig. 3.11G).

The herbivorous epifauna were usually found on more kelp at the moderate sites than at the exposed sites throughout the year, whereas some suspension feeders were more prevalent at exposed sites while others were found on more of the kelp at moderate sites (Fig. 3.11). Of the

14 months for which I have survey data from all sites, both amphipods (Fig. 3.11A) and isopods (Fig. 3.11C) were found on more of the kelp at the moderate sites than at the exposed sites in 10 of those months (Fig. 3.11A), limpets were found on more kelp at moderate sites in all 14 months (Fig. 3.11B), and, kelp crabs were found on more on more kelp at moderate sites in 12 months (Fig. 3.11D). Similarly, suspension-feeding mussels were found on a greater percentage of the kelp at moderate sties during 9 of the 14 months for which I have data for all sites (Fig. 3.11E). In contrast, the other suspension feeders were found on more of the kelp at the exposed sites: gooseneck barnacles for 9 months (Fig. 3.11F), and acorn barnacles for all 14 months (Fig. 3.11G).

3.4 DISCUSSION

3.4.1 Seasonal changes in kelp morphology

The morphology of a kelp can change via growth and via damage. Growth rates and patterns can be affected by environmental factors such as day length, nutrient concentrations in the water, temperature, and water flow (e.g. Koehl *et al*., 2008, Bearham *et al*., 2013), while damage can be caused by processes such as herbivory or wave action (e.g. Black, 1976; de Bettignies *et al*., 2012; Demes *et al*., 2013). *Egregia. menziesii* are perennial kelp (Abbott and Hollenberg, 1976), thus an individual's morphology is the result of growth during its first year, accrued frond breakage, and recent growth, all of which can be affected by the abiotic and biotic environment of a kelp.

I found that the morphology and epifauna of *E. menziesii* varied with season, both at sites that were exposed to heavy wave action (exposed) and at sites that encountered moderate waves (moderate). Throughout the year at both wave exposures, the kelp showed little variation in the number of fronds (N_f) from season to season (median N_f of 9 to 11 fronds at moderate sites, and of 8 to 10 fronds at exposed sites), but they did undergo changes in other morphological features. During spring, kelp at both moderate and exposed sites had short fronds (low mean frond length, L_{mean}, length of lonest frond, L_{max}, and total frond length, S), with a lot of variation in the lengths of fronds on an individual (low B). During spring, only a small percentage of kelp at both wave exposures were host to herbivorous epifauna (amphipods, limpets, isopods, kelp crabs), but many of the kelp were host to suspension feeding epifauna (mussels, gooseneck and acorn barnacles) (Fig. 3.11). However, there were some differences during spring between the kelp at sites with different wave exposure. At moderate sites, few of the fronds were intact (low percent of fronds with that had a terminal lamina and meristem, I), whereas at exposed sites, many of the fronds were intact (high I). During summer at both wave exposures, fronds grew longer (S, L_{mean}, L_{max} increased) and kelp became less bushy (the length of fronds per space through which the fronds could move in the water, D, decreased) with less variation in frond length (branching exponent, B, increased). More of the fronds were intact (high I) even though the percent of kelp infested with herbivores increased. However, kelp at moderate sites were host to herbivorous amphipods, limpets, and kelp crabs, whereas kelp at exposed sites were host only to amphipods and kelp crabs. During autumn at both wave exposures, the fronds reached their greatest lengths of the year (high S, L_{mean}, L_{max}) and kelp were less bushy (low D) with less variation in frond length (high B). The percent of intact fronds on kelp (I) decreased as the percent of kelp infested with herbivores, particularly amphipods, remained high. At the same time, the percent of kelp hosting suspension feeders increased at both wave exposures. During winter at both exposed and moderate sties, fronds became shorter (S, L_{mean}, L_{max} decreased) as more fronds broke (I

47

decreased), and kelp became bushier (*D* increased) with more variation in frond length (*B* decreased). In winter, the percent of kelp infested with herbivores decreased while the percent of kelp hosting suspension feeders continued to increase at both sites, but a greater percentage of kelp hosted suspension feeders at exposed sites than at moderate sites.

The total size (*S*) of an *E. menziesii* depends on both the number and length of fronds. I found that frond number did not vary with season, thus the size increases of these kelp were due to frond growth rather than generation of new fronds, as was also found by Black (1974), who suggested that *E. menziesii* only produce new fronds when old fronds break (Black, 1976).

The seasonal patterns of changes in *E. menziesii* morphology and epifauna that I measured were repeated on successive years during my study. However, during the winter and spring of 2016, the water temperatures were higher than during 2015 and 2017 (Fig. 3.12) and the waves were often bigger (National Buoy Data Center, http://www.ndbc.noaa.gov/) due to El Niño. *E. menziesii* were larger in February through May of 2016 than they were during those months in 2015 and 2017 (Fig. 3.7), which is not surprising since kelp growth rates increase with temperature (e.g. Bearham *et al*., 2013). In addition, the percent of kelp bearing amphipods or hosting limpets was lower during winter and spring of 2016 than in the other years monitored, which may have led to less herbivore damage and breakage of fronds. This reduction in epifauna during El Niño could have been caused by physiological stress due to anomalously high water temperatures and wave action (e.g. Donovan and Taylor, 2008; Bjelde and Todgham, 2013), and by waves dislodging epifauna from kelp (Kennelly, 1989; Duggins *et al*., 2001; Hughes 2010) or preventing their recruitment onto kelp (Black, 1976; Morton and Anderson, 2013).

3.4.2 Epifauna

E. menziesii at both exposed and moderate sites were host to a variety of herbivorous and suspension-feeding epifauna throughout the study period. The perennial life history of *E. menziesii* and its many complex, long fronds should make it a good refuge for epibionts, probably protecting them from predators and abiotic stresses such as heat and desiccation at low tide, and hydrodynamic forces at high tide. In turn, herbivores might enhance the survival of *E. menziesii.* Breakage of fronds at wounds caused by herbivores can prune the kelp to smaller size, thereby reducing hydrodynamic forces on the kelp and decreasing the risk that the entire thallus will be dislodged by large waves during winter storms (Black, 1976; de Bettignies *et al*., 2012; Demes *et al*., 2013; Lopez *et al*., 2014).

Previous studies of *E. menziesii* in southern California focused on the limpet, *Lottia insessa*, as the dominant epifaunal herbivore (Black, 1976). Although the range of *L. insessa* continues through northern California into Oregon and Washington (Black, 1976; Kuo and Sanford, 2013), I found that herbivorous amphipods fed on and damaged many more kelp than did *L. insessa* in northern California at both exposed and moderate sites (Fig. 311A,B).

Herbivorous epifauna were found on a greater percentage of the kelp at moderate sites than at exposed sites, whereas suspension-feeding epifauna were found on more of the kelp at exposed sites than at moderate sites. Suspension feeders were also more prevalent than herbivores during winter, when wave action was stronger. Similar patterns have been observed in communities of benthic invertebrates, with more suspension-feeding animals at sites with higher wave action (Christofoletti e*t al*., 2010). These patterns in the types of epibionts most prevalent in different wave exposures may have been due to the effects of water flow on the feeding performance of the animals, or on the ability of the animals to hang on to the kelp. It has been suggested that higher water motion increases the rate that water-borne food is delivered to

suspension-feeders (Sanford *et al*., 1994; Bertness *et al*., 1998), whereas heavy wave action can interfere with gastropod grazing activity (e.g. Denny, 1994). The most common suspension feeders on *E. menziesii* were sessile mussels and barnacles that can recruit to wave-battered substrata and that glue themselves to surfaces, whereas the abundant herbivores were motile. Rapid water motion has been shown to dislodge herbivores from kelp (Duggins *et al*., 2001; Kennelly, 1989; Hughes, 2010) and to interfere with their recruitment (Black, 1976; Morton and Anderson, 2013).

3.4.3 Effects of wave exposure on kelp morphology
Although *E. menziesii* at exposed and moderate sites showed similar seasonal patterns of morphological change, they did differ in structure at some times of the year (Table 3.2). During spring, summer, or autumn, kelp at exposed sites tended to have fewer, but longer, fronds than did kelp at moderate sites, and to have a greater proportion of intact fronds and less variation in frond length. These differences could be due to more breakage of fronds on kelp at moderate sites, where a greater proportion of the kelp were infested by herbivores than were those at exposed sites. However, during winter, when kelp from both sites were broken to smaller size (probably due to the increased wave action typical of winter storms in the northeastern Pacific Ocean, e.g. Wolcott, 2007), there were no differences in the morphology of *E. menziesii* at exposed or moderate sites. Although the size of other species of kelp can increase with wave-exposure (Pedersen *et al*., 2012), there was no difference in the total size (*S*) of *E. menziesii* from exposed versus moderate sites during any season.

3.4.4 Importance of size and other measures of morphology
Size is the morphological feature of macroalgae that is most easily and commonly measured. It can be used as a proxy for age, but this is problematic for seaweeds that can break to smaller size as they age. Size can also be used as a proxy for macrophyte performance in the environment since it can affect the magnitude of hydrodynamic forces, ability to resist drying and heating at low tide (e.g. reviewed in Denny, 1988, 1993), and the abundance of epibionts hosted (Norderhaug *et al*., 2007).
Although total size is very important, it is not a good predictor of other morphological features of macroalgae. For example, kelp with a few long fronds or many short fronds can be the same total size.   Furthermore, although I found that total size affected the rates at which *E. menziesii* increased or decreased in size during different seasons, as has been shown for other seaweeds (e.g. Black, 1974; González-Fragoso *et al*., 1991), I also found that thallus size rarely correlated with the rates of change of other morphological features. Structural features such as number, length, branching, and shape of fronds can affect ecologically-important factors such as tangling (see Chapter 2), self-shading (Koehl and Alberte, 1998; Holbrook *et al*.,1991), hydrodynamic forces (e.g. Koehl, 1984; Carrington, 1990; Martone *et al*., 2012; de Bettignies *et al*., 2013), heating and desiccation at low tide (e.g. Bell, 1995), and epibiont load (Hauser *et al*., 2006; see Chapter 2). I have shown that such features can change with season and wave exposure in different ways than does size.

Morphology	Month	Year Difference	Test	n
	February	2016 > 2017	**	23, 24
Kelp size	April	2015 < 2016	*	18, 33
	May	2015 < 2016	*	27, 47
Number of fronds	February	2015 > 2017 < 2016	**	30, 24, 23
	December	2015 < 2016	*	14, 24
	February	2015 < 2016 > 2017	**	30, 23, 24
Mean frond length	March	2015 < 2016	*	36, 18
	April	2015 < 2016	*	18, 33
	May	2015 < 2016	*	27, 47
	February	2015 < 2016 > 2017	**	30, 23, 24
Max frond length	March	2015 < 2016	*	36, 19
	April	2015 < 2016	*	18, 33
	May	2015 < 2016	*	27, 47
	January	2016 < 2017	*	12, 23
	February	2016 < 2015 > 2017	**	23, 30, 24
Frond density	March	2015 > 2016	*	36, 18
	April	2015 > 2016	*	18, 33
	December	2015 < 2016	*	14, 24
	February	2016 > 2015 < 2017	**	23, 30, 24
Intact fronds (%)	March	2015 < 2016	*	36, 18
	June	2015 > 2016	*	19, 57
	February	2015 < 2016	**	30, 23
	March	2015 < 2016	*	36, 18
Branching exponent	April	2015 < 2016	*	18, 33
	July	2015 > 2016	*	22, 77

Table 3.1: Inter-annual differences in morphology for each calendar month at Horseshoe Cove. Only months with significantly different morphologies between years are reported. * indicates a Mann-Whitney *U* test, $P < 0.05$. ** indicates a Kruskal-Wallis test with post hoc Dunn test, $P < 0.05$. Sample sizes for each year are given in the order of the corresponding years under 'Year Difference.'

Morphology	Spring	Summer	Autumn	Winter
Kelp size (S)	ns	ns	ns	ns
Number of fronds (N_f)	M > E	ns	ns	ns
Mean frond length (L_{mean})	ns	E > M	E > M	ns
Maximum frond length (L_{max})	ns	E > M	ns	ns
Frond density (D)	M > E	M > E	M > E	ns
Intact fronds (I)	E > M	E > M	E > M	ns
Branching exponent (B)	E > M	ns	E > M	ns

Table 3.2: Comparisons of morphological characters between kelp at exposed sites (E) and those at moderate sites (M) for each season. Significant difference between kelp from sites with different wave exposure (Mann-Whitney U tests, $P < 0.05$) are indicated by M > E if the values are higher at moderate sites, and E > M if they are higher at exposed sites, while 'ns' indicates no significant difference between wave-exposures. Sample sizes are reported in Fig. 3.8. Some kelp were measured in multiple seasons, but there was only one observation per kelp within a single season.

Morph. Feature	Waves	Spring	Summer	Autumn	Winter
Kelp size (cm wk^{-1})	M	4 (-12 to 27)	82 (12 to 136)	4 (-9 to 30)	-9 (-32 to 1) *
	E	8 (-23 to 48)	107 (28 to 160)	8 (-28 to 24)	8 (-7 to 28) *
Number of fronds (fronds wk^{-1})	M	0.25 (-0.21 to 0.64)	0.23 (-0.11 to 0.90)	0.00 (-0.19 to 0.50)	0.00 (-0.15 to 0.16) *
	E	0.00 (-0.50 to 0.37)	0.24 (-0.06 to 0.74)	0.00 (-0.23 to 0.33)	0.23 (0.00 to 0.53) *
Mean frond length (cm wk^{-1})	M	0.4 (-1.8 to 0.3) *	3.6 (2.0 to 6.0)	-0.6 (-1.3 to 0.5)	-1.8 (-3.2 to -0.8) *
	E	0.9 (0.1 to 3.1) *	3.9 (0.8 to 8.2)	1.4 (-3.3 to 2.9)	0.4 (-2.3 to 0.4) *
Max frond length (cm wk^{-1})	M	0.4 (-1.7 to 4.5)	11.3 (4.1 to 17.7)	0.5 (0.0 to 1.4)	-1.0 (-8.0 to -0.2)
	E	2.4 (0.3 to 6.8)	9.4 (3.1 to 13.4)	0.2 (-3.7 to 0.8)	-0.4 (-3.7 to 0.2)
Frond density (m m^{-3} wk^{-1})	M	0.83 (-2.27 to 4.22) *	-2.35 (-5.94 to -0.44) *	0.08 (-0.54 to 0.50)	0.64 (0.25 to 1.85)
	E	-1.18 (-5.02 to 0.04) *	-0.62 (-1.34 to 0.17) *	-0.08 (-0.36 to 0.30)	1.01 (0.02 to 5.52)
Intact fronds (% wk^{-1})	M	0.4 (-1.7 to 2.8)	0.0 (-2.5 to 1.9) *	0.0 (-2.3 to 0.1)	0.0 (-2.0 to 0.6)
	E	0.0 (-0.8 to 1.0)	-2.1 (-4.5 to -1.0) *	-1.1 (-3.1 to 0.6)	0.0 (-0.8 to 1.7)
Branching Exponent (wk^{-1})	M	-0.01 (-0.03 to 0.02)	0.01 (-0.01 to 0.04)	0.01 (0.00 to 0.05)	0.00 (-0.03 to 0.02)
	E	0.02 (-0.01 to 0.05)	0.00 (-0.02 to 0.04)	0.00 (-0.03 to 0.03)	-0.01 (-0.03 to 0.03)

Table 3.3: Comparisons of growth rates of morphological characters between exposed sites (E) and moderate sites (M) for each season. Values are medians with the ranges of the first quartile above and below the median given in parentheses. Cases in which there were significant differences between kelp at exposed versus moderate sites (Mann-Whitney U tests, $P < 0.05$) in the rates of change for a given morphological character are indicated by an asterisk to the right of the values. Samples sizes for moderate sites were 49 kelp for spring, 35 for summer, 26 for autumn, and 37 for winter, and for the exposed sites were 25 for spring, 28 for summer, 17 for autumn, and 24 for winter. Some kelp were measured in multiple seasons, but there was only one observation per kelp within a single season.

Wave-exposure	Morphology	Spring	Summer	Autumn	Winter
Moderate	Kelp size (S)	↑	↑	↓	↓
	Number of fronds (N_f)	ns	ns	↓	↓
	Mean frond length (L_{mean})	↓	ns	↓	↓
	Maximum frond length (L_{max})	ns	ns	↓	↓
	Frond density (D)	↓	↓	ns	↓
	% fronds intact (I)	↓	↓	ns	↓
	Branching exponent (B)	↓	ns	ns	ns
Exposed	Kelp size (S)	ns	↑	ns	ns
	Number of fronds (N_f)	↓	↑	ns	ns
	Mean frond length (L_{mean})	ns	ns	↓	↓
	Maximum frond length (L_{max})	ns	ns	↓	ns
	Frond density (D)	↓	ns	ns	ns
	% fronds intact (I)	↓	ns	↓	↓
	Branching exponent (B)	↓	↓	↓	↓

Table 3.4: Correlations between the rate of increase of a morphological feature and the prior value for that morphological feature for *E. menziesii* during different seasons at moderate and exposed sites. I tested for a significant association between the rate of change in the percent of fronds that were intact (I) and the prior I of each kelp using a Kendall Tau Correlation ($P < 0.05$). For all other morphological features, I used linear regression to test for significant correlations between the rate of change of a feature and its prior value for each kelp. Upward arrows (↑) indicate a positive correlation, downward arrows (↓) indicate a negative correlation, and 'ns' indicates no significant correlation. Sample sizes for the moderate sites were 59 individuals in spring, 52 in summer, 50 in autumn, and 44 in winter, and for the exposed sites were 20 in spring, 56 in summer, 26 in autumn, and 29 in winter. Some kelp were measured in multiple seasons, but there was only one observation per kelp within a single season.

Figure 3.1: An individual *Egregia menziesii* has a holdfast that attaches to the substratum and numerous strap-like fronds that come out of the holdfast.
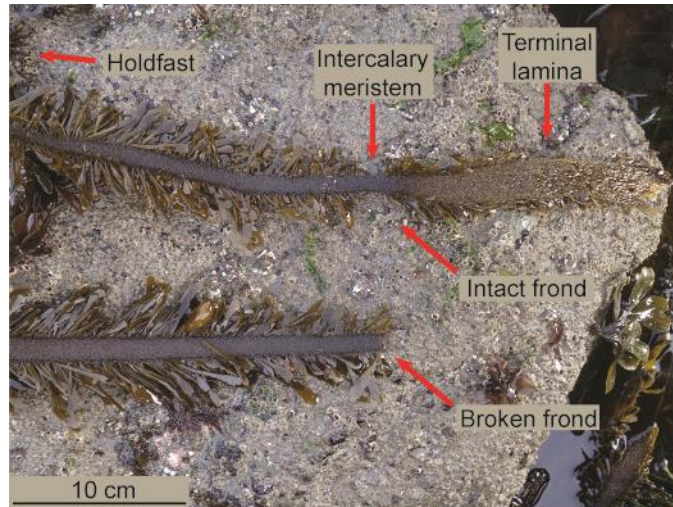
Figure 3.2: An "intact" frond of the kelp has an intercalary meristem and a terminal lamina at the distal end of the frond. A broken frond has lost its meristem and terminal lamina and cannot grow as rapidly as an intact frond.
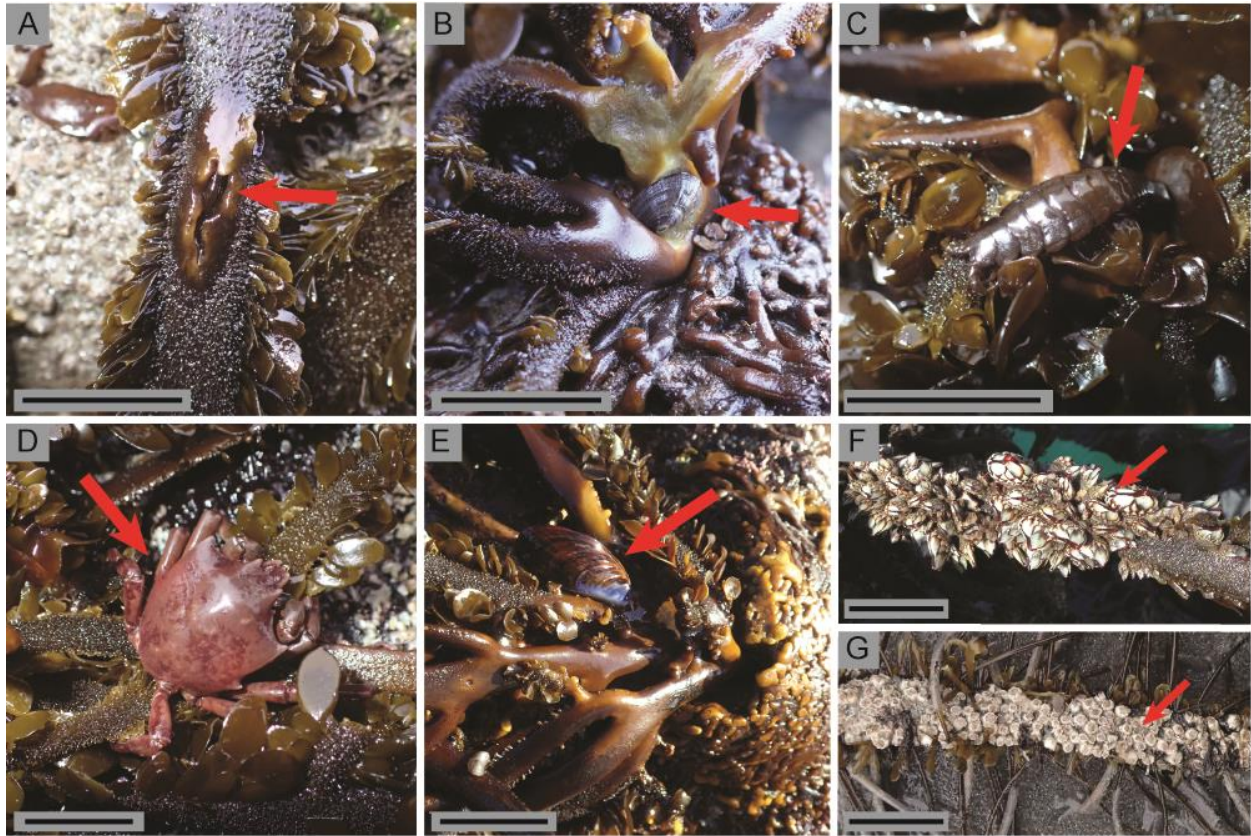
Figure 3.3: Common epifauna on fronds of kelp. Some herbivorous epifauna, such as amphipods (A) and limpets (B), create unique wounds on the kelp. Other herbivorous epifauna, such as isopods (C) and kelp crabs (D), inflict generic damage to the kelp. Non-herbivorous epifauna, such as mussels (E), gooseneck barnacles (F), and acorn barnacles (G), do not wound the kelp. The scale bar in each photo is approximately 2 cm. The red arrows show the epifauna.
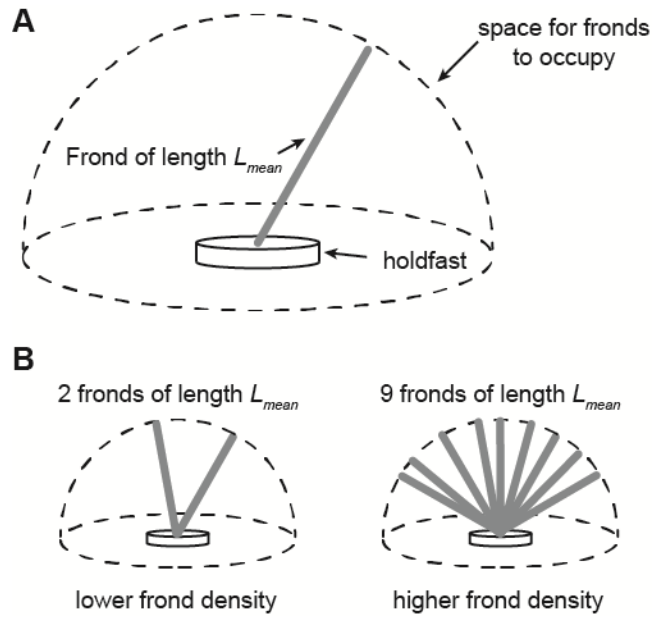
Figure 3.4: Frond density of the kelp is the length of fronds per space through which the fronds could move, calculated assuming the fronds can occupy a hemispherical space with a radius equal to the mean frond length, L_{mean} (A). The frond density is then a function of the number of fronds and the mean frond length (B).
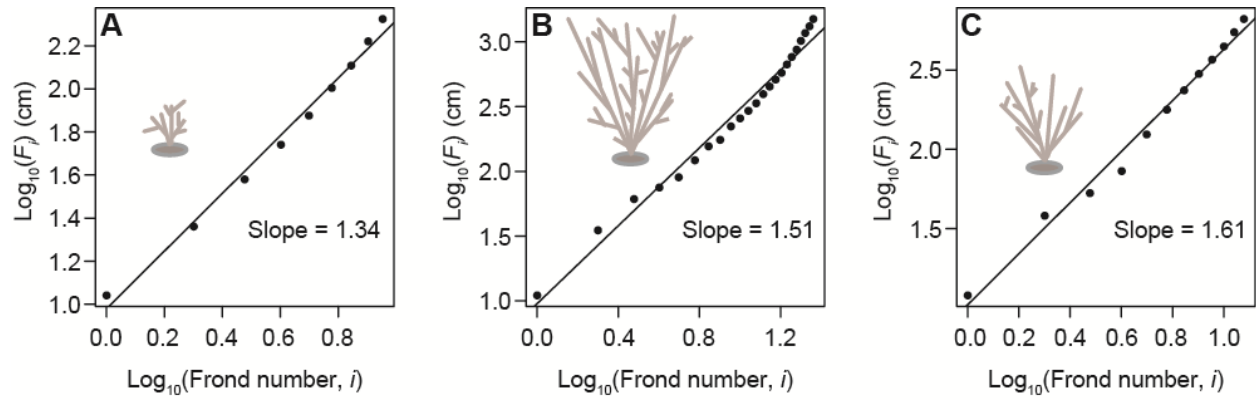
Figure 3.5: The branching exponent of kelp is the slope of the log-log regression of i and F_i, where i is the ordered rank of unique frond lengths (from shortest to longest), and F_i is the sum of the lengths of all fronds whose ranks are less than or equal to i. As an example, A-C show a scaled schematic of the fronds (in gray) used to calculate the branching exponent (slope) based on the frond lengths of real *E. menziesii*.
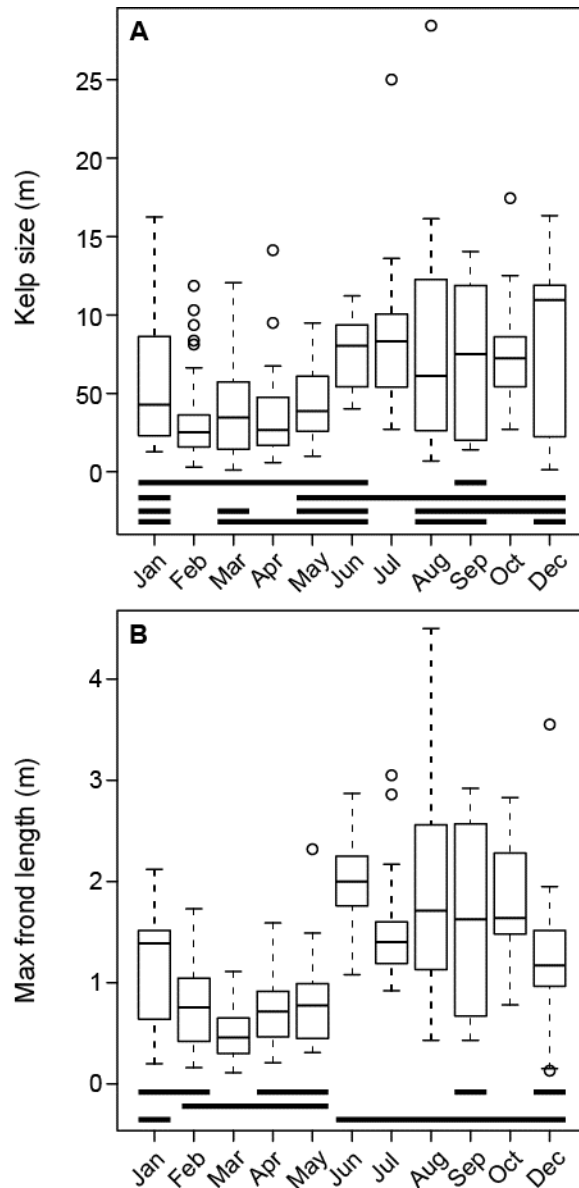
Figure 3.6: Kelp size (A) and the length of the longest frond (B) of *E. menziesii* at Horseshoe Cove (HC) during different months. The plots show the median values for all kelp measured along transects run during each month over a two-year period, (boxes indicate the first quartiles around the median, error bars show the most extreme data point that is no more than 1.5 times the interquartile range from the box, and circles indicate values beyond 1.5 time the interquartile range from the box). Bars under the horizontal axis indicate months for which the values were not significantly different from each other (Kruskal-Wallis tests with post hoc Dunn tests, $P < 0.05$ for significance). Sample sizes for each calendar month, in chronological order, were 19, 56, 23, 20, 46, 42, 73, 28, 8, 19, and 15 individuals.

59
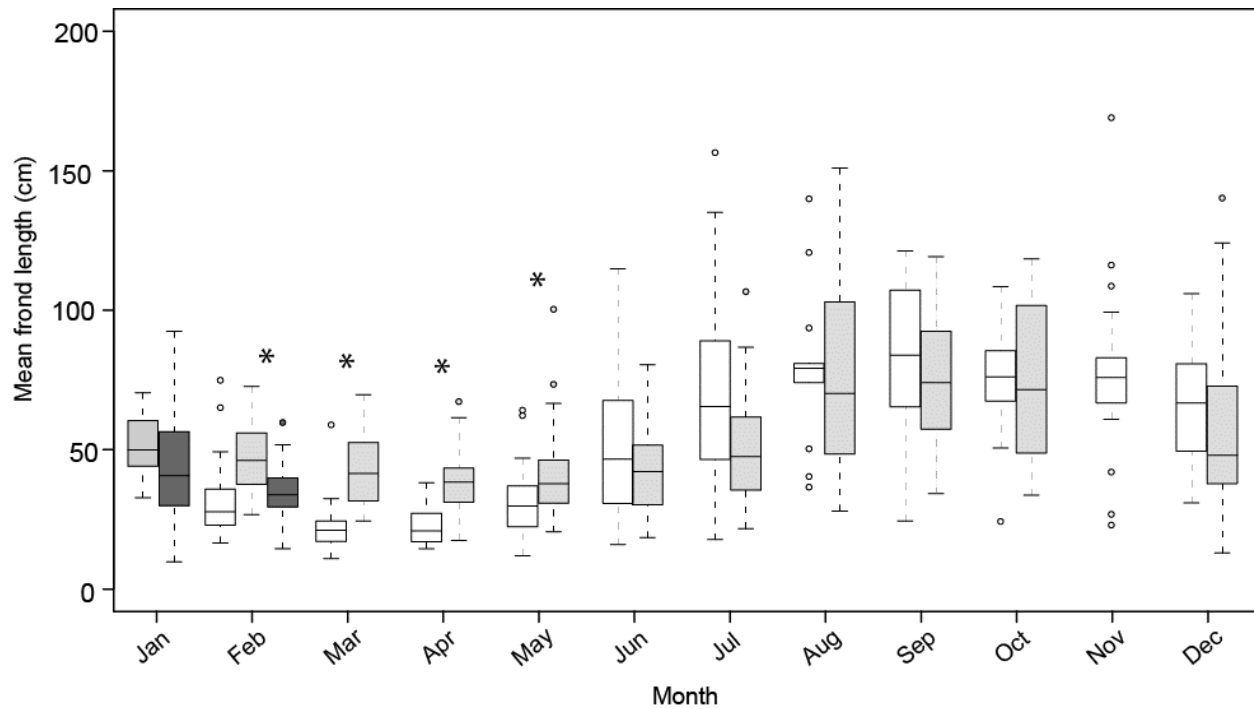
Figure 3.7: Inter-annual comparisons of the median values for mean frond length of kelp at Horseshoe Cove (HC). Data cover February through December 2015 (white bars), January through December 2016 (light grey bars), and January through February 2017 (dark grey bars). Boxes indicate the first quartiles around the median, error bars show the most extreme data point that is no more than 1.5 times the interquartile range from the box, and circles indicate values beyond 1.5 time the interquartile range from the box. Asterisks show months where kelp in 2016 had a significantly longer mean frond lengths than did kelp in the other surveyed years (Mann-Whitney U tests or Kruskal-Wallis test with post hoc Dunn test, depending on number of years, $P < 0.05$). Sample sizes for 2015, in chronological order, were 30, 36, 18, 27, 19, 22, 13, 15, 16, 16, 14. Sample sizes for 2016, in chronological order, were 12, 23, 18, 33, 47, 57, 77, 31, 15, 11, and 24. Sample sizes for 2017, in chronological order, were 23 and 24. There was only one observation per kelp for the entire data set.
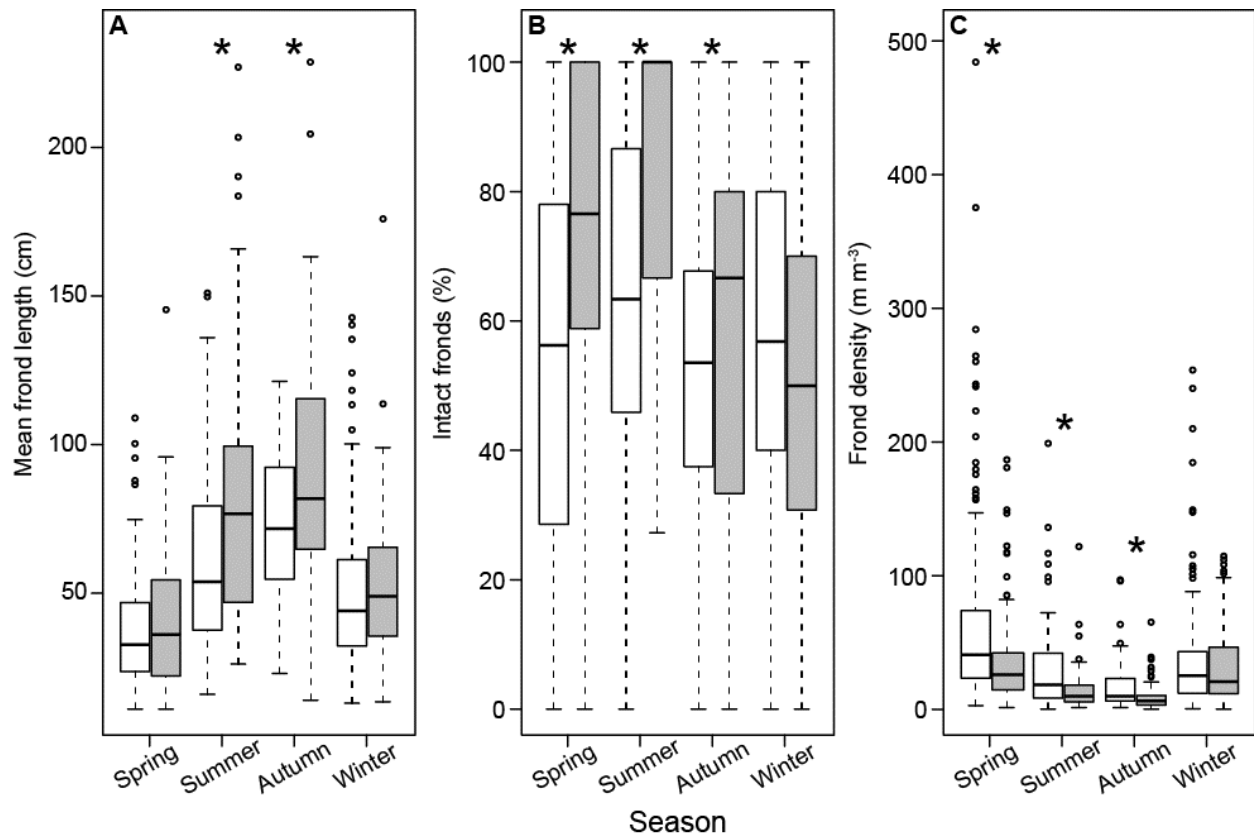
Figure 3.8: Seasonal variation in mean frond length (A), intact fronds (B), and frond density (C) for kelp at moderate sites (white bars) and exposed sites (gray bars). Asterisks indicated significantly different morphologies between wave exposures during that season (Mann-Whitney *U* tests, $P < 0.05$). Sample sizes at moderate sites were 195, 232, 75, and 193, for spring, summer, autumn, and winter, respectively. Sample sizes at exposed sites were 164, 201, 58, and 91 for spring, summer, autumn, and winter, respectively. Some kelp were measured in multiple seasons, but there was only one observation per kelp within a single season.
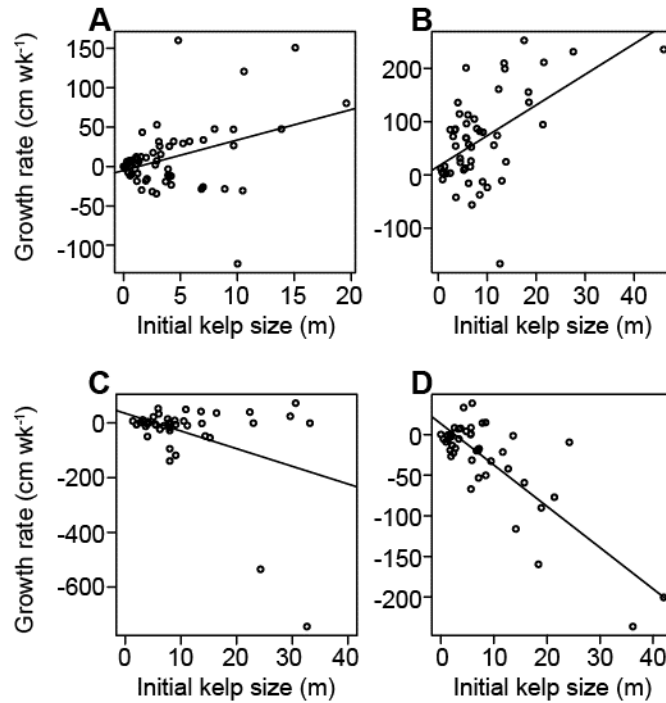
Figure 3.9: Growth rates of *E. menziesii* (eqn. 3.2) at moderate sites in spring (A), summer (B), autumn (C), and winter (D) depend on the initial kelp size (S) (linear regressions, $P < 0.005$). In spring and summer, growth rates were positively correlated to the initial size, whereas in the autumn and winter, growth rates were negative (i.e. kelp were becoming smaller) and were negatively correlated to the initial size (i.e. large kelp got smaller at a greater rate than did little kelp). Sample sizes for seasons were 59 individuals for spring, 52 for summer, 49 for autumn, and 44 for winter. Some kelp were measured in multiple seasons, but there was only one observation per kelp within a single season.
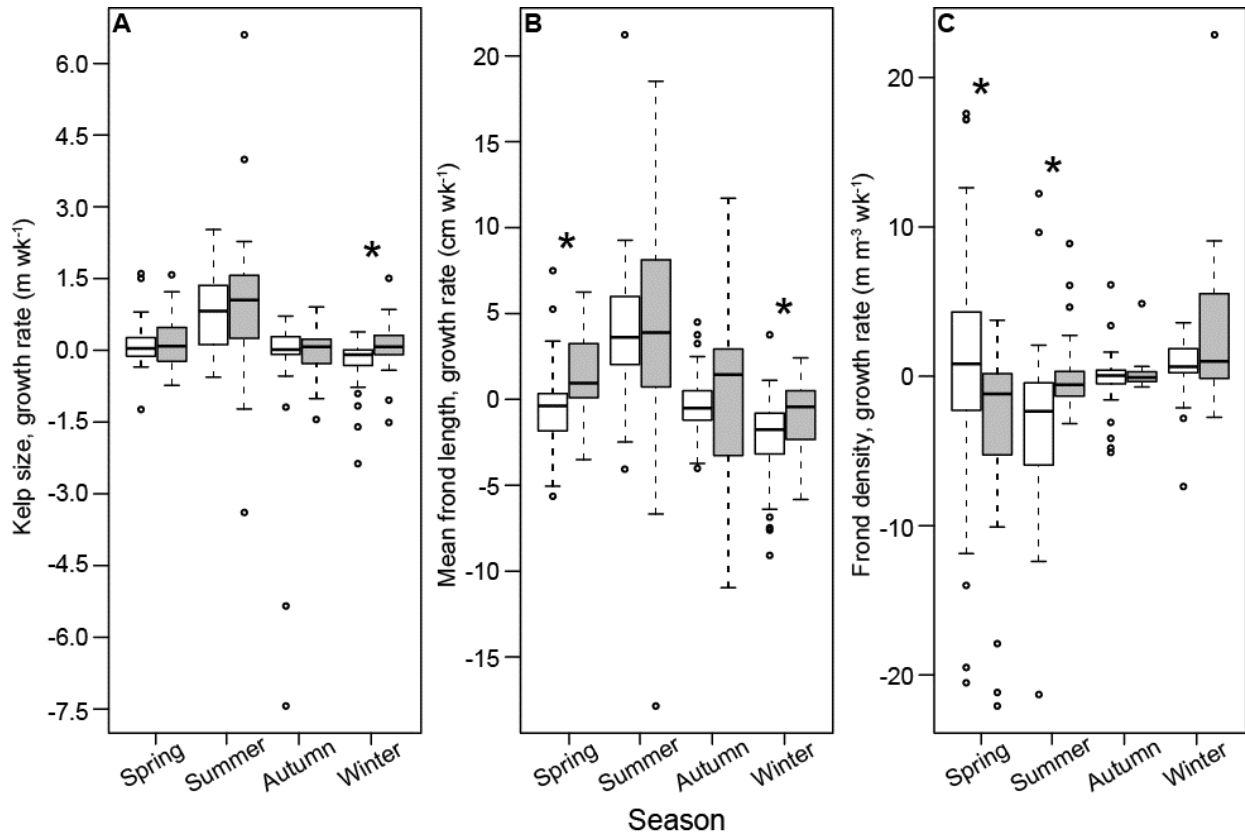
Figure 3.10: Rates of change for total kelp size, S (A), mean frond length, L_{mean} (B), and frond density, D (C) during different seasons at the moderate sites (white bars) and at the exposed sites (gray bars). Asterisks indicated significantly different growth rates between moderate and exposed sites during a given season (Mann-Whitney U tests, $P < 0.05$). Sample sizes at the moderate sites were 49 individuals for spring, 35 for summer, 26 for autumn, and 37 for winter. and at the exposed sites they were 25 for spring, 28 for summer, 17for autumn, and 24 for winter. Some kelp were measured in multiple seasons, but there was only one observation per kelp within a single season.
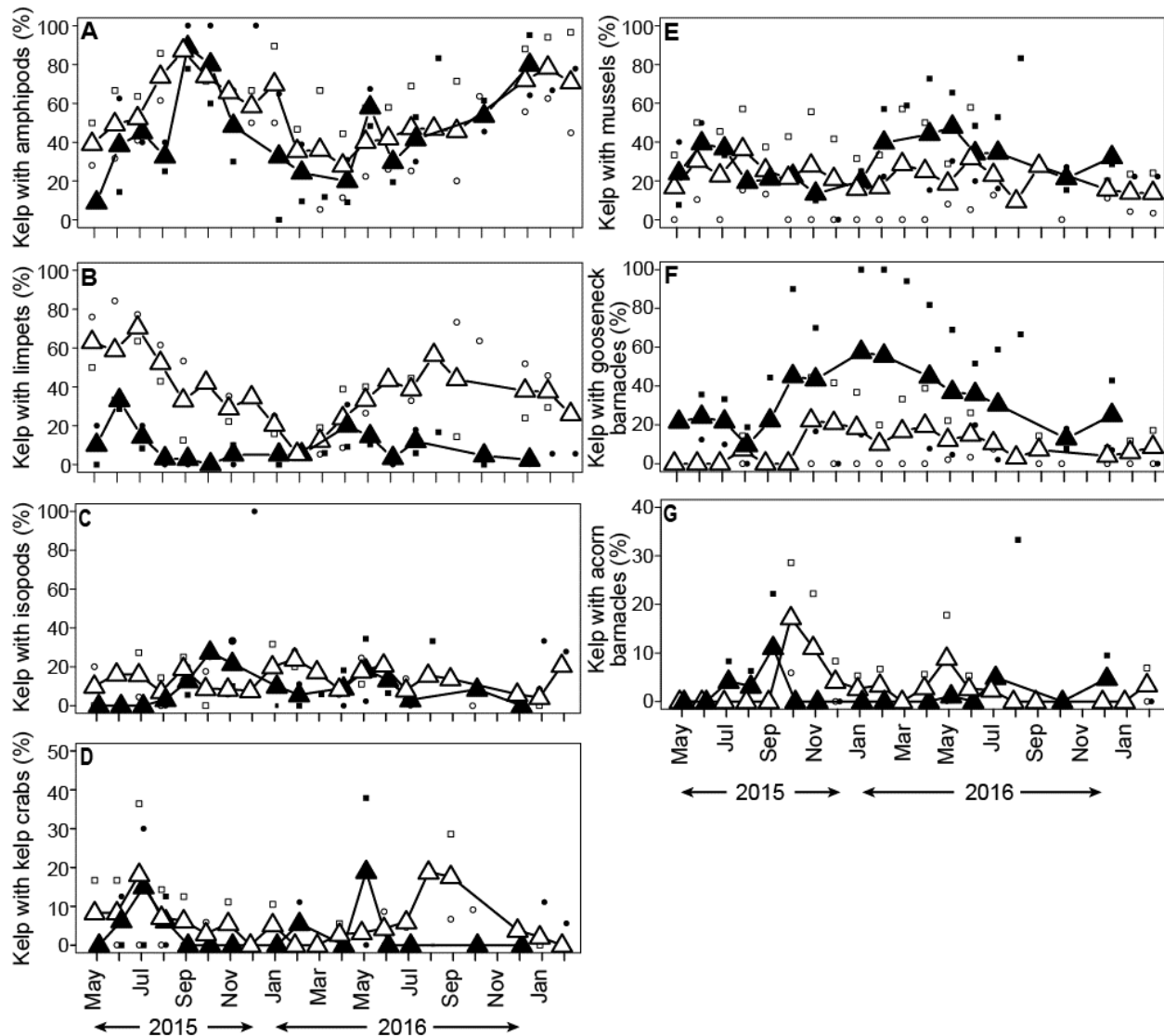
Figure 3.11: The percent of *E. menziesii* individuals hosting amphipods (A), limpets (B), isopods (C), kelp crabs (D), mussels (E), gooseneck barnacles (F), and acorn barnacles (G) at moderate sites (white) and exposed sites (black) from May 2015 to February 2017. Values for individual sites are the squares and circles, and median values for the moderate and exposed sites are the large triangles. Sample sizes for each month are listed in Table S2. Some kelp were surveyed in multiple months, but there was only one observation per kelp within a single month.

64
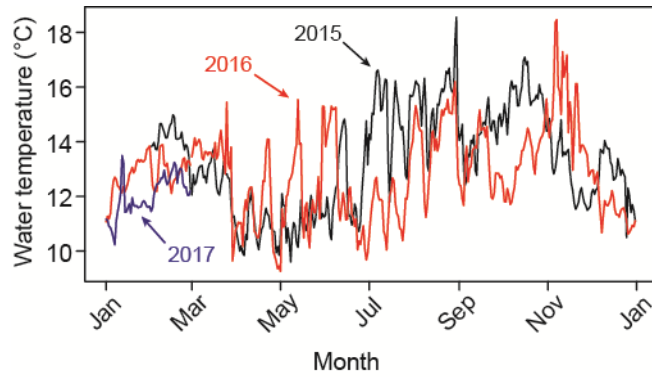
Figure 3.12: Daily mean sea surface temperature near the study sites (all sites < 20 km from measurement site). In Spring 2016, water temperatures were frequently warmer than they had been in the previous year. Data provided by the University of California, Davis, Bodega Marine Laboratory's Bodega Ocean Observing Node, delivered via the BOON website (http://boon.ucdavis.edu/).

REFERENCES

Abbott, I.A., Hollenberg, G.J., 1976. Marine Algae of California. Stanford University Press, Stanford, CA.

Bearham D., Vanderklift, M.W., Gunson, J.R. 2013. Temperature and light explain spatial variation in growth and productivity of the kelp *Ecklonia radiata*. *Marine Ecology Progress Series*, 476, 59-70.

Beermann AJ, Ellrich JA, Molis M, Scrosati RA (2013) Effects of seaweed canopies and adult barnacles on barnacle recruitment: the interplay of positive and negative influences. J Exp Mar Biol Ecol 448, 162-170.

Bell, E.C., 1995. Environmental and morphological influences on thallus temperature and desiccation of the intertidal alga *Mastocarpus papillatus* Kützing. *Journal of Experimental Marine Biology and Ecology*, 191, 29-55.

Bell, E., Denny, M.W., 1994. Quantifying "wave exposure": a simple device for recording maximum velocity and results of its use at several field sites. *Journal of Experimental Marine Biology and Ecology*, 181, 9-29.

Bertness, M.D., Gaines, S.D., Yeh S.M., 1998. Making mountains out of barnacles: the dynamics of acorn barnacle hummocking. *Ecology*, 79, 1382-1394.

Bertness, M.D., Leonard, G.H., Levine, J.M., Schmidt, P.R., Ingraham, A.O., 1999. Testing the relative contribution of positive and negative interactions in rocky intertidal communities. *Ecology*, 80, 2711-2726.

de Bettignies, T., Thomsen, M.S., Wernberg, T., 2012. Wound kelps: patterns and susceptibility to breakage. *Aquatic Biology*, 17, 223-233.

de Bettignies, T., Wernberg, T., Lavery, P.S., 2013. Size, not morphology, determines hydrodynamic performance of a kelp during peak flow. *Marine Biology*, 160, 843-851.

Bjelde, B.E., Todgham, A.E., 2013. Thermal physiology of the fingered limpet *Lottia digitalis* under emersion and immersion. *Journal of Experimental Biology*, 216, 2858-2869.

Black, R., 1974. Some biological interactions affecting intertidal populations of the kelp *Egregia laevigata*. *Marine Biology*, 28, 189-198.

Black, R., 1976. The effects of grazing by the limpet, *Acmaea insessa*, on the kelp, *Egregia laevigata*, in the intertidal zone. *Ecology* 57, 265-277.

Blanchette, C.A., Miner, B.G., Gaines, S.D., 2002. Geographic variability in form, size and survival of *Egregia menziesii* around Point Conception, California. *Marine Ecology Progress Series*, 239, 69-82.

Burnaford, J.L., 2004. Habitat modification and refuge from sublethal stress drive a marine plant-herbivore association. *Ecology*, 85, 2837-2849.

Burrows, M.T., Harvey, R., Robb. L., 2008. Wave exposure indices from digital coastlines and the prediction of rocky shore community structures. *Marine Ecology Progress Series*, 353, 1-12.

Bustamante, R.H., Branch, G.M., Eekhout, S., 1995. Maintenance of an exceptional intertidal grazer biomass in South Africa: subsidy by subtidal kelps. *Ecology*, 76, 2314-2329.

Carrington, E., 1990. Drag and dislodgment of an intertidal macroalga: consequences of morphological variation in *Mastocarpus papillatus* Kutzing. *Journal of Experimental Marine Biology and Ecology,* 139, 185-200.

Christie, H., Norderhaug, K.M., Fredriksen, S., 2009. Macrophytes as habitat for fauna. *Marine Ecology Progress Series,* 396, 221-233.

Christofoletti, R.A., Takahashi, C.K., Oliveira, D.N., Flores, A.A.V., 2010. Abundance of sedentary consumers and sessile organisms along the wave exposure gradient of subtropical rocky shores of the south-west Atlantic. *Journal of the Marine Biological Association of the United Kingdom*, 91, 961-967.

Colvard, N.B., Carrington, E., Helmuth, B., 2014. Temperature-dependent photosynthesis in the intertidal alga *Fucus gardneri* and sensitivity to ongoing climate change. *Journal of Experimental Marine Biology and Ecology,* 458, 6-12.

Demes, K.W., Pruitt, J.N., Harley, C.D.G., Carrington, E., 2013. Survival of the weakest: increased frond mechanical strength in a wave-swept kelp inhibits self-pruning and increases whole-plant mortality. *Functional Ecology,* 27, 439-445.

Denny, M.W., 1988. *Biology and the Mechanics of the Wave-swept Environment*. Princeton University Press, Princeton, NJ.

Denny, M.W., 1993. *Air and Water: the Biology and Physics of Life's Media*, Princeton University Press, Princeton, NJ.

Denny, M.W., 1994. Roles of hydrodynamics in the study of life on wave-swept shores, pp. 169-204 in *Ecological Morphology*. Wainwright, P.C., Reilly, S.M. [Eds], University of Chicago Press, Chicago, IL.

Denny, M.W., Blanchette, C.A., 2000. Hydrodynamics, shell shape, behavior and survivorship in the Owl Limpet *Lottia gigantea*. *Journal of Experimental Biology,* 203, 2623-2639.

Donovan, D.A., Taylor, H.H., 2008. Metabolic consequencese of living in a wave-swept environment: effects of simulated wave forces on oxygen consumption, heart rate, and activity of the shell adductor muscle of the abalone *Haliotis iris*. *Journal of Experimental Marine Biology and Ecology*, 354, 231-240.

Duggins, D., Eckman, J.E., Siddon, C.E., Klinger, T., 2001. Interactive roles of mesograzers and current flow in survival of kelps. *Marine Ecology Progress Series*, 223, 143-155.

Denny, M.W., Gaylord, B.P., Helmuth, B., Daniel, T., 1998. The menace of momentum: dynamic forces on flexible organisms. *Limnology and Oceanography,* 43, 955-968.

Fenwick, G.D., 1976. The effect of wave exposure on the amphipod fauna of the alga *Caulerpa brownie*. *Journal of Experimental Marine Biology and Ecology,* 25, 1-18.

Friedland, M.T., Denny, M.W., 1995. Surviving hydrodynamic forces in a wave-swept environment: consequences of morphology in the feather boa kelp, *Egregia menziesii* (Turner). *Journal of Experimental Marine Biology and Ecology,* 190, 109-133.

Gaylord, B., 1999. Detailing agents of physical disturbance: wave-induced velocities and accelerations on a rocky shore. *Journal of Experimental Marine Biology and Ecology,* 239, 85-124.

Gaylord, B., Denny, M.W., 1997. Flow and Flexibility. I. Effects of size, shape and stiffness in determining wave forces on the stipitate kelps *Eisenia arborea* and *Pterygophora californica*. *Journal of Experimental Biology,* 200, 3141-3164.

Gaylord, B., Denny, M.W., Koehl, M.A.R., 2008. Flow forces on seaweeds: Field evidence for roles of wave impingement and organism inertia. *Biological Bulletin,* 215, 295-308.

Gere, J.M., Timoshenko, S.P., 1997. *Mechanics of materials* (4th ed.). PWS Publishing Company, Boston, MA.

González-Fragoso, J., Ibarra-Obando, S.E., North, W.J., 1991. Frond elongation rates of shallow water *Macrocystis pyrifera* (L.) Ag. in northern Baja California, Mexico. *Journal of Applied Phycology*, 3, 311-318.

Graham, M.H., 2004. Effects of local deforestation on the diversity and structure of southern California giant kelp forest food webs. *Ecosystems* 7, 341-357.

Graham, M.H., Vásquez, J.A., Buschmann, A.H., 2007. Global ecology of the giant kelp *Macrocystis*: from ecotypes to ecosystems. *Oceanography and marine Biology*, 45, 39-88.

Harley, C.D.G., Anderson, K.M., Demes, K.W., Jorve, J.P., Kordas, R.L., Coyle, T.A., 2012. Effects of climate change on global seaweed communities. *Journal of Phycology*, 48, 1064-1078.

Harley, C.D.G., Helmuth, B.S.T., 2003. Local- and regional-scale effects of wave exposure, thermal stress, and absolute versus effective shore level on patterns of intertidal zonation. *Limnology and Oceanography*, 48, 1498-1508.

Hauser, A., Attrill, M.J., Cotton, P.A., 2006. Effects of habitat complexity on the diversity and abundance of macrofaunal colonizing artificial kelp holdfasts. *Marine Ecology Progress Series*, 325, 93-100.

Henkel, S.K., Murray, S.N., 2007. Reproduction and morphological variation in southern California populations of the lower intertidal kelp *Egregia menziesii* (Laminariales). *Journal of Phycology,* 43, 242-255.

Holbrook, N.M., Denny, M.W., Koehl, M.A.R., 1991. Intertidal "trees": consequences of aggregation on the mechanical and photosynthetic properties of sea-palms *Postelsia palmaeformis* Ruprecht. *Journal of Experimental Marine Biology and Ecology,* 146, 39-67.

Hunter, T., 1988. Mechanical design of hydroids: flexibility, flow forces, and feeding in *Obelia longissima*. Doctoral dissertation, University of California, Berkeley, California, 228 pp.

Hughes, B.B., 2010. Variable effects of a kelp foundation species on rocky intertidal diversity and species interactions in central California. *Journal of Experimental Marine Biology and Ecology*, 393, 90-99.

Johnson, A.J., Koehl, M.A.R., 1994. Maintenance of dynamic strain similarity and environmental stress factor in different flow habitats: thallus allometry and material properties of a giant kelp. *Journal of Experimental Biology*, 195, 381-410.

Kennelly, S.J., 1989. Effects of kelp canopies on understory species due to shade and scour. *Marine Ecology Progress Series*, 50, 215-224.

Koehl, M.A.R., 1984. How do benthic organisms withstand moving water? *American Zoologist*, 24, 57-70.

Koehl, M.A.R., 1999. Ecological biomechanics of benthic organisms: life history, mechanical design and temporal patterns of mechanical stress. *Journal of Experimental Biology*, 202, 3469-3476.

Koehl, M.A.R., Alberte, R.S., 1988. Flow, flapping, and photosynthesis of *Nereocystis luetkeana*: a functional comparison of undulate and flat blade morphologies. *Marine Biology,* 99, 435-444.

Koehl, M.A.R., Silk, W.K., Liang, H., Mahadevan, L., 2008. How kelp produce blade shapes suited to different flow regimes: a new wrinkle. *Integrative and Comparative Biology*, 48, 318-330.

Koehl, M.A.R., Wainwright, S.A., 1977. Mechanical adaptations of a giant kelp. *Limnology and Oceanography,* 22, 1067-1071.

Kregting, L., Blight, A., Elsäßer, B., Savidge, G., 2013. The influence of water motion on the growth rate of the kelp *Laminaria hyperborea*. *Journal of Experimental Marine Biology and Ecology*, 448, 337-345.

Kroeker, K.J., Sanford, E., Rose, J.M., Blanchette, C.A., Chan, F., Chavez, F.P., Gaylord, B., Helmuth, B., Hill, T.M., Hofmann, G.E., McManus, M.A., Menge, B.A., Nielsen, K.J., Raimondi, P.T., Russell, A.D., Washburn, L., 2016. Interacting environmental mosaics drive geographic variation in mussel performance and predation vulnerability. *Ecology Letters*, 19, 771-779.

Krumhansl, K.A., Demes, K.W., Carrington, E., Harley, C.D.G., 2015. Divergent growth strategies between red algae and kelps influence biomechanical properties. *American Journal of Botany*, 102, 1938-1944.

Krumhansl, K.A., Scheibling, R.E., 2012. Production and fate of kelp detritus. *Marine Ecology Progress Series,* 467, 281-302.

Kuo, E.S.L., Sanford, E., 2013. Northern distribution of the seaweed limpet *Lottia insessa* (Mollusca: Gastropoda) along the Pacific coast. *Pacific Science*, 67, 303-313.

Leighton, D.L., 1971. Grazing activities of benthic invertebrates in southern California kelp beds, pp 421-453. In: North, W.J. [ed] *The Biology of Giant Kelp Beds (*Macrocystis*) in California*. J. Cramer, Lehre, Germany.

Lopez, D., Eloy, C., Michelin, S., de Langre, E., 2014. Drag reduction, from bending to pruning. *Europhysics Letters*, 108,48002.

Lowell, R.B., Markham, J.H., Mann, K.H., 1991. Herbivore-like damage induces increased strength and toughness in a seaweed. *Proceedings of the Royal Society of London B,* 243, 31-38.

Martone, P.T., Kost, L., Boller, M., 2012. Drag reduction in wave-swept macroalgae: Alternative strategies and new predictions. *American Journal of Botany,* 99, 806-815.

Meluzzi, D., Smith, D.E., Arya, G., 2010. Biophysics of knotting. *Annual Review of Biophysics*, 39, 349-366.

Mislan, K.A.S., Blanchette, C.A., Broitman, B.R., Washburn, L., 2011. Spatial variability of emergence, splash, surge, and submergence in wave-exposed rocky-shore ecosystems. *Limnology and Oceanography*, 56, 857-866.

Morton, D.N., Anderson, T.W., 2013. Spatial patterns of invertebrate settlement in giant kelp forests. *Marine Ecology Progress Series*, 485, 75-89.

Norderhaug, K.M., Christie, H., Andersen, G.S., Beekby, T., 2012. Does the diversity of kelp forest macrofaunal increase with wave-exposure? *Journal of Sea Research*, 69, 36-42.

Norderhaug, K.M., Christie, H., Fredriksen, S., 2007 Is habitat size an important factor for faunal abundances on kelp (*Laminaria hyperborea*)? *Journal of Sea Research*, 58, 120-124.

Ogle, D.H., 2017. FSA: fisheries stock analysis. R package version, 0.8.12

Pedersen, M.F., Nejrup, L.B., Fredriksen, S., Christie, H., Norderhaug, K.M., 2012. Effects of wave exposure on population structure, demography, biomass and productivity of the kelp *Laminaria hyperborea*. *Marine Ecology Progress Series*, 451, 45-60.

Peng, C.J., Lee, K.L., Ingersoll, G.M., 2002. An introduction to logistic regression analysis and reporting. *Journal of Educational Research*, 96, 3-14.

Pfister, C.A., 1991. Reproductive plasticity in the kelp *Alaria nana* (Phaeophyceae). *Journal of Phycology*, 27, 763-766.

Pieranski, P., Kasas, S., Dietler, G., Dubochet, J., Stasiak, A., 2001. Localization of breakage points in knotted strings. *New Journal of Physics*, 3, 1-13.

Poore, A.G.B., Gutow, L., Pantoja, J.S., Tala, F., Madariaga, D.J., Thiel, M., 2014. Major consequences of minor damage: impacts of small grazers on fast-growing kelps. *Oecologia*, 174, 789-801.

R Development Core Team. (2014). R: A Language and Environment for Statistical Computing. R Foundation for Statistical Computing, Vienna, Austria. http://www.R-project.org

Rodriguez, G.E., Rassweiler, A., Reed, D.C., Holbrook, S.J., 2013. The importance of progressive senescence in the biomass dynamics of giant kelp (*Macrocystis pyrifera*). *Ecology*, 94, 1848-1858.

Rohde, S., Hiebenthal, C., Wahl, M., Karez, R., Bischof, K., 2008. Decreased depth distribution of *Fucus vesiculosus* (Phaeophyceae) in the Western Baltic: effects of light deficiency and epibionts on growth and photosynthesis. *European Journal of Phycology,* 43, 143-150.

Sanford, E., Bermudez, D., Bertness, M.D., Gaines, S.D., 1994. Flow, food supply and acorn barnacle population dynamics. *Marine Ecology Progress Series*, 104, 49-62.

Seuront, L., 2010. *Fractals and Multifractals in Ecology and Aquatic Science*. CRC Press, New York, NY.

Simonson, E.J., Metaxas, A., Scheibling, R.E., 2015. Kelp in hot water: II. effects of warming seawater temperature on kelp quality as a food source and settlement substrate. *Marine Ecology Progress Series*, 537, 105-119.

Sotka, E.E., 2007. Restricted host used by the herbivorous amphipod *Peramphithoe tea* is motivated by food quality and abiotic refuge. *Marine Biology*, 151, 1831-1838.

Stewart, H.L., 2004. Hydrodynamic consequences of maintaining an upright posture by different magnitudes of stiffness and buoyancy in the tropical alga *Turbinaria ornata. Journal of Marine Systems,* 49, 157-167.

Stewart, H.L., 2006a. Hydrodynamic consequences of flexural stiffness and buoyancy for seaweeds: a study using physical models. *Journal of Experimental Biology,* 209, 2170-2181.

Stewart, H.L., 2006b. Ontogenetic changes in buoyancy, breaking strength, extensibility, and reproductive investment in a drifting macroalga *Turbinaria ornata* (Phaeophyta). *Journal of Phycology,* 42, 43-50.

Stewart, H.L., Payri, C.E., Koehl, M.A.R., 2007. The role of buoyancy in mitigating reduced light in macroalgal aggregations. *Journal of Experimental Marine Biology and Ecology,* 343, 11-20.

Teagle, H., Hawkins, S.J., Moore, P.J., Smale, D.A., 2017. The role of kelp species as biogenic habitat formers in coastal marine ecosystems. *Journal of Experimental Marine Biology and Ecology*, 492, 81-98.

Wainwright, S.A., Biggs, W.D., Currey, J.D., Gosline, J. M., 1976. *Mechanical Design in Organisms*. John Wiley, New York, NY.

Wolcott, B., 2007. Mechanical size limitation and life-history strategy of an intertidal seaweed. *Marine Ecology Progress Series,* 338, 1-10.

Vogel, S., 1994. *Life in Moving Fluids*. Princeton University Press, Princeton, NJ.

Vogel, S., 1989. Drag and reconfiguration of broad leaves in high winds. *Journal of Experimental Botany,* 40, 941-948.

Appendix

Contents:

Figure S1.1: Sites for surveying intertidal populations of *Egregia menziesii*. Moderately wave-exposed sites (Miwok Beach and Horseshoe Cove) were located near Bodega, CA, wave-exposed sites (McClures Beach and Kehoe Beach) were located in the Point Reyes National Seashore. The two groups of sites are approximately 23 km apart.

Waves	Morph. Feature	Spring	Summer	Autumn	Winter
Moderate	Number of fronds (Nf)	↑, $p = 0.016$, $R^2 = 0.08$	ns	↓, $p = 0.008$, $R^2 = 0.12$	ns
	Mean frond length (Lmean)	ns	ns	ns	ns
	Max frond length (Lmax)	ns	ns	↓, $p = 0.001$, $R^2 = 0.19$	ns
	Frond density (D)	ns	ns	ns	ns
	Intact fronds (I)	ns	↓, $p = 0.009$, tau = -0.25	ns	ns
	Branching exponent (B)	ns	ns	ns	ns
Exposed	Number of fronds (Nf)	ns	ns	ns	ns
	Mean frond length (Lmean)	ns	ns	ns	ns
	Max frond length (Lmax)	ns	ns	ns	ns
	Frond density (D)	ns	ns	ns	ns
	Intact fronds (I)	ns	ns	ns	ns
	Branching exponent (B)	ns	ns	ns	ns

Table S3.1: Results of correlations between the rate of change of a morphological feature and the initial size of the kelp at sites across a wave-exposure gradient. A linear regression was used to test for a correlation for all morphological features except for Intact Fronds, which was tested using a Kendall Tau Correlation. An upward pointing arrow indicates a positive correlation and a downward pointing arrow indicate a negative correlation.

Month	Horseshoe Cove	Miwok Beach	Kehoe Beach	McClures Beach
May 2015	25	6	13	10
June 2015	19	6	14	8
July 2015	22	11	12	10
August 2015	13	7	16	5
September 2015	15	8	18	5
October 2015	17	7	10	4
November 2015	17	9	10	6
December 2015	14	12	0	1
January 2016	12	19	4	20
February 2016	25	15	21	18
March 2016	19	21	17	0
April 2016	35	18	11	13
May 2016	49	45	29	43
June 2016	58	19	31	5
July 2016	79	45	17	50
August 2016	32	0	6	0
September 2016	15	7	0	0
October 2016	11	0	13	11
December 2016	27	25	21	14
January 2017	24	17	0	14
February 2017	29	29	0	18

Table S3.2: Sample sizes for epifauna surveys at all study sites.
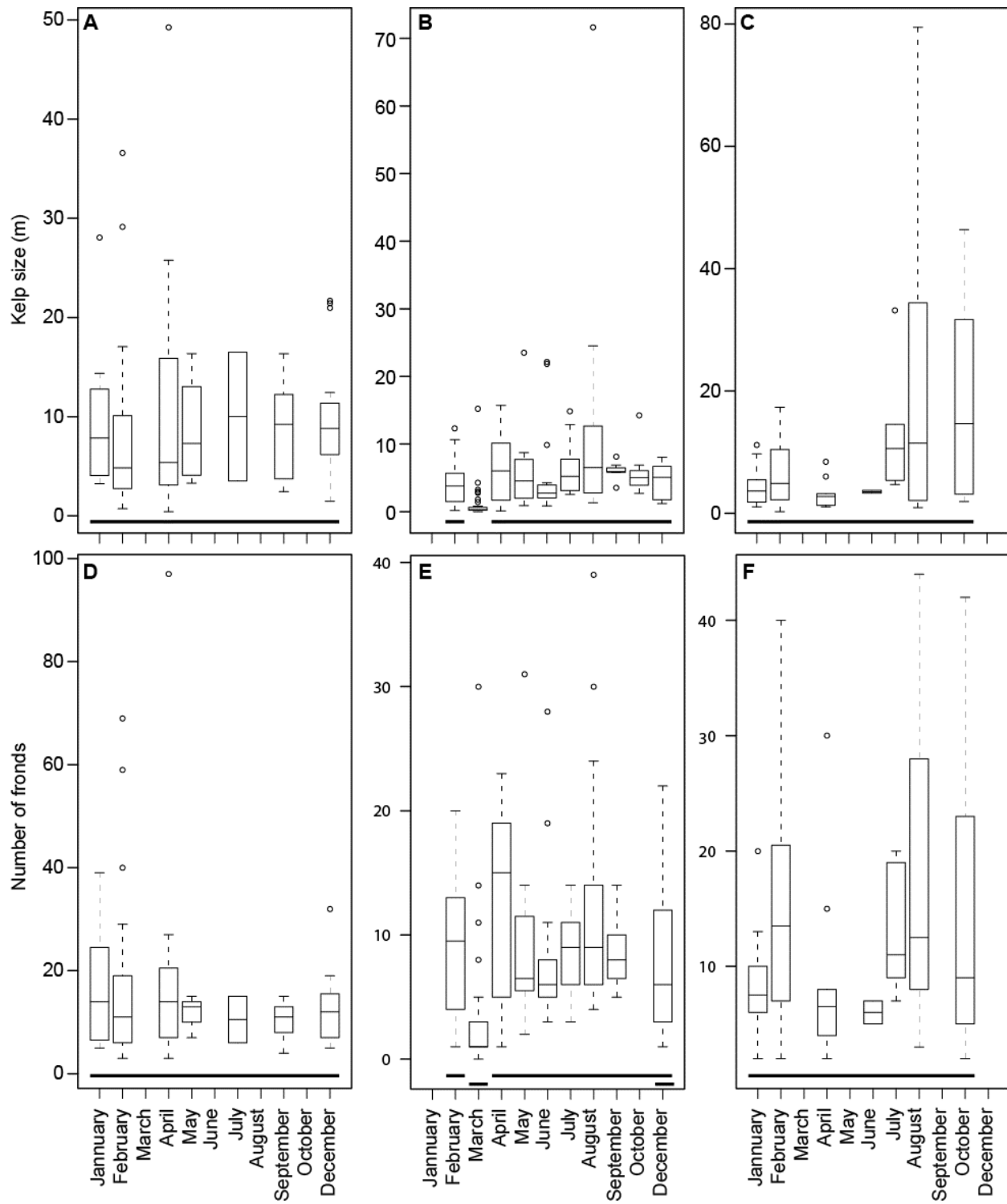
Figure S3.1: Comparisons of kelp size at Miwok Beach (A), Kehoe Beach (B), and McClures Beach and number of fronds per kelp at Miwok Beach (D), Kehoe Beach (E), and McClures Beach (F) during different months. The plots show the median values for all kelp measured along transects run during each month over a two-year period (boxes indicate the first quartiles

around the median, error bars show the most extreme data point that is no more than 1.5 times the interquartile range from the box, and circles indicate values beyond 1.5 time the interquartile range from the box). Bars under the horizontal axis indicate months for which the values were not significantly different from each other (Kruskal-Wallis tests with post hoc Dunn tests, $P <$ 0.05 for significance). Sample sizes for each month at Miwok B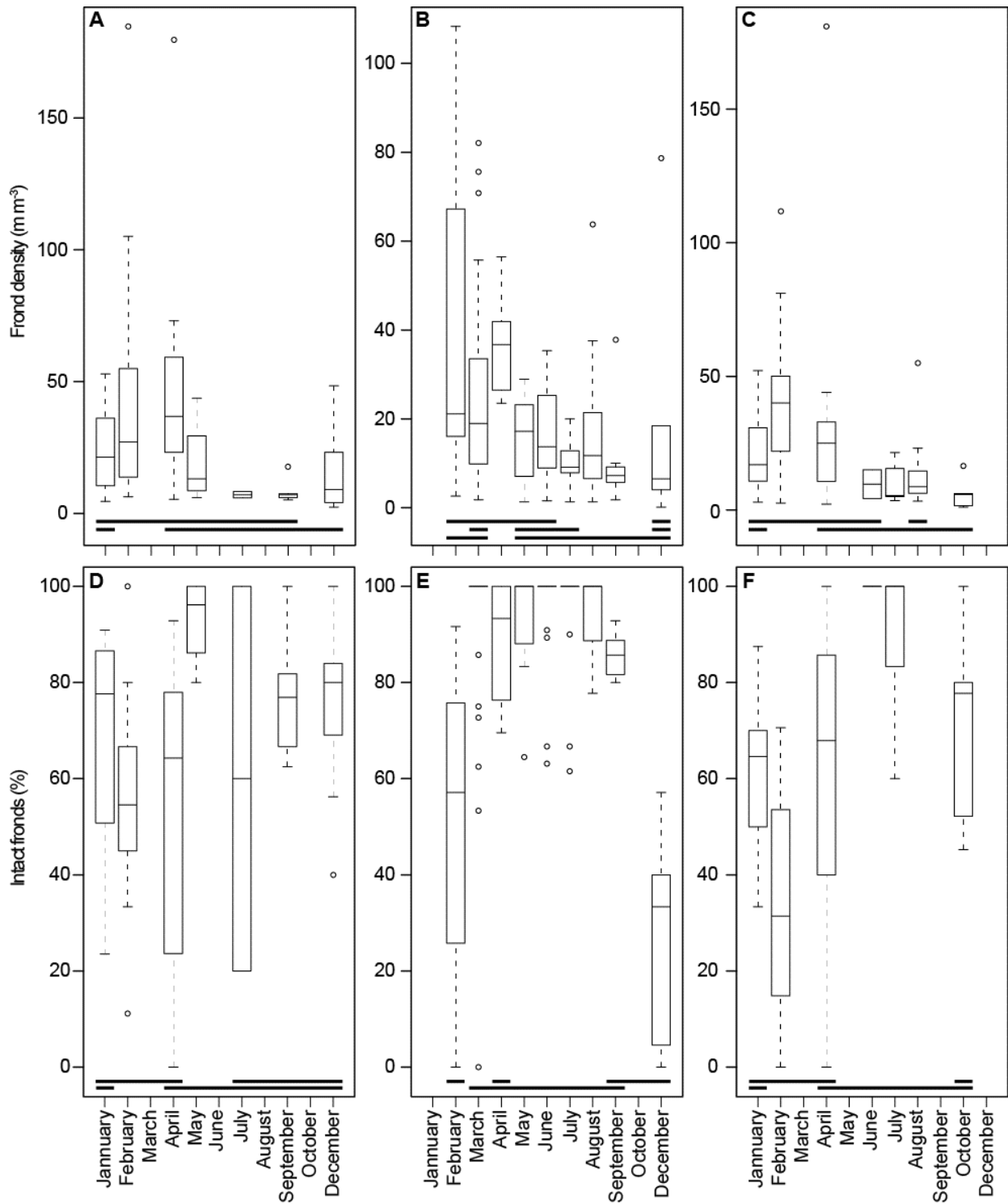each, in chronological order, were 10, 40, 7, 31, 29, 5, and 15. Sample sizes for each month at Kehoe Beach were 20, 41, 7, 20, 22, 13, 22, 7, and 6. Sample sizes for each month at McClures Beach were 16, 18, 10, 30, 50, 47, 10, and 5.
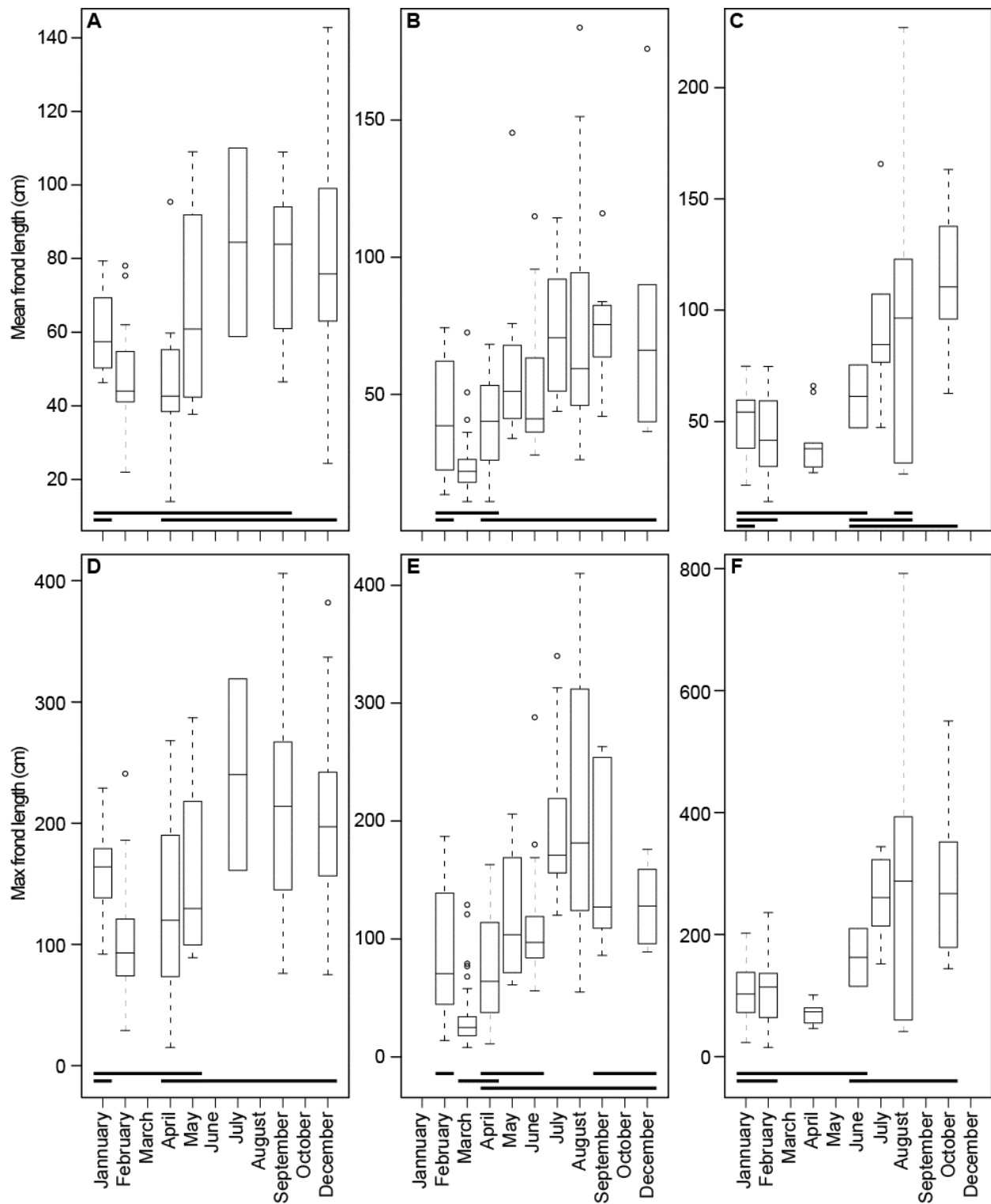
Figure S3.2: Comparisons of the mean frond length per kelp at Miwok Beach (A), Kehoe Beach (B), and McClures Beach and maximum frond length per kelp at Miwok Beach (D), Kehoe Beach (E), and McClures Beach (F) during different months. The plots show the median values for all kelp measured along transects run during each month over a two-year period (boxes

indicate the first quartiles around the median, error bars show the most extreme data point that is no more than 1.5 times the interquartile range from the box, and circles indicate values beyond 1.5 time the interquartile range from the box). Bars under the horizontal axis indicate months for which the values were not significantly different from each other (Kruskal-Wallis tests with post hoc Dunn tests, $P < 0.05$ for significance). Sample sizes are reported in Fig. S3.1.

Figure S3.3: Comparisons of the frond density of kelp at Miwok Beach (A), Kehoe Beach (B), and McClures Beach and the percent of intact fronds per kelp at Miwok Beach (D), Kehoe Beach (E), and McClures Beach (F) during different months. The plots show the median values for all kelp measured along transects run during each month over a two-year period (boxes indicate the first quartiles around the median, error bars show the most extreme data point that is no more than 1.5 times the interquartile range from the box, and circles indicate values beyond 1.5 time

79

the interquartile range from the box). Bars under the horizontal axis indicate months for which the values were not significantly different from each other (Kruskal-Wallis tests with post hoc Dunn tests, $P < 0.05$ for significance). Sample sizes are reported in Fig. S3.1.
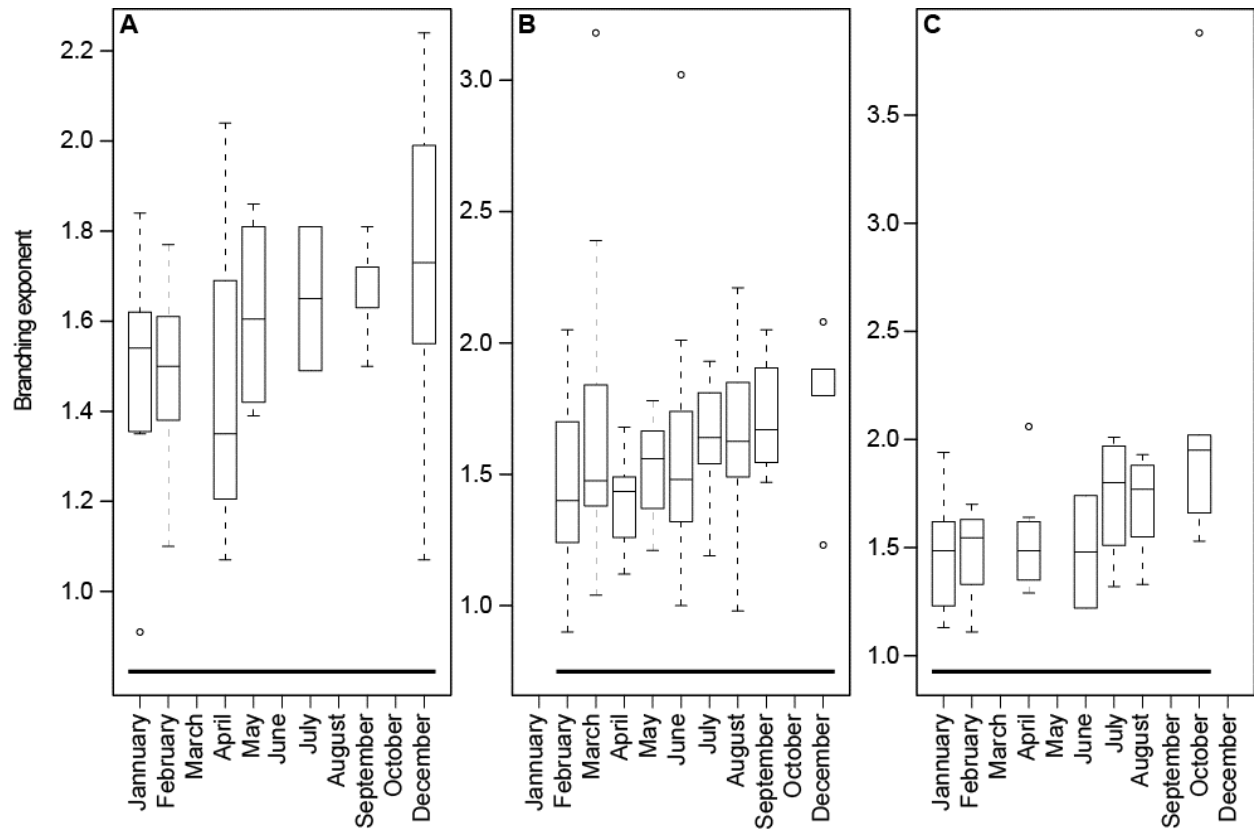
Figure S3.4: Comparisons of the branching exponent of kelp at Miwok Beach (A), Kehoe Beach (B), and McClures Beach during different months. The plots show the median values for all kelp measured along transects run during each month over a two-year period (boxes indicate the first quartiles around the median, error bars show the most extreme data point that is no more than 1.5 times the interquartile range from the box, and circles indicate values beyond 1.5 time the interquartile range from the box). Bars under the horizontal axis indicate months for which the values were not significantly different from each other (Kruskal-Wallis tests with post hoc Dunn tests, $P < 0.05$ for significance). Sample sizes are reported in Fig. S3.1.
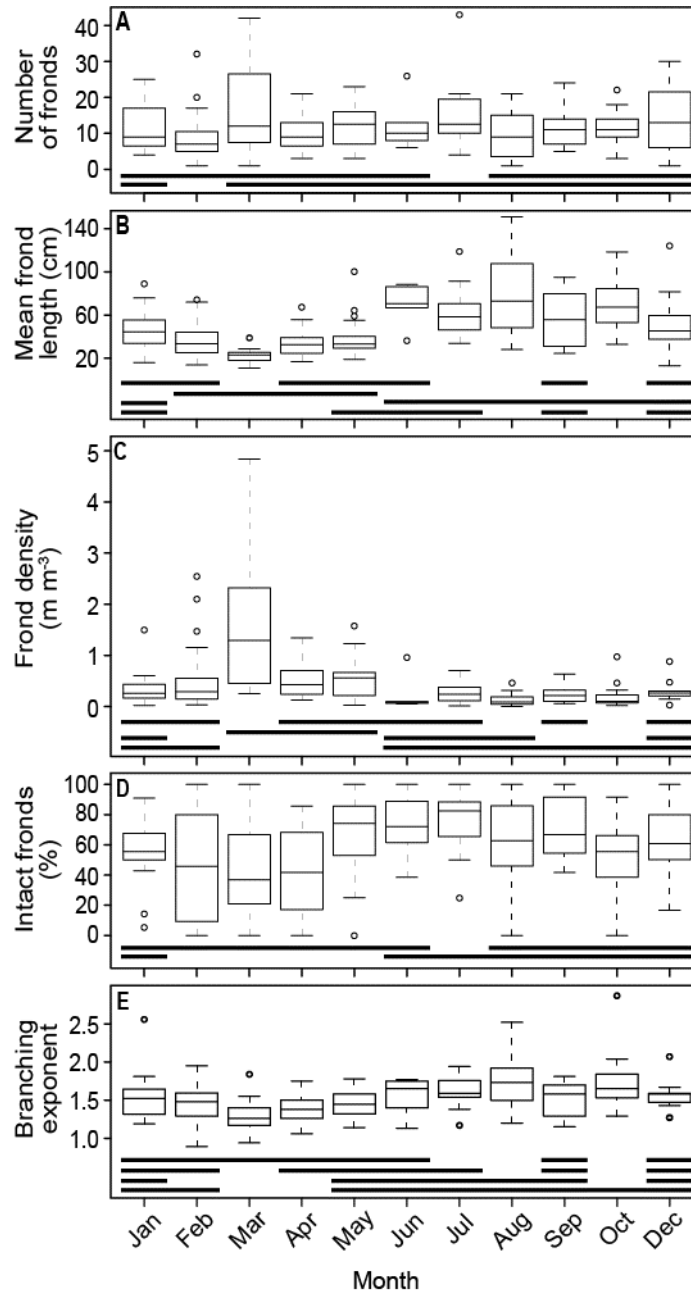
Figure S3.5: Comparisons of number of fronds (A), mean frond length (B), frond density (C), intact fronds (D) and branching exponent (E) of the kelp among calendar years. Each pair of bars above the data shows two groups of months with different values (Kruskal-Wallis tests with post hoc Dunn tests, $P < 0.05$). Sample sizes are reported in Fig. 3.6. There was only one observation per kelp for each morphological character.
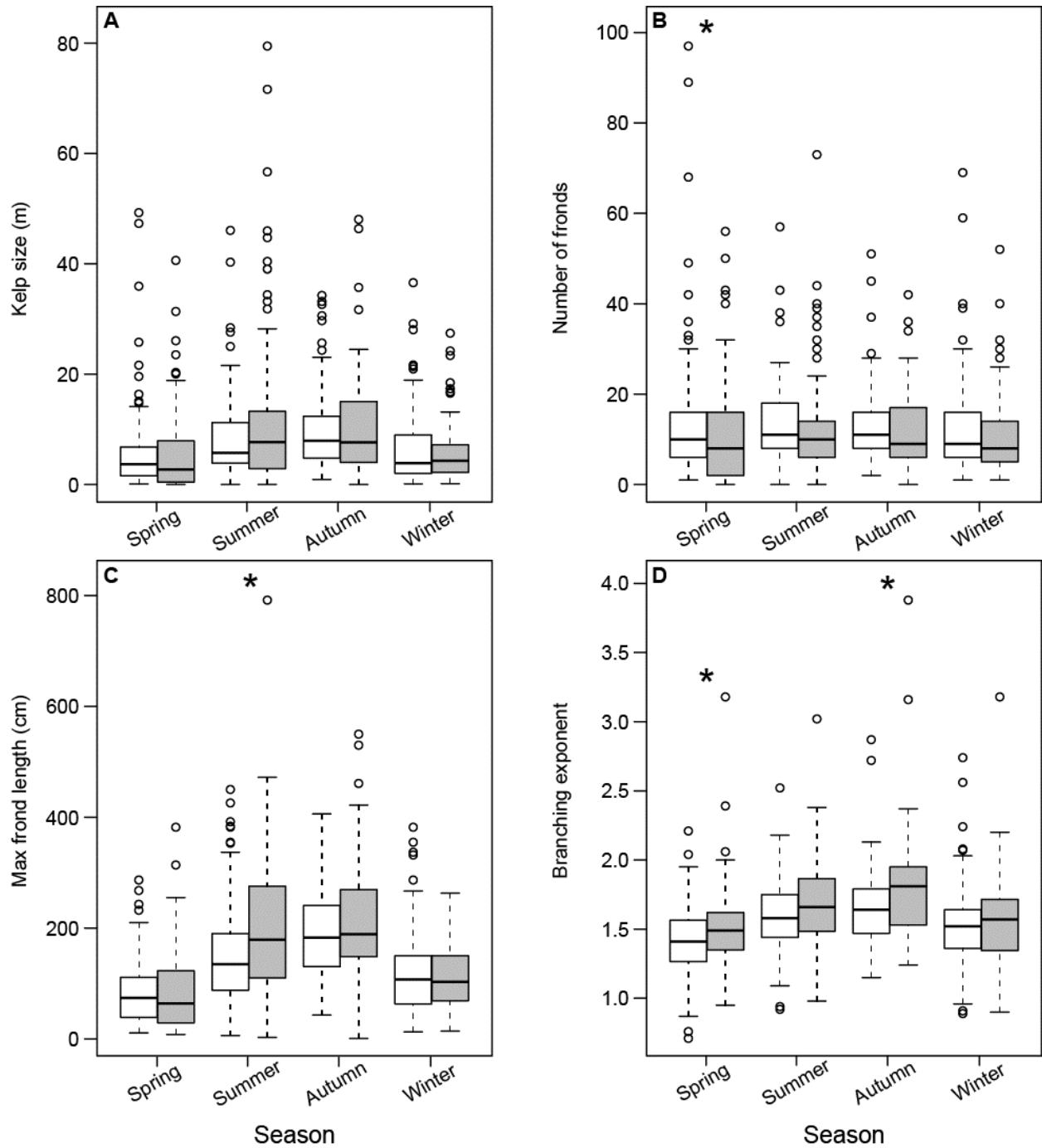
Figure S3.6: Seasonal variation in kelp size (A), number of fronds (B), maximum frond length (C), and branching exponent (D) for kelp at moderately wave-exposed sites (white bars) and wave-exposed sites (gray bars). Asterisks indicate a significant difference in a morphological character between wave-exposures during that season (Mann-Whitney U tests, $P < 0.05$). Sample sizes are reported in Fig. 3.8. Some kelp were measured in multiple seasons, but there was only one observation per kelp within a single season.
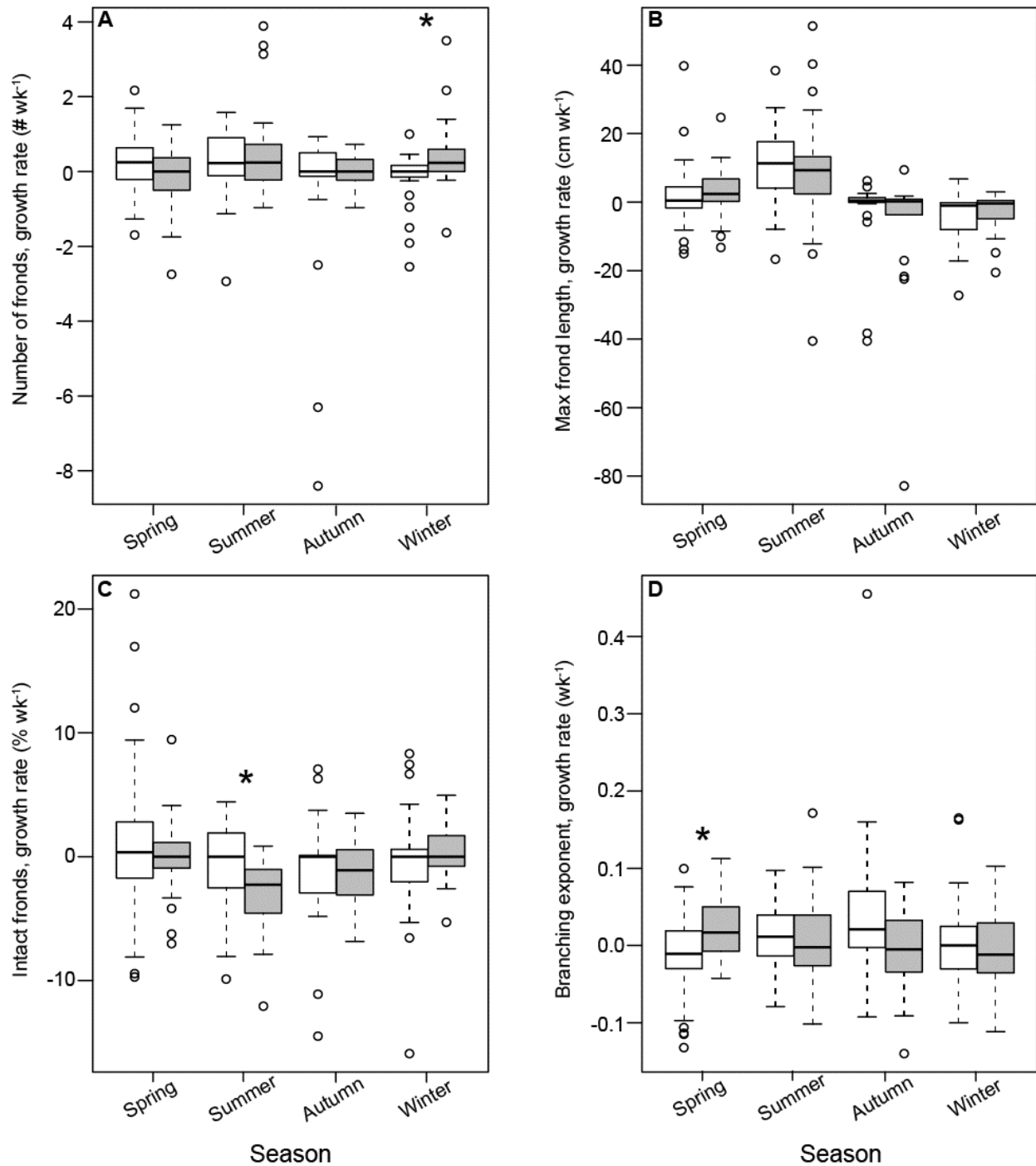
Figure S3.7: Seasonal variation in growth rates for number of fronds (A), maximum frond length (B), intact fronds (C), and branching exponent (D) for kelp at moderately wave-exposed sites (white bars) and wave-exposed sites (gray bars). Asterisks indicate a significant difference in growth rates between wave-exposures during that season (Mann-Whitney U tests, $P < 0.05$). Sample sizes are reported in Fig. 3.10. Some kelp were measured in multiple seasons, but there was only one observation for each kelp within a single season.